Tomas Bata University in Zlín
Faculty of Technology

Doctoral Thesis

Intelligent Fluids – Electro-Rheological (ER) and Magneto-Rheological (MR) Suspensions

Inteligentní tekutiny – elektroreologické (ER) a magnetoreologické (MR) suspenze

Michal Sedlačík

July 2012

Zlín, Czech Republic

Doctoral study programme: P 2808 Chemistry and Materials Technology

2808V006 Technology of Macromolecular Compounds

Supervisor: Assoc. Prof. Vladimír Pavlínek

CONTENT

ABSTRACT

Nowadays, a large number of modern technologies employ intelligent materials, which generally change their properties according to the external stimulus applied. Recently, a new class of intelligent systems with extraordinary rheological behaviour in an external field has attracted much interest from both academics and engineers.

The main representatives of such rheologicaly-active field-responsive systems are Magneto-Rheological (further only MR) and Electro-Rheological (further only ER) fluids. The rheology of these fluids is very attractive since it can be controlled by the application of a field - either magnetic or electric. Typically, MR or ER fluids comprise suspensions of nano/micrometre-sized magnetic or dielectric particles respectively, dispersed in a suitable carrier liquid. The key feature of these fluids is their capability to alter viscosity by several orders of magnitude in milliseconds.

Although MR and ER behaviour was discovered 60 years ago, the first use of MR and ER fluids in real applications happened in the 1990s owing to progress in the Chemistry, Physics, Materials Science, and Mechanical and Electrical Engineering fields [1, 2]. Currently, MR fluids are mainly used in various systems in which variable control of the applied damping/force adjustment is required. Nevertheless, several obstacles - such as particle sedimentation due to density mismatch between the dispersed magnetic particles and the carrier liquid in MR fluids; or the low efficiency of ER fluids, still hinder their wider utilisation.

Therefore, the primary focus of this work is to design novel MR/ER fluids which would not suffer from these drawbacks. Taking into account the differing requirements of the intelligent fluids studied resulted in the development of two different approaches. The first part of the presented work deals with Carbonyl Iron, which, being the most commonly-used dispersed phase in MR, was modified via Wet (coating with polyaniline) or Dry (plasma treatment) chemical methods in order to improve its compatibility, with silicone oil used as a carrier liquid and - thus, to enhance the long-term stability of MR fluids. Furthermore, the effect of annealing temperature, used for the synthesis of Cobalt Ferrite particles, on MR behaviour was studied to prepare novel types of dispersed particles for MR fluids, with controlled magnetic properties. The second part of the work concentrates on the fabrication of hollow globular clusters of Titanium Oxide/Polypyrrole particles with a core-shell structure - representing a novel dispersed phase for ER fluids of improved ER efficiency.

Keywords: Magneto-rheology • Electro-rheology • Carbonyl iron • Cobalt Ferrite • Titanium Oxide • Polyaniline • Polypyrrole • Core-shell •Plasma treat-

ment • Silicone oil • Sedimentation • Steady Shear • Dynamic Shear measurements

ABSTRAKT

V dnešní době je velké množství moderních technologií úzce spjato s využíváním inteligentních materiálů. Obecně u těchto systémů dochází k požadované změně jedné nebo více vlastností v reakci na vnější stimuly. V poslední době poutá pozornost nejen vědecké, ale i praktické oblasti využití nová skupina inteligentních systémů vykazující neobyčejnou změnu svých reologických vlastností v závislosti na vnějším aplikovaném poli.

Hlavními zástupci těchto systémů aktivně měnících své reologické chování v závislosti na působícím poli jsou magnetoreologické (MR) a elektroreologické (ER) tekutiny. Jak již název napovídá, tyto tekutiny vykazují velmi zajímavé reologické chování, které může být kontrolováno účinky buď magnetického anebo elektrického pole. MR nebo ER tekutiny lze charakterizovat jako suspenze nano/mikro částic s magnetickými nebo výhradně dielektrickými vlastnostmi ve vhodné nosné kapalině. Největší výhodou těchto tekutin oproti obvyklým tekutinám je jejich schopnost měnit viskozitu v širokém rozsahu (několik řádů) a to ve zlomcích milisekundy.

Ačkoliv první vysvětlení MR a ER chování byla provedena již před 60 lety, reálné aplikace MR a ER tekutin na trhu byly možné až v devadesátých letech díky rozvoji chemie, fyziky, materiálových věd strojního a elektroinženýrství [1, 2]. V dnešní době jsou zejména MR tekutiny s oblibou používány v různých systémech, kde je požadováno proměnné ovládání tlumení/působící síla. Nicméně jejich širšímu využití neustále brání několik překážek jako sedimentace částic v důsledku velkého rozdílu hustot mezi dispergovanými částicemi a nosnou kapalinou v MR tekutinách nebo nízká účinnost ER tekutin.

Prvořadá pozornost je tudíž v této práci upřena na návrh nových MR/ER tekutin, u nichž jsou zmíněné nedostatky potlačovány. V závislosti na odlišných požadavcích studovaných typů inteligentních tekutin jsou uplatňovány dva různé přístupy. V první části práce bylo karbonyl železo, jakožto nejpoužívanější dispergovaná složka v MR tekutinách, upraveno pomocí mokrých (potažení polyanilínem) nebo suchých (plasmové opracování) chemických metod za účelem zvýšení kompatibility se silikonovým olejem použitým jako nosná kapalina a tím i zvýšením dlouhodobé stability MR tekutin. Kromě toho byl studován vliv žíhací teploty použité při výrobě částic kobalt feritu na MR chování s cílem připravit nový typ dispergovaných částic s řízenými magnetickými vlastnostmi pro MR tekutiny. V druhé části práce byly vyrobeny duté kulovité aglomeráty oxidu titaničitého s polypyrolem se strukturou jádro-slupka (core-shell) jako novou dispergovanou fází pro ER tekutiny s vylepšenou ER účinností.

Klíčová slova: Magnetoreologie • Elektroreologie • Karbonyl železo • Kobalt ferit • Polyanilín • Polypyrol • Jádro-slupka • Plasmové opracování • Silikonový olej • Sedimentace • Ustálené smýkání • Oscilační měření

LIST OF PAPERS

PAPER I

SEDLACIK, M., PAVLINEK, V., SAHA, P., SVRCINOVA, P., FILIP, P., STEJSKAL, J. Rheological properties of magnetorheological suspensions based on core–shell structured polyaniline–coated carbonyl iron particles. *Smart Mater. Struct.* 2010, vol. 19, 115008.

PAPER II

SEDLACIK, M., PAVLINEK, V., LEHOCKY, M., GRULICH, O., MRACEK, A., SVRCINOVA, P., FILIP, P., VESEL, A. Plasma–treated carbonyl iron particles as a dispersed phase in magnetorheological fluids. *Colloid Surf. A-Physicochem. Eng. Asp*. 2011, vol. 387, p. 99-103.

PAPER III

SEDLACIK, M., PAVLINEK, V., SAHA, P., SVRCINOVA, P., FILIP, P. The role of particles annealing temperature on magnetorheological effect. *Mod. Phys. Lett. B*. 2012, vol. 26, 1150013.

PAPER IV

SEDLACIK, M., MRLIK, M., PAVLINEK, V., SAHA, P., QUADRAT, O. Electrorheological properties of suspensions of hollow globular titanium oxide/polypyrrole particles. *Colloid Polym. Sci.* 2012, vol. 290, p. 41-48.

PAPER V

SEDLACIK, M., MRLIK, M., KOZAKOVA, Z., PAVLINEK, V., KURITKA, I. Synthesis and electrorheology of rod-like TiO_2 particles prepared via microwave-assisted molten-salt method. *manuscript*. 2012.

THEORETICAL BACKGROUND

1. Intelligent fluids in static field

Smart systems modifying their fluidity in the external static field stand out as materials of enormous scientific and applicative interest. Such materials are polyphasic fluids made up of microparticles dispersed in the carrier fluid and additives which prevent irreversible aggregation or sedimentation. The microparticles can be magnetic or exclusively dielectric resulting in two types of intelligent fluids. The former are called MR fluids (see section 6), while the latter are referred to as ER fluids (see section 7). The remarkable field-induced changes in rheological behaviour are driven by dipolar magnetic or dielectric attractive forces causing the formation of particles into chains aligned in direction of static magnetic (MR fluid) or electric (ER fluid) field, respectively [3].

2. MR and ER phenomenon

Despite the differences in their composition and properties, the physical phenomenon responsible for the changes in rheological behaviour of MR and ER fluid called MR and ER effects are quite similar. The MR or ER phenomenon can be simply demonstrated by means of Scheme 1 showing the intelligent fluid placed between two electrodes producing either magnetic (expressed in magnetic flux density, B) or electric (expressed in electric field strength, E) field. In the absence of an applied field, the system exhibits Newtonian-like behaviour and, thus it has the consistency of the oil body with randomly distributed particles (Scheme 1a). The application of field induces a dipole moment in each suspended particle and, in the first stage, interparticle attractive forces promote the formation of labyrinthine structures (Scheme 1b) within the system. Further increase in the applied field causes the particles to form columnar structures, parallel to the applied field (Scheme 1c). The formed chain-like or columnar structures restrict the motion of the fluid and, thereby, increase the elastic characteristics of the suspension. For practical applications, the characteristic time of structure transformation, t_{sc}, i.e., time of formation or break-up of solid-like structure, is an important factor. From practical application point of view this time must be in the range of 1-10 ms [4]. The use of MR or ER fluids in real systems is based on the simultaneous application of magnetic or electric field, respectively, and shear, oscillatory or pressure driven force (Scheme 1d–f). Although the mechanical loading evokes rupturing of created internal structure, the field-induced attractive forces cause “self healing” of particles alignment (see section 3) until the moment, when hydrodynamic forces overcome the field-induced ones and material starts to exhibit yielding behaviour. This phenomenon is associated with a yield stress, τ_0, (see also section 4.2) of the system, which corresponds to the minimum energy required to rupture the aggregates [5].

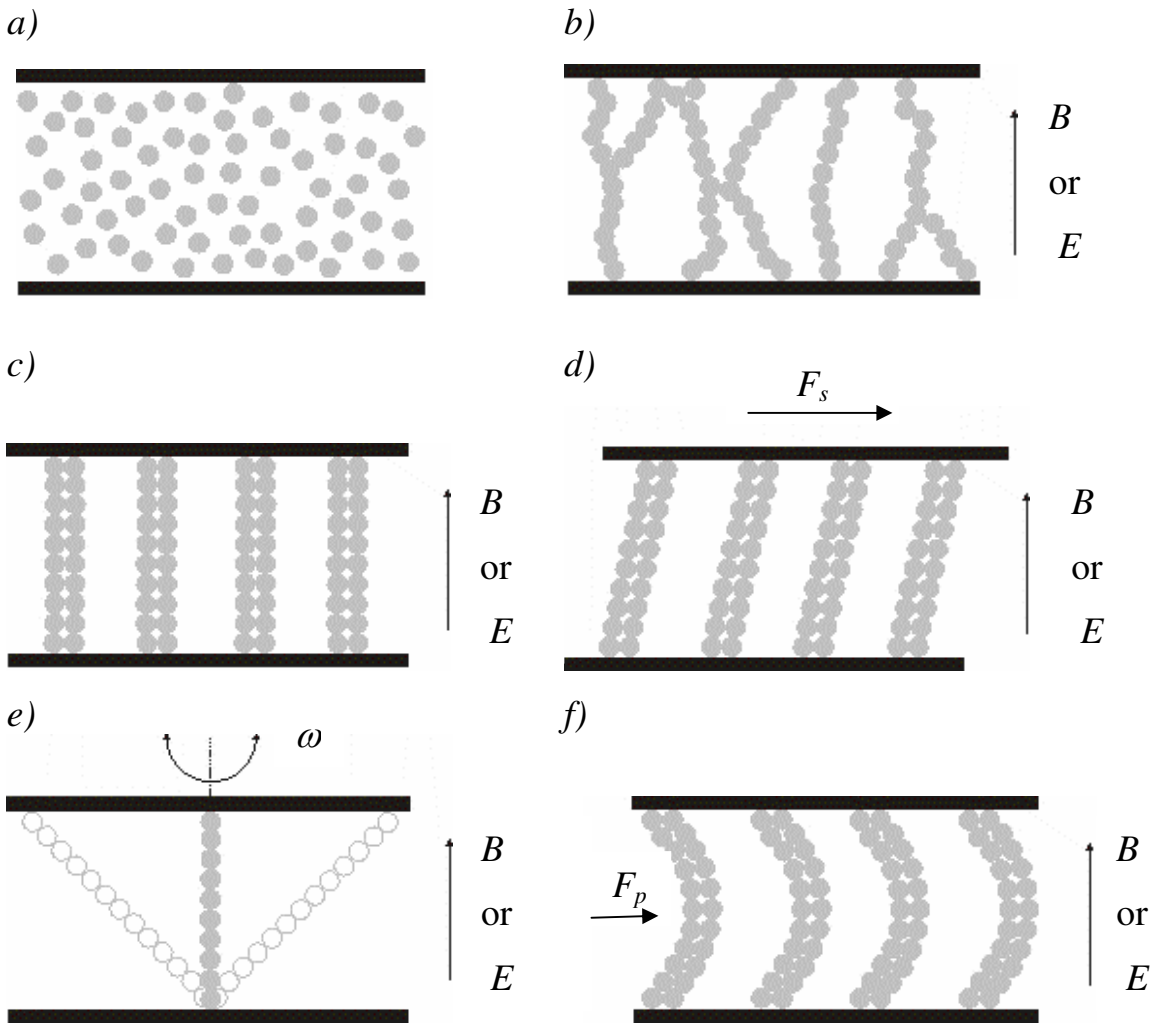

Scheme 1: Structural changes in MR or ER fluid before (a), and after (b, c) application of an external magnetic, B, or electric, E, field, respectively. Furthermore, in simultaneous application of shear force, F_s, (d), dynamic shear force driven by angular frequency, ω, (e) and pressure force, F_p, (f) on formed structure. Redrawn from Ref. [6, 7].

3. Microstructure changes of MR or ER fluids

As mentioned earlier, the liquid to solid-like state transition of the system, which is closely connected with changes of its rheological properties, is attributed to the formation of chain-like or columnar internal structure of particles in the presence of external field.

In case of MR fluids the mechanism is based upon the alignment of each particle with its north magnetic pole facing the north pole of the external magnetic field and likewise with the south magnetic poles [8]. These particles are then aligned similarly and in close proximity to each other and, thus the north pole of one particle will find itself attracted to a nearby particle's south pole

(Scheme 2a). Evidently, the highest probability of particles attraction occurs, when two induced dipoles are situated in the same field stream line; i.e. the angle, θ_{ij}, between the field direction and particles center-to-center line, R_{ij}, is 0°. However, when the north pole of one particle is next to the north pole of another particles; i.e. θ_{ij} = 90 °, the particles will repeal each other (Scheme 2b). Among these two limiting values of θ_{ij} the particles will rotate attempting two align their R_{ij} and attract each other (Scheme 2c).

In case of ER fluids the mechanism of particles alignment into chain-like or columnar structures is different compared to MR fluids. Here, the external electric field induces electric dipoles on each particle due to its interfacial polarization [9]. Such dipoles are then oriented according to the electric field direction and positive pole of one particle attracts itself to a nearby negative pole of another particles by electrostatic forces. Hence, the polarization rate, i.e. polarizability, $\Delta\varepsilon'$, of dispersed particles is assumed to be the most important factor in generating of noticeable liquid to solid-like state transition [10].

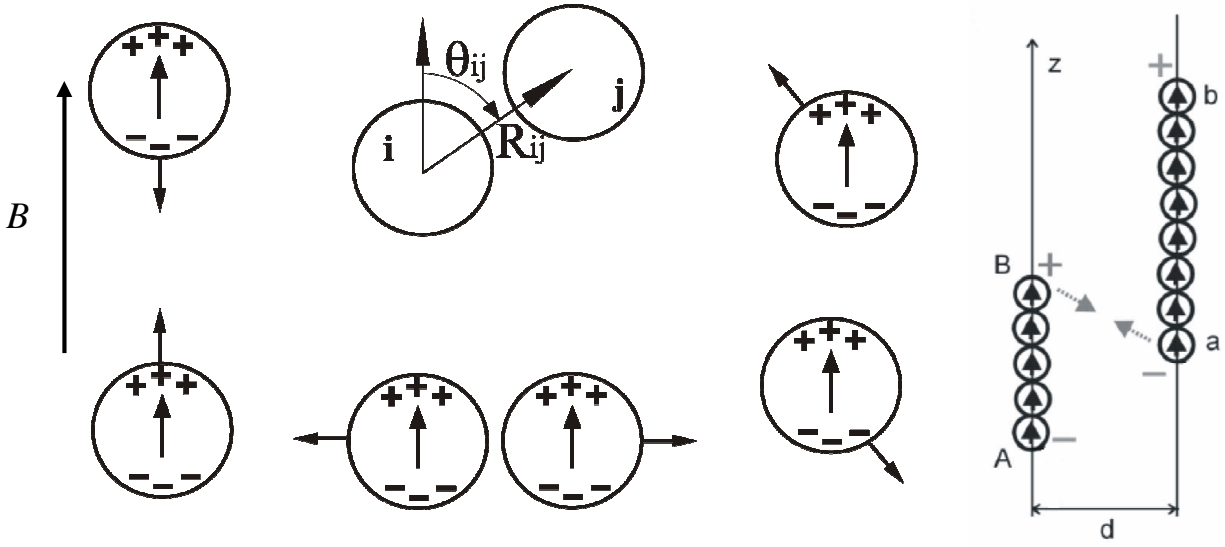

Scheme 2: Magnetostatic interactions between particles dipoles in a magnetic field (B). Dipoles aligned with the field attract each other (a), dipoles with their line-of-centers; i.e. angle θ_{ij} between the field direction and center-to-center line R_{ij}, normal to the field repeal each other (b), while other θ_{ij} produces a torque attempting to align the R_{ij} with the field. Attraction of two rotating ruptured chains (d). Redrawn from Ref. [7, 11]

As mentioned in previous section, the chain-like structure rupturing in the simultaneous application of the force and external static field has a self healing ability. This can be explained by the existence of torque which makes the separated chains to rotate. Well before shifting enough (by strong hydrodynamic forces) these two chains connect end by end (Scheme 2d). After two particles of

each chain have joined the coalescence occurs [11]. All the illustrated changes happen in milliseconds and, once the external field is removed, the structure rapidly disappears under flow and the system immediately returns to its liquid character [12].

4. Rheological properties

If the particles interaction energy in MR or ER fluids is higher compared to thermal energy, the particle chains become rigid [13]. Just this feature evokes practical interest of intelligent materials for applied science. Structures made up in the whole volume of MR or ER fluid exposed to static external field lead to losses of fluidity at stresses lower than the strength of the structure and system becomes a viscoplastic medium with yield stress corresponding to the strength of particle structure [14].

Out of doubt it is necessary to use standard methods and characteristics for evaluation of internal structure properties. Therefore, rheological parameters as shear stress, shear viscosity or yield stress in steady shear and/or storage and loss moduli or complex viscosity in oscillatory mode are employed in MR and ER fluids investigation.

4.1 Steady shear

In the absence of external field, MR or ER suspensions exhibit nearly Newtonian character in steady shear flow [15] and, hence can be expressed by Eq. 1:

$$\tau = \eta \cdot \dot{\gamma} \tag{1}$$

Shear stress, τ, is linearly proportional to the shear rate, $\dot{\gamma}$. The shear viscosity, η, does not depend on $\dot{\gamma}$ but only on the particles volume fraction, Φ. Viscosity of concentrated suspensions containing even anisotropic and polydispersed particles [16] can be calculated according to Eq. 2:

$$\eta = \eta_0 \, [1 + 0.75 \, / \, (\Phi_{max} \, / \, \Phi - 1)]^2 \tag{2}$$

where η_0 is the viscosity of Newtonian liquid and Φ_{max} the maximal particle fraction (at maximum packing).

Application of field results in drastic changes of rheological properties, i.e. system changes from a purely viscous liquid to a viscoplastic medium (Figure 1).

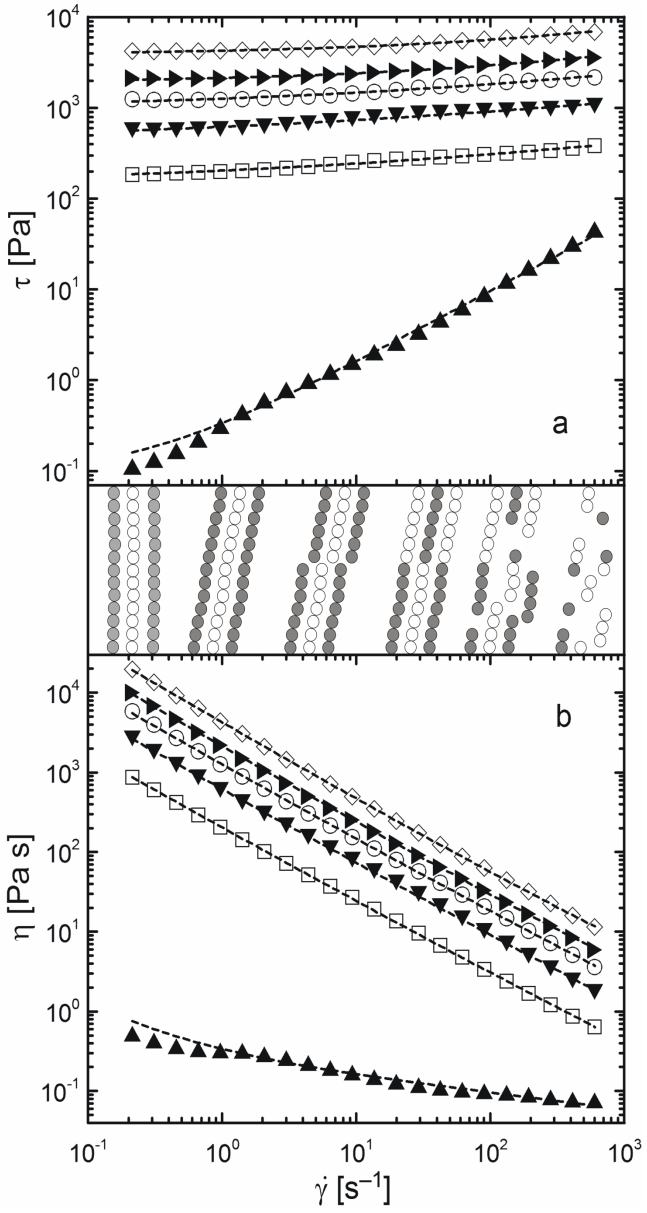

Figure 1: Double-logarithmic plot of the shear stress, τ, (a) and shear viscosity, η, (b) vs. shear rate, $\dot{\gamma}$, for typical MR suspension of carbonyl iron particles coated with polyaniline in silicone oil under various magnetic flux densities, B [mT]: (▲) 0, (□) 50, (▼) 95, (○) 145, (►) 192, (◇) 290. Dash lines are fits of Herschel-Bulkley model (Eq. 4). Based on data from Ref. [17]

The efficiency of a magneto or electro-sensitive fluid is firstly judged through its yield stress, $\tau_{0,}$ which measures the strength of the structure formed by the application of the field. Then, for stresses $\tau > \tau_0$, the viscoplastic body is gradually brought to the fluid phase. Bingham plastic constitutive model has been widely used for predictions of system behaviour [18, 19]:

$$\tau = \tau_0 + \eta_{pl} \cdot \dot{\gamma} \tag{3}$$

Actually, the Bingham model is not applicable, when MR or ER fluids exhibit shear thinning in the post-yield region. Herschel Bulkley fluid model theoretically and experimentally demonstrated successful evaluation of non-Newtonian MR or ER fluids behaviour above the yield stress [13, 20]:

$$\tau = \tau_0 + \eta_{pl} \cdot \dot{\gamma}^n \tag{4}$$

where η_{pl} is the plastic viscosity of the suspension in both models (Eq. 3, 4) and n is the Herschel-Bulkley index.

Generally, there are two types of yield stress according to the experimental setup, namely dynamic yield stress and static yield stress [21, 22]. The former is obtained in control shear rate (CSR) mode, in which a shear rate is applied to the material and shear stress required to make material flow is measured. Then, the dynamic yield stress is obtained by extrapolation of shear stress curve to zero shear rate. On the other hand, the static yield stress is produced in control shear stress (CSS) mode, in which the necessary stress for initiation of shear flow of material originally been at rest is determined [23]. Thus, the static yield stress is more predictive value about the structure strength [24].

4.2 Viscoelastic measurements

MR or ER materials having Bingham plastic behaviour under a superimposed external magnetic or electric field can be successfully described as viscoelastic system in the range of small strains of oscillatory flow. In some applications, e.g. vibrating damping [25], such characterization is even more realistic than via the yield stress. In contrast to the steady shear flow experiment, the internal structure is only deformed and not destroyed. Since this deformation is dynamic, the obtained shear modulus is complex quantity:

$$G^* = G' + iG'' \tag{5}$$

where the real part, G', is storage modulus (elastic portion), and imaginary part, G'', is loss modulus (viscous portion). In the interest of real applications, there is important to know angular frequency dependence of G' and G'' in the linear viscoelastic region (LVR); i.e. at strain amplitude in which the structure of the MR or ER fluid is basically undisturbed [26]. Generally, G'' is higher at low concentration or approximately the same as G' at high concentration of particles in suspension in the absence of an external field. However, when the field is applied; i.e. the fluid undergoes liquid to solid-like state transition, both viscoelastic moduli abruptly increase and especially G' starts to dominate over G'' attaining several decimal orders of magnitude [14]. A typical example is shown in Fig. 2 for MR fluids of variously large magnetic particles. While the intensity of magnetic field gradually increases, G' grows up which is an evidence of stiffer

structure development. Nevertheless, the increase is particles size dependent (for more details see section 5.3).

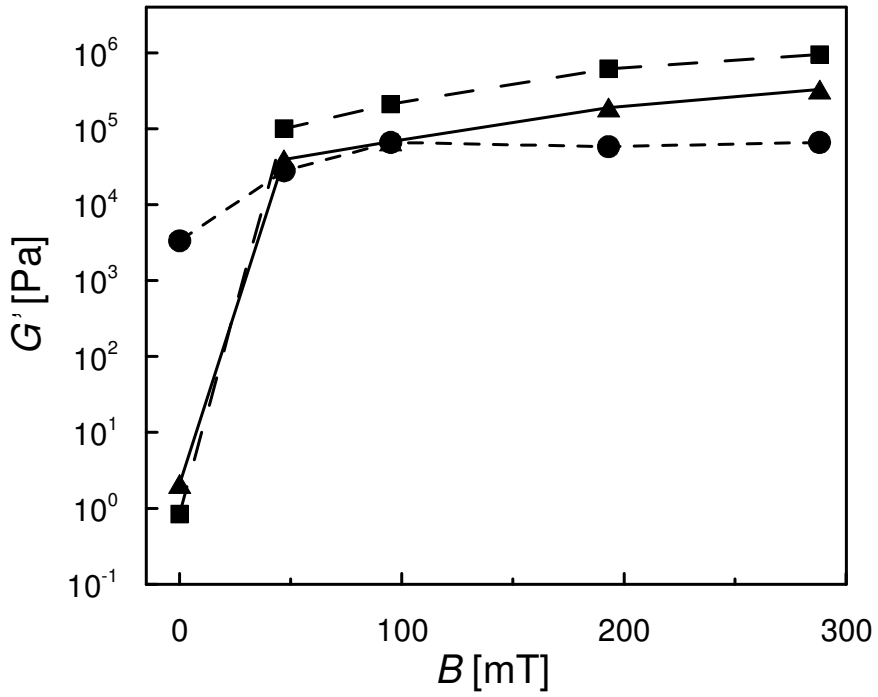

Figure 2: Magnetorheological effect: influence of magnetic field on storage modulus, G', of suspensions based on 35 nm $CoFe_2O_4$ (●), 3.5 μm (▲), and 9 μm (■) carbonyl iron particles at angular frequency $\omega = 0.92$ rad·s^{-1} and strain amplitude $\gamma = 2 \cdot 10^{-5}$. Based on data from Ref. [17, 27]

5. Important factors influencing the MR or ER effect

It is worth also noting, that the main parameters characterizing the efficiency of MR or ER systems such as yield stress and storage modulus are strongly dependent on many factors, among others, on the external field strength, the working temperature and particles concentration, size, particles size distribution, and shape, as described below.

5.1 External field strength

The external field strength is a key factor for efficient MR or ER fluid; since, until certain critical field strength, the higher the field is the more compact and stiffer chains or columns are created. The critical field strength is not strictly given quantity for all MR or ER fluids, but depends on many variables such as dispersed phase and/or carrier liquid properties, concentration or temperature influencing the particles coalescence mechanism [6].

In case of ER fluids, the yield stress as one of the critical evaluation parameters of the ER performance changes its electric field dependency just at the criti-

cal electric field strength, E_C [28]. Below this value, the predicted ER mechanism is polarization model [7, 29] and, generally, τ_0 scales E^2. On the other hand, above the E_C, the proposed ER mechanism is conductivity model [30, 31] and $\tau_0 \approx E^{3/2}$.

If using the analogy between linear electrostatic and magnetostatic, it seems, that models developed for ER fluids can be modified to treat MR fluids. However, these models fail to treat the nonlinearity inherent in all magnetic materials [32]. The magnetization, M, in such materials does not increase indefinitely with increasing applied field, but rather it saturates at the saturation magnetization, M_s [33]. In MR fluids, local saturation magnetization of dispersed particles determines the field dependence of the yield stress and shear modulus over a wide range of applied external magnetic fields. There have been used a numerous finite-element techniques [34] and analytical approximations [35] for the calculation of the field distribution in magnetizable particles chains (Scheme 3). These calculations revealed that magnetic nonlinearity and saturation have a significant impact on the field dependence of the yield stress and shear moduli of MR fluids.

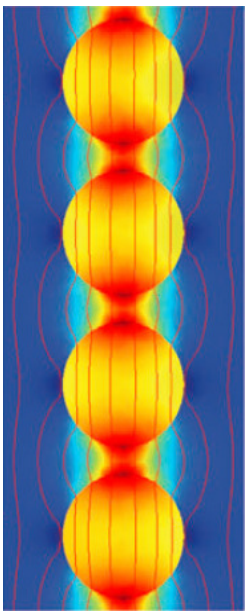

Scheme 3: Magnetic flux lines in an idealized particle chain obtained by finite-element analysis. Adopted from Ref. [36]

Only at low applied fields, τ_0 and G' increase, as expected from linear magnetostatics, with B^2. For higher applied fields, the contact regions of each particle are saturated (Scheme 3) and $\tau_0 \approx B^{3/2}$ while G' scales linearly with B. At high fields, the particles saturate completely, and τ_0 and G' scale with M_S^2 [32].

It is necessary to distinguish here the real values of yield stresses of MR or ER fluids in magnetic or electric field used in commercial applications. Generally, it is possible to obtain yield stresses close to 100 kPa for common MR fluids whereas 10 kPa only for special types of ER fluid [37]. The detailed discussion about composition will be given in section 6 for MR fluids and in section 7 for ER fluids, respectively.

5.2 Temperature

The temperature variation basically influences both dispersed phase and carrier liquid properties. The former case is especially important in ER fluids, where increase in temperature changes dielectric properties and particle conductivity resulting in higher polarizability and better internal structure development [6, 38]. The magnetic properties of particles used in MR fluids are not so temperature sensitive in working temperature range of – 30 to 120 °C. On the other hand, increased temperature evokes higher Brownian motion counteracting the chain formation and, thus, the final influence of temperature on dispersed phase depends on the ratio of these two contributions.

As mentioned above, the properties of liquid continuum are affected by temperature as well. Generally, with increasing temperature the medium viscosity decreases and dispersed particles form chain-like structures much easier. However, the thermal stability of the system and Brownian motion have to be considered again.

5.3 Particles concentration, size, particle size distribution, shape

MR or ER effect is also strongly affected by concentration of dispersed particles, their size, particle size distribution and shape. In each system, there exists an optimum in volume fraction of field-responsible particles. Basically, this ratio ranges from 15 to 40 vol.% for both types of systems [3, 39]. In the presence of external field applied to the system below the minimal concentration only weak internal structure is formed. The MR or ER effect increases significantly with particles concentration. Nevertheless, the particles mobility is reasonably inhibited and field-off viscosity increased above the maximal concentration which, subsequently, decreases MR or ER efficiency.

Particles should be generally large enough that attraction forces can overcome Brownian motion and small enough in order to prevent sedimentation [40]. From more detailed point of view, particles in MR fluids should be rather larger in the range of 1 – 10 μm due to sufficient intrinsic magnetic properties as shown in Figure 2. The problem of sedimentation within the systems having bigger particles in the mentioned range can be eliminated using bimodal particles, i.e. one fraction in nanometre and the other one in micrometer range [41,

42]. On the other hand, recent studies in ER fluids proved that reasonably higher ER effect is achieved with nanometre-sized particles due to their much higher surface area reflecting in higher surface polarization [43].

The effect of particles shape on the generation of higher MR or ER effect is more reasonable in systems with lower concentration and/or lower external field strengths applied. In principle, particles having their major axis aligned with the external field, i.e. rod-like particles, will have greater induced moment and, consequently, stiffer internal structure formed compared to their spherical analogues [40, 44, 45].

6. Materials used for MR systems

MR fluids are generally two-phase systems, in which micrometer-sized ferro- or ferrimagnetic multi-domain particles are suspended in a variety of carrier liquids like silicone or mineral oils [8]. It is worth to mention here, that MR fluids differ from so called ferrofluids which contain nanometre-sized magnetizable particles. An acceptable MR fluid is characterized by low initial viscosity, high τ_0 in external field applied, negligible temperature dependence, and high stability [46, 47]. The significant difference between dispersed particles density and carrier liquid density however makes MR fluids susceptible to long-term separation [17, 48]. Thus, additives such as thixotropic agents [49] or surfactants [50] are used to inhibit sedimentation and particles agglomeration.

More details about general description of MR fluids are available from reviews in *Refs*. [37, 51, 52].

6.1 Dispersed phase

The dispersed phase is the most important component in MR fluids. The strength of induced magnetic dipoles in particles and, consequently, the stiffness of formed internal structure markedly depend on magnetic properties of dispersed particles such as high M_S and low coercive magnetic force, H_C. Systems with very low H_C are called magnetically soft materials and are characterized by their high permeability resulting in easy magnetization by relatively low-strength magnetic fields. Moreover, when the applied field is removed, they return to the state of relatively low residual magnetism [33]. The magnetic materials which satisfy the above mentioned requirements and have size of 1 – 10 μm are some ferro- or ferrimagnetic materials (Scheme 4).

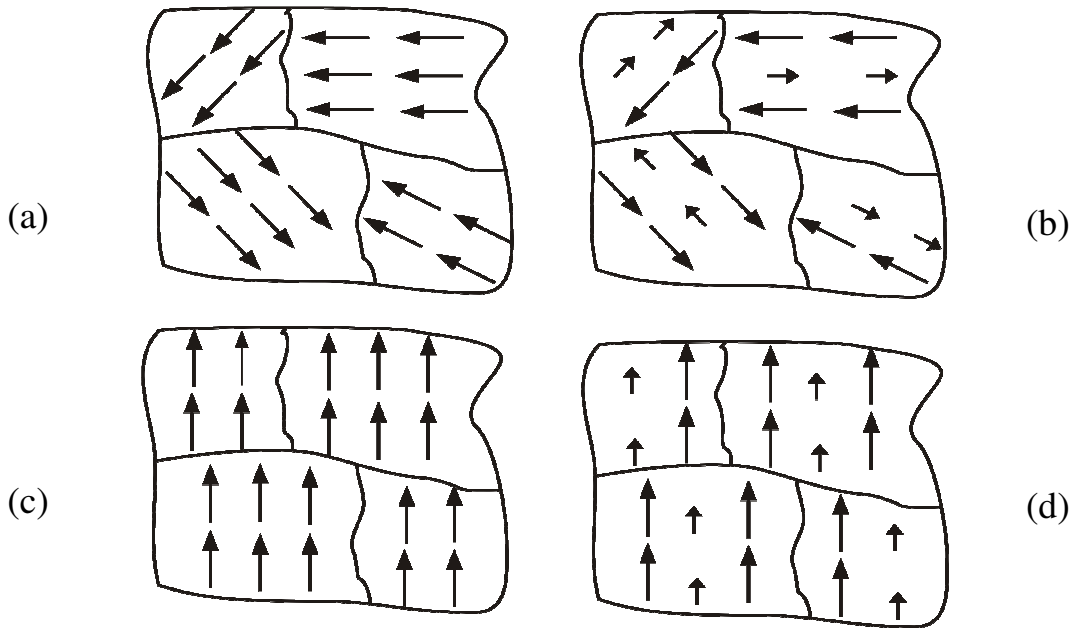

Scheme 4: Magnetic domain structure of ferro- (a), ferrimagnetic (b) material in the absence of external field, and ferro- (c), ferrimagnetic (d) material in the presence of external field. Redrawn from Ref. [33]

Since the number of magnetizable elements and alloys is limited, the choice for MR dispersed phase is much more limited than for ER fluids [52]. The element with highest M_S is iron ($\mu_0 M_S$ = 2.1 Tesla) [47]. Thus, iron, especially that made by chemical vapour deposition (CVD) technique from iron pentacarbonyl precursors and known as carbonyl iron (CI), is the most used material as a dispersed phase in MR fluids. The iron particles prepared by CVD technique are preferred as opposed to, for example, those prepared by using the electrolytic or spray atomization process due to their chemical purity, optimal size and spherical shape [3]. CI was firstly used by Rabinow [53] and later on by many other teams [3, 48, 54-56]. The MR efficiency of these fluids in the loading of 30 vol.% is typically 50 kPa in applicative fields [11].

Alloys of iron and cobalt can be ranged among other candidates as a dispersed phase in MR fluids. Although such systems have $\mu_0 M_S$ = 2.43 Tesla [47], they posses lower magnetic permeability than CI particles. It means that the theoretical yield stress of 48 kPa for MR fluids based on iron-cobalt alloys [57] can not be reach at magnetic field strengths normally used in real devices. Furthermore, there exist many other materials used as dispersed phase in MR fluids including iron oxides like magnetite [58, 59] or ceramic ferrites [3] which, however, exhibit relatively low MR efficiency compared to previously mentioned variants.

Unfortunately, large size of magnetic particles constitutes the origin of some limitations to practical applications of MR fluids. The density of iron (ρ = 7.87 g cm^{-3}) is much higher than that of carrier liquid ($\rho \approx$ 1 g cm^{-3}) resulting in the instability of the fluid caused by the particles sedimentation. More-

over, once the dispersed phase is settled, the poor redispersibility due to an irreversible aggregation can occur [40]. Many concepts for obtaining a stable dispersion of magnetic particles in carrier liquid have already been established. One strategy, for example, deals with addition of gel forming or thixotropic additives [49, 60]. Another idea is based on the use of two types of stabilisers: sedimentation stabilisers, which prevent the particles from settling, and agglomerative stabilisers preventing the ferromagnetic particles from sticking together [46, 51]. However, the low shear viscosity without magnetic field after such stabilization is often not maintained. Recently, the core-shell structuralized particles with magnetic material as a core and polymer as a shell has been used [48, 55, 61]. The polymeric layer does not only reduce the total density of particle, but, particularly, improve the compatibility between hydrophobic carrier liquid and hydrophilic iron particle dispersed [58, 62]. Moreover, the coating protects iron particles against corrosion [63].

In summary, further studies should be made in the task of long-term stability of MR fluids rather than in increasing the yield stress which have already reached sufficient values for practical utilization of these intelligent systems.

6.2 Carrier liquid

The carrier liquid of MR fluid is basically selected based upon its rheological and tribological properties, chemical and temperature stability, and price. Much greater freedom is possible in selecting carrier liquid for MR fluid, since the dielectric properties of the suspending fluid, necessary in ER fluid, do not influence the MR effect [64]. By reason of large density mismatch between carrier liquid and dispersed phase, the surfactants or/and dielectric nano/microparticles are frequently added for the prevention of sedimentation of magnetic particles [3]. Typically, silicone [17], mineral [65] oils, glycol [66] or water [67], which is not suitable for ER fluids, are widely used as carrier liquid in MR fluids.

7. Materials used for ER systems

ER fluids are typically composed of non-conducting or semiconducting particles dispersed in a non-conducting carrier liquid in loading between 5 to 50 vol.%. In contrast to MR fluids, in ER systems dielectric breakdown occurs long before saturation mechanism is reached and, thus, the achieved yield stresses are typically two orders of magnitude lower than yield stresses reached in MR fluids [51]. However, an expressive progress have been done since their discovery by Winslow in 1947 [68]. Firstly, the systems were based on materials such as silica particles [69], starch [68], or crystalline cellulose [70]. Nevertheless, these materials contain a small amount of water to be ER active which was connected with several drawbacks as high leaking current, narrow working tem-

perature range, and devices corrosion. To overcome these limitations, water-free ER systems have been developed later [71] and are discussed below.

7.1 Dispersed phase

In contrast to MR fluids, the choice of materials suitable for dispersed phase is much wider in ER systems. Particles polarization plays crucial role in efficiency of ER fluids. Required polarization can be obtained in various types of materials.

First variant of dispersed phase consists in the use of inorganic materials like titanium oxide (TiO_2) [72], talc [73] or zeolite [74]. The main advantage of these materials over others is their high particles polarization, which even totally changes previous concepts on the ER mechanism. Together with nanometre scale of particles and the use of surfactants enable to reach yield stresses comparable to common MR fluids [43, 75]. Unfortunately, high abrasion and particles sedimentation decline the above mentioned benefit of inorganic materials.

Second type of materials used as ER fluids dispersed phase are conducting polymers. Chemical structure of polypyrrole (PPy) [76], polyaniline (PANI) [77] or poly(p-phenylene) [78] is formed by conjugated system of σ and π bonds which together with charge carriers enable to obtain conductive material. By using polymers as a dispersed phase in ER fluids, there is no sedimentation, but the loading of dispersed phase in the system is limited. Interestingly, the use of inorganic material as a core and conducting polymer as a shell in the core-shell structure is a new way in the designing of efficient ER fluids with low sedimentation and improved compatibility with continuum liquid [79-81]. Hence, dispersed phase particles based on core-shell structures are promising challenge for efficient ER fluids in the future.

Third possible materials as a dispersed phase in ER fluids are either immiscible or miscible liquids in the insulating oil which, as a consequence, also solve the problem of sedimentation. However, high field-off viscosity and weak ER efficiency belong to limitations of such systems. Liquid-crystalline materials can be ranged into this group [82, 83].

7.2 Carrier liquid

The choice of carrier liquid for ER systems is more restricted than in their MR counterparts. Along with properties inherent to MR fluids such as low viscosity, wide temperature range, high chemical stability and low toxicity; the ER carried liquids should have low relative permittivity, high electric breakdown strength, and low conductivity. Thus, various types of oils such as silicone [76], mineral [84], transformer [85] or kerosene [86] can be use as carrier liquid for ER fluids.

AIMS OF THE DOCTORAL STUDY

The main goal of the doctoral study is to synthesise and evaluate MR or ER properties of novel particles used as a dispersed phase in MR or ER fluids.

In case of MR fluids, various techniques for synthesis of core-shell particles including wet or dry methods are employed. Here, CI particles are used as a magnetic core and polymeric (PANI or fluoropolymer) layer as a shell. Moreover, the influence of annealing temperature on the magnetic properties of cobalt ferrite particles as alternative dispersed phase in MR fluids is also studied.

In case of ER fluids, the attention is paid to the synthesis of hollow globular clusters of titanium oxide/polypyrrole (TiO_2/PPy) core-shell structured particles. Elucidation of relation between ER efficiency and the structure of particles via rheological measurements and dielectric spectra analysis is performed.

SUMMARY OF THE PAPERS

In the following, short summaries and major results presented in Papers I to V are given. This chapter is divided into three parts corresponding to the main aims of the thesis.

8. Improved long-term stability of magnetorheological fluids

To analyze the effect of polymeric coating on long-term stability of magnetorheological (MR) fluids, the carbonyl iron (CI) was encapsulated with polyaniline (PANI) by using PANI colloidal dispersion in chloroform in **Paper I "Rheological properties of magnetorheological suspensions based on core-shell structured polyaniline-coated carbonyl iron particles"** (Figure 3) to obtain core-shell particles.

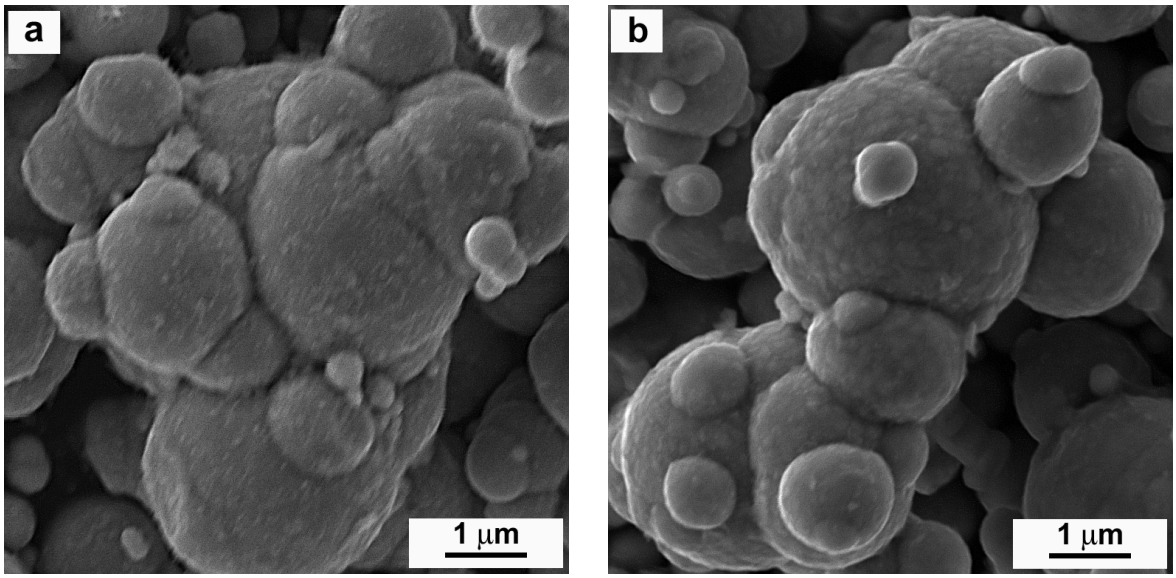

Figure 3: SEM images of CI (a) and CI/PANI core-shell (b) particles.

Vibrating sample magnetometry experiments revealed almost unchanged magnetic properties of PANI-coated CI. With a view to subsequent measurements, CI particles coated with PANI were suspended in silicone oil. MR properties of such fluids were investigated by steady and oscillatory shear experiments. Core-shell particles based MR fluids showed typical MR behaviour under the applied magnetic field following the characteristic $\tau_0 \propto B^{3/2-2}$ correlation. The results further revealed that polymeric coating positively affects the mutual compatibility between dispersed particles and silicone oil resulting in lower field-off viscosity in the absence of magnetic field. Thus, relative increase in viscosity, $e = (\eta_M - \eta_0)/\eta_0$, indicating MR efficiency was higher (Figure 4). Moreover, the improved mutual compatibility and reduced density of dispersed core-shell particles made particles sedimentation significantly lower.

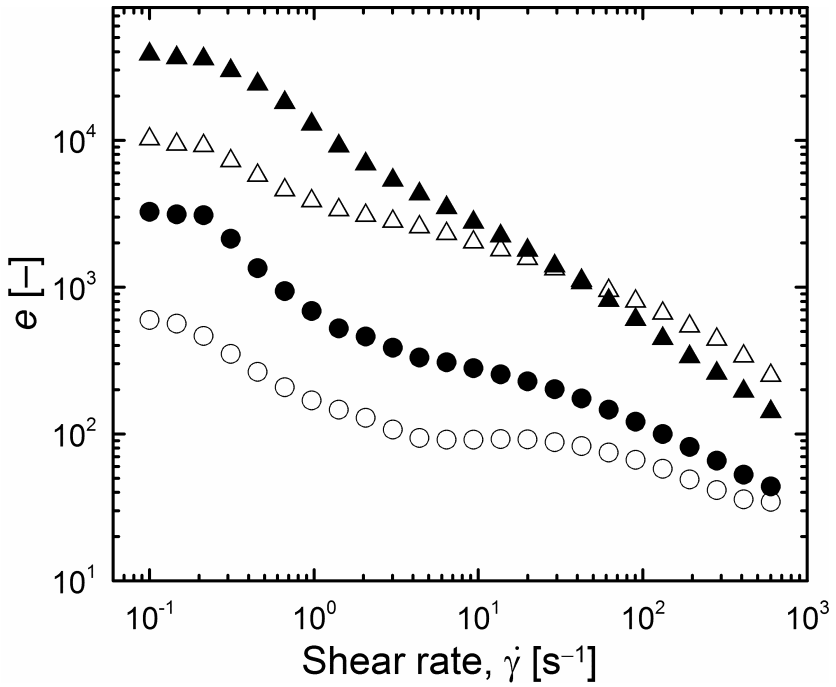

Figure 4: The dependence of MR efficiency, e, on the shear rate, $\dot{\gamma}$, for 60 (△, ▲) and 80 (○, ●) wt.% suspensions of mere CI (open symbols) and CI/PANI core-shell particles (solid symbols) in silicone oil. Calculated for magnetic flux density of 0 and 308 mT.

Paper II "Plasma-treated carbonyl iron particles as a dispersed phase in magnetorheological fluids" deals with the MR performance of core-shell particles prepared via innovative plasma enhanced chemical vapour deposition of fluoropolymer formed from octafluorocyclobutane onto CI particles. The successful coating was proved by X-ray photoelectron spectroscopy. The composition of surface layer and, consequently, the MR performance of prepared particles varied with the time of treatment in the plasma reactor as can be seen in Figure 5.

Compared to MR fluid based on mere CI, plasma-treated core-shell structured CI particles based MR fluids show enhanced sedimentation stability probably due to the interaction forces between fluorine bonded on particle surface and methyl groups of silicone oil used as a carrier liquid (Figure 6). The time of treatment in the plasma has also significantly influenced the sedimentation stability of MR fluids. Thus, MR fluid of particles treated for 60 s exhibits the best stability due to the presence of higher total concentration of atoms with electronegative nature, i.e. fluorine, oxygen and nitrogen, in the surface layer than in the case of particles treated for 120 s. This is supposedly caused by etching phenomenon which occurs and removes the surface atoms along with the functionalized groups at higher treatment times.

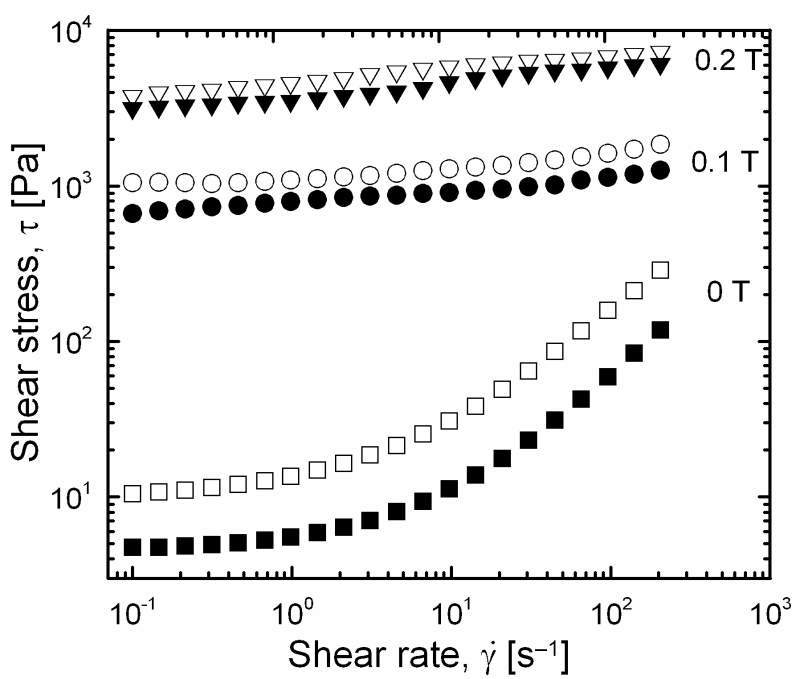

Figure 5: Flow curves of 80 wt.% MR fluids based on CI/fluoropolymer particles obtained from the plasma treatment of CI particles for 60 s (open symbols) and 120 s (solid symbols) under various magnetic fields applied.

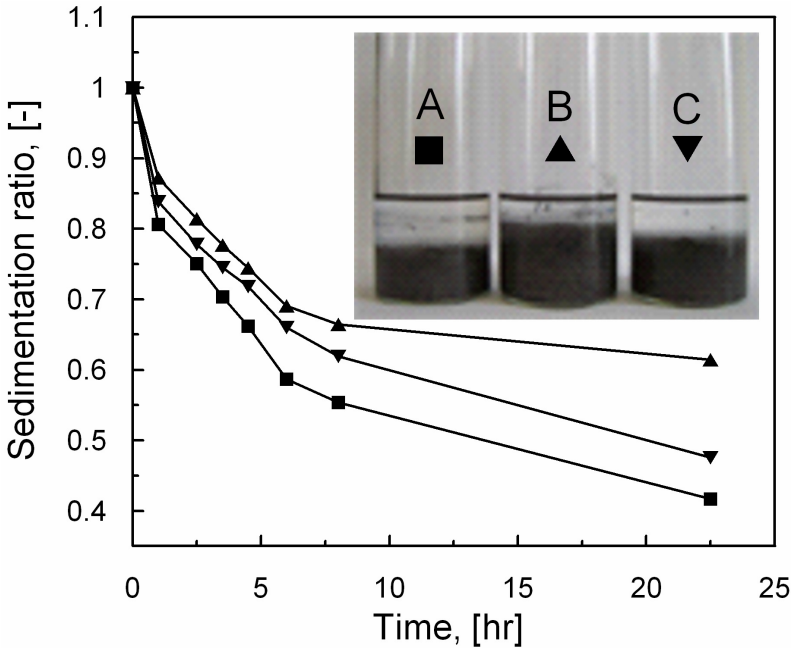

Figure 6: Sedimentation ratio vs. time for MR fluids based of mere CI (A: ■), core-shell CI/fluoropolymer particles treated in the plasma for 60 s (B: ▲), and 120 s (C: ▼). Inset: results of the sedimentation after 24 hrs.

9. Controlling of magnetic properties of particles

The possibility to control magnetic properties of cobalt ferrite particles via their annealing at different temperatures after the sol-gel synthesis is presented in **Paper III "The role of particles annealing temperature on magnetorheological effect"**. The X-ray diffraction analysis and vibrating sample magnetometry revealed that finite crystallite size of spinel cobalt ferrite particles and, consequently, magnetization saturation increased with increasing annealing temperature due to more proper magnetic domain development. Attention has also been paid to the analysis of the effect of particles annealing temperature on their MR behaviour.

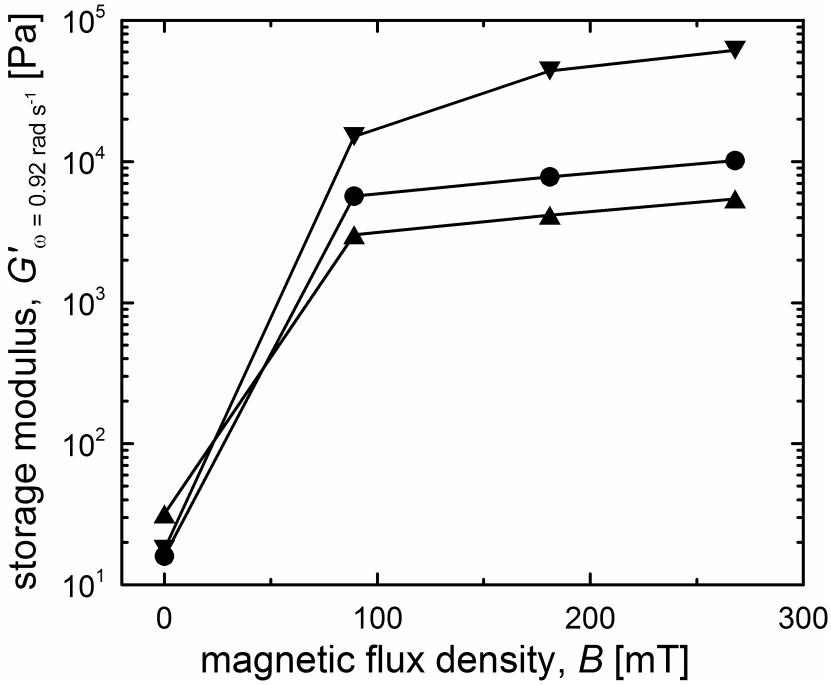

Figure 7: Storage modulus, G', dependence on magnetic flux density, B, at the angular frequency $\omega = 0.92$ rad s^{-1} for MR suspensions (40 wt.%) of cobalt ferrite particles annealed at 400 °C (▲), 850 °C (●), and 1000 °C (▼) dispersed in silicone oil.

MR performance, dynamic yield stress, as well as storage modulus were chosen as suitable criterions for this purpose. It was found that the intensity of MR effect of variously annealed cobalt ferrite particles based MR fluids increased with increasing annealing temperature (Figure 7).

10. Improved ER efficiency

Electrorheological characteristics of novel hollow globular clusters of TiO_2/PPy with core-shell structure are described in **Paper IV "Electrorheological properties of suspensions of hollow globular titanium oxide/polypyrrole particles"**. Mere TiO_2 particles were prepared via solvothermal synthesis and subsequently encapsulated by PPy layer. The structure and morphology (Figure 8) were characterized by X-ray diffraction analysis and scanning electron microscopy, respectively. Further, mere TiO_2 and PPy-modified particles were used as dispersed phase in silicone oil suspensions for ER investigation.

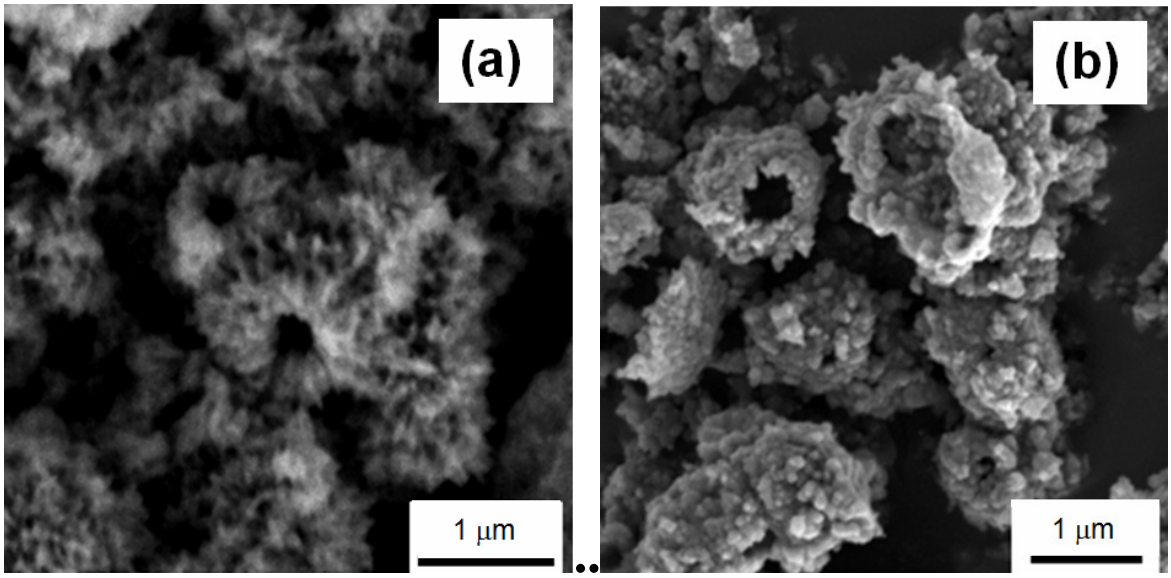

Figure 8: SEM images of TiO_2 (a) and TiO_2/PPy (b) hollow globular clusters.

While the ER activity of mere TiO_2 was low, the PPy coating of these hollow globular clusters improved the compatibility of dispersed particles and silicone oil and increased ER efficiency of the system considerably. Moreover, in contrast to maximum possible concentration of about 10 wt.% of mere TiO_2, 25 wt.% suspension of PPy-modified particles with low field-off viscosity could be prepared. Oscillatory shear experiment within the linear viscoelastic region further revealed that G' of core-shell structured particles based ER fluid increased around 2.5 orders of magnitude after the application of electric field (E = 3 kV mm^{-1}) compared to its initial value due to strong particles polarization. These observations were well interpreted by dielectric spectra analysis (Figure 9); the particles polarizability determining the dynamical response of a bound system to external electric fields, $\Delta\varepsilon' = \varepsilon'_0 - \varepsilon'_\infty$, considerably increased by coating of TiO_2 particles with PPy and also the relaxations times were shorter in case of core-shell structured particles since the maximum of dielec-

tric loss factor, ε'', was shifted to higher frequencies, which is positive for ER efficiency.

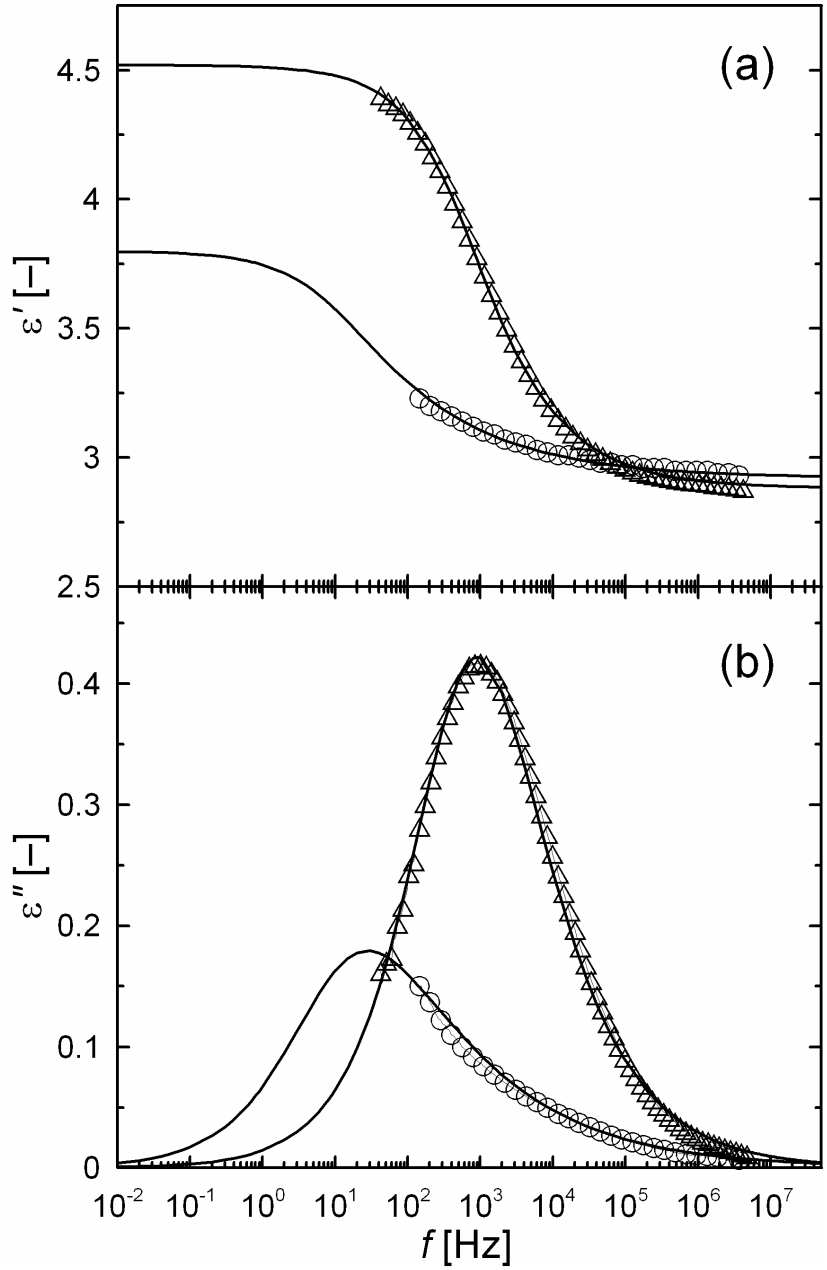

Figure 9: Relative permittivity, ε′, (a) and dielectric loss factor, ε″, (b) as a function of the frequency, f, for 5 wt.% TiO_2 hollow globular clusters (○), and TiO_2/PPy (△) particles ER fluids.

The object of aim in **Paper V "Synthesis and electrorheology of rod-like TiO_2 particles prepared via microwave-assisted molten-salt method"** is the synthesis and ER characterization of TiO_2 rod-like particles. A novel microwave-assisted molten-salt synthesis was employed for the preparation of these particles. This technique brings benefits in the use of low-melting salts which accelerate diffusion and thus formation of required structure and shortened re-

action time due to the incorporation of microwave heating which uniformly heats the system and make the reaction faster compared to conventional processes. The X-ray diffraction analysis confirmed the transformation from anatase crystalline phase of starting TiO_2 nanopowder into rutile of prepared TiO_2 particles while the scanning electron microscopy depicted their rod-like morphology. Rod-like TiO_2 particles were subsequently adopted as a dispersed phase of novel ER fluid and its ER performance was compared to that of starting TiO_2 particle based ER fluid (Figure 10). The dielectric spectra analysis confirmed higher ER activity of rod-like particles since these have higher interfacial polarizability and shorter relaxation time probably due to the one dimensional structure. The results further revealed that shear stress at very low shear rate, τ_C, i.e. close to the yield stress, scales with the electric field, E, according to $\tau_C = q \cdot E^{\alpha}$, which corresponds very well to assumption from polarization model ($\alpha = 2$). Finally, the ER efficiency increased with the particle concentration. The maximal concentration for which the ER efficiency will attain a maximum, e_{max}, was still not reached. Comparing these results with those obtained for ER fluids consisted of spherical TiO_2 particles, it is evident, that rod-like particles possess higher ER efficiency probably due to lower field-off viscosity given by one dimensional character of particles.

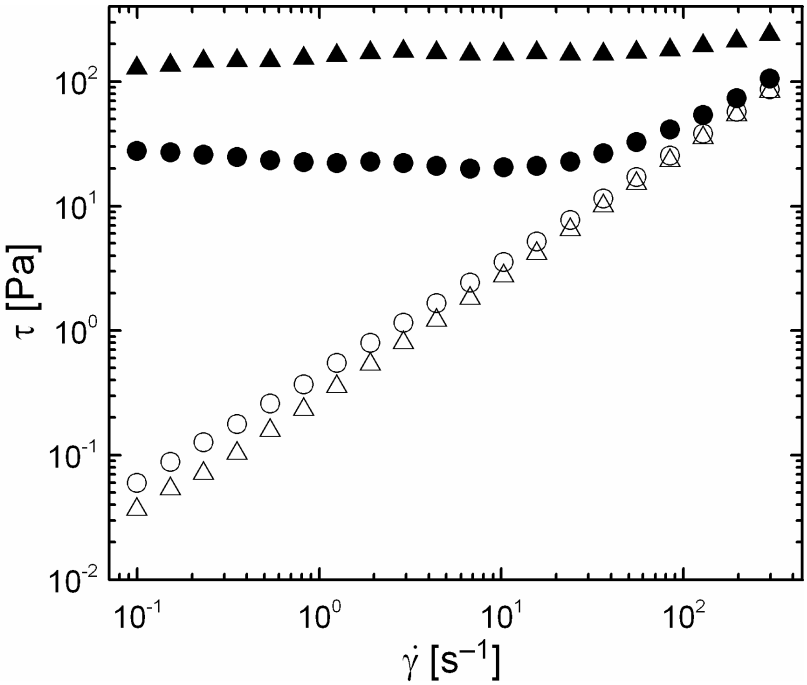

Figure 10: The dependence of the shear stress, t, vs. shear rate, $\dot{\gamma}$, for 15 wt.% ER fluid of starting anatase TiO_2 (●, ○) and prepared rutile TiO_2 rod-like (▲, △) particles in silicone oil. The electric field strengths ($kV \cdot mm^{-1}$): 0 (○, △), 3 (●, ▲).

CONTRIBUTIONS TO THE SCIENCE AND PRACTICE

The presented doctoral thesis deals with intelligent fluids, namely MR and ER phenomenon – basic mechanisms of these effects, role of various factors and materials on the MR and ER performance. However, the main attention is focused on the elimination of drawbacks of particular systems such as low sedimentation stability in case of MR fluids and weak ER efficiency of common ER fluids. All measurements have been carried out in accordance with MR and ER standards enabling the comparison of obtained results with literature. The benefits of current study to the scientific world are as follows:

- The use of core-shell structured particles with magnetic agent as a core and polymer layer as a shell improves the sedimentation stability of MR fluids compared to mere magnetic particles based systems.

- Mutual compatibility between core-shell particles and silicone oil used as a carrier liquid positively influences a relative increase in MR effect.

- The magnetic properties of cobalt ferrite particles, and subsequently MR performance, can be tailored during their synthesis via annealing temperature used.

- ER fluids based on core-shell structured composite particles with hollow globular clusters of titanium oxide as a core material and shell from conducting polymer polypyrrole show optimal dielectric properties resulting in high interfacial polarization and considerably higher ER performance than uncoated titanium oxide particles based system.

- One dimensional rod-like titanium oxide particles prepared via simple and rapid microwave-assisted molten-salt method exhibit much higher ER effect than common ER fluids consisted of spherical titanium oxide particles.

- Most of obtained results were already published and provide a new knowledge in research of intelligent MR and ER fluids.

ACKNOWLEDGEMENT

First, I would like to express my personal and profession respect to my supervisor, Assoc. Prof. Vladimír Pavlínek. He created an excellent research environment and gave me quanta of encouraging, personal and valuable advices all the time of my studies. My thanks belong to him also for support of my conferences abroad and my stay in Slovenia and making corrections of my scientific papers.

Special gratitude goes to my co-authors, who came up with ideas improving the research quality.

I cannot fail to mention all colleagues from Polymer Centre and sincerely thanks them for their friendly help, especially to Dr. Robert Moučka, Assoc. Prof. Ivo Kuřitka, Assoc. Prof. Marián Lehocký and Dr. Aleš Mráček.

Finally, I would like to thank my family and girlfriend for their understanding, patience and support during the studying period. It would have been impossible to finish without the strong support of them.

Thank you very much to all.

LIST OF SYMBOLS AND ACRONYMS

B	[T]	magnetic flux density
CI		carbonyl iron
CSS		control shear stress mode
CSR		control shear rate mode
CVD		chemical vapour deposition
e	[–]	MR or ER efficiency
E	[kV mm^{-1}]	electric field strength
E_C	[kV mm^{-1}]	critical electric field strength
ER		electrorheological
f	[Hz]	frequency
F_p	[N]	pressure force
F_s	[N]	shear force
G'	[Pa]	storage modulus
G''	[Pa]	loss modulus
LVR		linear viscoelastic region
M	[A m^{-1}]	magnetization
M_S	[A m^{-1}]	saturation magnetization
MR		magnetorheological
n		Herschel-Bulkley index
PANI		polyaniline
PPy		polypyrrole
R_{ij}		particles center-to-center line

t_{sc}	[s]	structure changing time
$\Delta\varepsilon'$	[–]	polarizability
ε''	[–]	dielectric loss factor
ε'_0	[–]	static relative permittivity
ε'_∞	[–]	high frequency relative permittivity
Φ	[vol.%]	volume fraction
Φ_{max}	[vol.%]	maximum particle fraction (at maximum packing)
γ		strain amplitude
$\dot{\gamma}$	[s^{-1}]	shear rate
η	[Pa s]	shear viscosity
η_0	[Pa s]	shear viscosity of Newtonian liquid
η_M	[Pa s]	shear viscosity in magnetic field
η_{pl}	[Pa s]	plastic viscosity
μ_0	[N A^{-2}]	magnetic permeability of vacuum
θ_{ij}	[°]	angle between the field direction and particles center-to-center line
ρ	[g cm^{-3}]	density
τ	[Pa]	shear stress
τ_0	[Pa]	yield stress
ω	[rad s^{-1}]	angular frequency

REFERENCES

1. DYKE, S.J., SPENCER, B.F., SAIN, M.K., CARLSON, J.D. Modeling and control of magnetorheological dampers for seismic response reduction. *Smart Mater. Struct.* 1996, vol. 5, no. 5, p. 565-575.
2. KORDONSKY, W.I. Magnetorheological effect as a base of new devices and technologies. *J. Magn. Magn. Mater.* 1993, vol. 122, no. 1-3, p. 395-398.
3. BICA, I. Advances in magnetorheological suspension: Production and properties. *J. Ind. Eng. Chem.* 2006, vol. 12, no. 4, p. 501-515.
4. HAO, T. Electrorheological suspensions. *Adv. Colloid Interface Sci.* 2002, vol. 97, no. 1-3, p. 1-35.
5. EKWEBELAM, C., SEE, H. Microstructural investigations of the yielding behaviour of bidisperse magnetorheological fluids. *Rheol. Acta*. 2009, vol. 48, no. 1, p. 19-32.
6. HAO, T. *Electrorheological fluids*. The non-aqueous suspensions. 1st ed. Amsterdam: Elsevier, 2005. 561 p. ISBN 1-44452180-1.
7. PARTHASARATHY, M., KLINGENBERG, D.J. Electrorheology: Mechanisms and models. *Mater. Sci. Eng. R-Rep.* 1996, vol. 17, no. 2, p. 57-103.
8. RINGLE, D.R. *A review of electromagnetic material properties* [online]. Textinfo calvin.edu [cited 10th March 2011]. Available from: <http://www.calvin.edu/~pribeiro/courses/engr302/Samples/ringle.doc>.
9. BLOCK, H., KELLY, J.P., QIN, A., WATSON, T. Materials and mechanisms in electrorheology. *Langmuir*. 1990, vol. 6, no. 1, p. 6-14.
10. IKAZAKI, F., KAWAI, A., UCHIDA, K., KAWAKAMI, T., EDAMURA, K., SAKURAI, K., ANZAI, H., ASAKO, Y. Mechanisms of electrorheology: the effect of the dielectric property. *J. Phys. D-Appl. Phys.* 1998, vol. 31, no. 3, p. 336-347.
11. BOSSIS, G., VOLKOVA, O., LACIS, S., MEUNIER, A. Magnetorheology: Fluids, structures and rheology. In ODENBACH, S. *Ferrofluids. Magnetically controllable fluids and their applications*. 1st ed. Berlin Heidelberg: Springer-Verlag, 2002, vol. 594, p. 202-230.
12. KLINGENBERG, D.J. Magnetorheology: Applications and challenges. *Aiche J.* 2001, vol. 47, no. 2, p. 246-249.
13. AI, H.X., WANG, D.H., LIAO, W.H. Design and modeling of a magnetorheological valve with both annular and radial flow. *J. Intell. Mater. Syst. Struct.* 2006, vol. 17, no. 4, p. 327-334.

14. MALKIN, A.Y., ISAYEV, A.I. *Rheology: Concepts, methods, and applications*. 1st ed. Toronto: ChemTec Publishing, 2006. 553 p. ISBN 1-895198-33-X.

15. MACOSKO, C.W. *Rheology. Principles, measurements and applications*. 1st ed. New York: VCH Publishers, 1994. 568 p. ISBN 1-56081-579-5.

16. CHONG, J.S., CHRISTIA.EB, BAER, A.D. Rheology of concentrated suspensions. *J. Appl. Polym. Sci.* 1971, vol. 15, no. 8, p. 2007-2021.

17. SEDLACIK, M., PAVLINEK, V., SAHA, P., SVRCINOVA, P., FILIP, P., STEJSKAL, J. Rheological properties of magnetorheological suspensions based on core-shell structured polyaniline-coated carbonyl iron particles. *Smart Mater. Struct.* 2010, vol. 19, no. 11, p. 115008.

18. FILISKO, F.E., RADZILOWSKI, L.H. An intrinsic mechanism for the activity of aluminosilicate based electrorheological materials. *J. Rheol.* 1990, vol. 34, no. 4, p. 539-552.

19. BINGHAM, E.C. An investigation of the laws of plastic flow. *U.S. Bureau Stand. Bull.* 1916, vol. 13, no. 1, p. 309-353.

20. HERSCHEL, W.H., BULKLEY, R. Konsistenzmessungen von Gummi-Benzol-Lösungen. *Kolloid Z.* 1926, vol. 39, no. 4, p. 291-300.

21. MEZGER, T.G. *The rheology handbook*. 2nd ed. Hannover: William Andrew Publishing, 2006. 252 p. ISBN 0815515294.

22. BARNES, H.A. The yield stress - a review or 'παντα ρει' - everything flows? *J. Non-Newton. Fluid Mech.* 1999, vol. 81, no. 1-2, p. 133-178.

23. MA, H.R., WEN, W.J., TAM, W.Y., SHENG, P. Dielectric electrorheological fluids: theory and experiment. *Adv. Phys.* 2003, vol. 52, no. 4, p. 343-383.

24. KORDONSKI, W., GORODKIN, S., ZHURAVSKI, N. Static field stress in magnetorheological fluid. *Int. J. Mod. Phys. B*. 2001, vol. 15, no. 6-7, p. 1078-1084.

25. LAUN, H.M., GABRIEL, C., KIEBURG, C. Magnetorheological fluid in oscillatory shear and parameterization with regard to MR device properties. *J. Intell. Mater. Syst. Struct.* 2010, vol. 21, no. 15, p. 1479-1489.

26. HE, Y., CHENG, Q.L., PAVLINEK, V., LI, C.Z., SAHA, P. Synthesis and electrorheological characteristics of titanate nanotube suspensions under oscillatory shear. *J. Ind. Eng. Chem.* 2009, vol. 15, no. 4, p. 550-554.

27. SEDLACIK, M., PAVLINEK, V., SAHA, P., SVRCINOVA, P., FILIP, P. The role of particles annealing temperature on magnetorheological effect. *Mod. Phys. Lett. B*. 2012, vol. 26, no. 3, 1150013.

28. SEO, Y. A new yield stress scaling function for electrorheological fluids. *J. Non-Newton. Fluid Mech.* 2011, vol. 166, no. 3-4, p. 241-243.

29. HAO, T., KAWAI, A., IKAZAKI, F. Mechanism of the electrorheological effect: Evidence from the conductive, dielectric, and surface characteristics of water-free electrorheological fluids. *Langmuir*. 1998, vol. 14, no. 5, p. 1256-1262.

30. TAN, Z.H., ZHANG, Q.J., LIU, L.S., ZHAI, P.C. A new modified conductivity model for prediction of shear yield stress of electrorheological fluids based on face-center square structure. *J. Wuhan Univ. Technol.-Mat. Sci. Edit.* 2004, vol. 19, no. 4, p. 91-94.

31. DAVIS, L.C. Polarization forces and conductivity effects in electrorheological fluids. *J. Appl. Phys.* 1992, vol. 72, no. 4, p. 1334-1340.

32. GINDER, J.M., DAVIS, L.C., ELIE, L.D. Rheology of magnetorheological fluids: Models and measurements. *Int. J. Mod. Phys. B*. 1996, vol. 10, no. 23-24, p. 3293-3303.

33. BROŽ, J. *Moderní problémy ferromagnetismu*. 1st ed. Praha: Nakladatelství Československé akademie věd, 1962. 192 p. ISBN 1062-21-140-62.

34. GINDER, J.M., DAVIS, L.C. Shear stresses in magnetorheological fluids - Role of magnetic saturation. *Appl. Phys. Lett.* 1994, vol. 65, no. 26, p. 3410-3412.

35. FANG, F.F., CHOI, H.J., JHON, M.S. Magnetorheology of soft magnetic carbonyl iron suspension with single-walled carbon nanotube additive and its yield stress scaling function. *Colloid Surf. A-Physicochem. Eng. Asp.* 2009, vol. 351, no. 1-3, p. 46-51.

36. GINDER, J.M. Magnetorheological materials. *APS News*. 2004, vol. 13, no. 6, p. 5.

37. BOSSIS, G., LACIS, S., MEUNIER, A., VOLKOVA, O. Magnetorheological fluids. *J. Magn. Magn. Mater.* 2002, vol. 252, no. 1-3, p. 224-228.

38. HAO, T., KAWAI, A., IKAZAKI, F. Direct differentiation of the types of polarization responsible for the electrorheological effect by a dielectric method. *J. Colloid Interface Sci.* 2001, vol. 239, no. 1, p. 106-112.

39. XU, Y.Z., LIANG, R.F. Electrorheological properties of semiconducting polymer-based suspensions. *J. Rheol.* 1991, vol. 35, no. 7, p. 1355-1373.

40. DE VICENTE, J., SEGOVIA-GUTIERREZ, J.P., ANDABLO-REYES, E., VEREDA, F., HIDALGO-ALVAREZ, R. Dynamic rheology of sphere- and rod-based magnetorheological fluids. *J. Chem. Phys.* 2009, vol. 131, no. 19, p. 194902.

41. TRENDLER, A.M., BOSE, H. Influence of particle size on the rheological properties of magnetorheological suspensions. *Int. J. Mod. Phys. B*. 2005, vol. 19, no. 7-9, p. 1416-1422.

42. LOPEZ-LOPEZ, M.T., DE VICENTE, J., BOSSIS, G., GONZALEZ-CABALLERO, F., DURAN, J.D.G. Preparation of stable magnetorheological fluids based on extremely bimodal iron-magnetite suspensions. *J. Mater. Res.* 2005, vol. 20, no. 4, p. 874-881.

43. WEN, W.J., HUANG, X.X., YANG, S.H., LU, K.Q., SHENG, P. The giant electrorheological effect in suspensions of nanoparticles. *Nat. Mater.* 2003, vol. 2, no. 11, p. 727-730.

44. DE VICENTE, J., VEREDA, F., SEGOVIA-GUTIERREZ, J.P., MORALES, M.D., HIDALGO-ALVAREZ, R. Effect of particle shape in magnetorheology. *J. Rheol.* 2010, vol. 54, no. 6, p. 1337-1362.

45. BELL, R.C., KARLI, J.O., VAVRECK, A.N., ZIMMERMAN, D.T., NGATU, G.T., WERELEY, N.M. Magnetorheology of submicron diameter iron microwires dispersed in silicone oil. *Smart Mater. Struct.* 2008, vol. 17, no. 1, 015028.

46. ASHOUR, O., ROGERS, C.A., KORDONSKY, W. Magnetorheological fluids: Materials, characterization, and devices. *J. Intell. Mater. Syst. Struct.* 1996, vol. 7, no. 2, p. 123-130.

47. JOLLY, M.R., BENDER, J.W., CARLSON, J.D. Properties and applications of commercial magnetorheological fluids. *J. Intell. Mater. Syst. Struct.* 1999, vol. 10, no. 1, p. 5-13.

48. VEKAS, L. Ferrofluids and Magnetorheological Fluids. In VINCENZINI, P., DARRIGO, G. *Smart Materials & Micro/Nanosystems*. 1st ed. Stafa-Zurich: Trans Tech Publications Ltd, 2009, vol. 54, p. 127-136.

49. DE VICENTE, J., LOPEZ-LOPEZ, M.T., GONZALEZ-CABALLERO, F., DURAN, J.D.G. Rheological study of the stabilization of magnetizable colloidal suspensions by addition of silica nanoparticles. *J. Rheol.* 2003, vol. 47, no. 5, p. 1093-1109.

50. LOPEZ-LOPEZ, M.T., KUZHIR, P., BOSSIS, G., MINGALYOV, P. Preparation of well-dispersed magnetorheological fluids and effect of dispersion on their magnetorheological properties. *Rheol. Acta*. 2008, vol. 47, no. 7, p. 787-796.

51. HIETANEN, S. ER fluids and MR materials - Basic properties and some application developments. In VESSONEN, I. *Smart Materials and Structures - Vtt Research Programme 2000-2002*. Espoo: Technical Research Centre Finland, 2003, vol. 225, p. 33-50.

52. PARK, B.J., FANG, F.F., CHOI, H.J. Magnetorheology: Materials and application. *Soft Matter*. 2010, vol. 6, no. 21, p. 5246-5253.

53. RABINOW, J. The magnetic fluid clutch. *AIEE Trans.* 1948, vol. 67, no. 2, p. 1308-1315.

54. BOSSIS, G., KHUZIR, P., LACIS, S., VOLKOVA, O. Yield behavior of magnetorheological suspensions. *J. Magn. Magn. Mater.* 2003, vol. 258, p. 456-458.

55. FANG, F.F., CHOI, H.J., CHOI, W.S. Two-layer coating with polymer and carbon nanotube on magnetic carbonyl iron particle and its magnetorheology. *Colloid Polym. Sci.* 2010, vol. 288, no. 3, p. 359-363.

56. BOMBARD, A.J.F., ALCANTARA, M.R., KNOBEL, M., VOLPE, P.L.O. Experimental study of MR suspensions of carbonyl iron powders with different particle sizes. In LU, K.Q., SHEN, R., LIU, J.X. *Electrorheological fluids and magnetorheological suspensions*. Singapore: World Scientific Publ Co Pte Ltd, 2005, p. 349-355.

57. MARGIDA, A.J., WEISS, K.D., CARLSON, J.D. Magnetorheological materials based on iron alloy particles. *Int. J. Mod. Phys. B*. 1996, vol. 10, no. 23-24, p. 3335-3341.

58. VIOTA, J.L., DELGADO, A.V., ARIAS, J.L., DURAN, J.D.G. Study of the magnetorheological response of aqueous magnetite suspensions stabilized by acrylic acid polymers. *J. Colloid Interface Sci.* 2008, vol. 324, no. 1-2, p. 199-204.

59. VIOTA, J.L., DE VICENTE, J., DURAN, J.D.G., DELGADO, A. Stabilization of magnetorheological suspensions by polyacrylic acid polymers. *J. Colloid Interface Sci.* 2005, vol. 284, no. 2, p. 527-541.

60. LOPEZ-LOPEZ, M.T., ZUGALDIA, A., GONZALEZ-CABALLERO, F., DURAN, J.D.G. Sedimentation and redispersion phenomena in iron-based magnetorheological fluids. *J. Rheol.* 2006, vol. 50, no. 4, p. 543-560.

61. PARK, B.J., KIM, M.S., CHOI, H.J. Fabrication and magnetorheological property of core/shell structured magnetic composite particle encapsulated with cross-linked poly(methyl methacrylate). *Mater. Lett.* 2009, vol. 63, no. 24-25, p. 2178-2180.

62. BOMBARD, A.J.F., KNOBEL, M., ALCANTARA, M.R. Phosphate coating on the surface of carbonyl iron powder and its effect in magnetorheological suspensions. *Int. J. Mod. Phys. B*. 2007, vol. 21, no. 28-29, p. 4858-4867.

63. ABSHINOVA, M.A., KAZANTSEVA, N.E., SAHA, P., SAPURINA, I., KOVAROVA, J., STEJSKAL, J. The enhancement of the oxidation resistance of carbonyl iron by polyaniline coating and consequent changes in

electromagnetic properties. *Polym. Degrad. Stabil.* 2008, vol. 93, no. 10, p. 1826-1831.

64. RANKIN, P.J., GINDER, J.M., KLINGENBERG, D.J. Electro- and magneto-rheology. *Curr. Opin. Colloid Interface Sci.* 1998, vol. 3, no. 4, p. 373-381.
65. LOPEZ-LOPEZ, M.T., GOMEZ-RAMIREZ, A., IGLESIAS, G.R., DURAN, J.D.G., GONZALEZ-CABALLERO, F. Assessment of surfactant adsorption in oil-based magnetic colloids. *Adsorpt.-J. Int. Adsorpt. Soc.* 2010, vol. 16, no. 4-5, p. 215-221.
66. BARBER, D.E., CARLSON, J.D. Performance characteristics of prototype MR engine mounts containing glycol MR fluids. *J. Intell. Mater. Syst. Struct.* 2010, vol. 21, no. 15, p. 1509-1516.
67. BICA, D., VEKAS, L., AVDEEV, M.V., MARINICA, O., SOCOLIUC, V., BALASOIU, M., GARAMUS, V.M. Sterically stabilized water based magnetic fluids: Synthesis, structure and properties. *J. Magn. Magn. Mater.* 2007, vol. 311, no. 1, p. 17-21.
68. WINSLOW, W.M. 1947 *US Patent* 2,417,850.
69. CHEN, T.Y., LUCKHAM, P.F. A study of the electrical-current passing through water-activated electrorheological fluids. *J. Phys. D-Appl. Phys.* 1994, vol. 27, no. 7, p. 1556-1563.
70. KORDONSKY, V.I., KOROBKO, E.V., LAZAREVA, T.G. Electrorheological polymer-based suspensions. *J. Rheol.* 1991, vol. 35, no. 7, p. 1427-1439.
71. BOSSIS, G., ABBO, C., CUTILLAS, S., LACIS, S., METAYER, C. Electroactive and electrostructured elastomers. *Int. J. Mod. Phys. B*. 2001, vol. 15, no. 6-7, p. 564-573.
72. SHEN, R., WANG, X.Z., WEN, W.J., LU, K.Q. TiO2 based electrorheological fluid with high yield stress. In LU, K.Q., SHEN, R., LIU, J.X. *Electrorheological fluids and magnetorheological suspensions*. Singapore: World Scientific Publ Co Pte Ltd, 2005, p. 42-47.
73. YILMAZ, H., YILMAZ, U. Electrorheological properties of talc powder/silicone oil suspensions under DC fields. *Chin. J. Polym. Sci.* 2007, vol. 25, no. 3, p. 245-252.
74. TIAN, Y., MENG, Y.G., WEN, S.Z. Dynamic responses of zeolite-based ER fluid sheared between two concentric cylinders. *J. Intell. Mater. Syst. Struct.* 2004, vol. 15, no. 8, p. 621-626.
75. QIAO, Y.P., YIN, J.B., ZHAO, X.P. Oleophilicity and the strong electrorheological effect of surface-modified titanium oxide nano-particles. *Smart Mater. Struct.* 2007, vol. 16, no. 2, p. 332-339.

76. CHENG, Q.L., PAVLINEK, V., LENGALOVA, A., LI, C.Z., BELZA, T., SAHA, P. Electrorheological properties of new mesoporous material with conducting polypyrrole in mesoporous silica. *Microporous Mesoporous Mat.* 2006, vol. 94, no. 1-3, p. 193-199.

77. STENICKA, M., PAVLINEK, V., SAHA, P., BLINOVA, N.V., STEJSKAL, J., QUADRAT, O. The electrorheological efficiency of polyaniline particles with various conductivities suspended in silicone oil. *Colloid Polym. Sci.* 2009, vol. 287, no. 4, p. 403-412.

78. CHOI, H.J., JHON, M.S. Electrorheology of polymers and nanocomposites. *Soft Matter*. 2009, vol. 5, no. 8, p. 1562-1567.

79. FANG, F.F., LIU, Y.D., CHOI, H.J. Synthesis and electrorheological characteristics of polyaniline/organoclay nanoparticles via Pickering emulsion polymerization. *Smart Mater. Struct.* 2010, vol. 19, no. 12, p. 6.

80. HONG, J.Y., KWON, E., JANG, J. Fabrication of silica/polythiophene core/shell nanospheres and their electrorheological fluid application. *Soft Matter*. 2009, vol. 5, no. 5, p. 951-953.

81. CHENG, I.C., HWU, W.H., LEE, W.S., SUN, C.C. Theoretical studies on the inter-force enhancement of core-shell particles dispersed in an electrorheological fluid. *J. Chin. Inst. Chem. Eng.* 2005, vol. 36, no. 5, p. 475-485.

82. HAO, T. Electrorheological fluids. *Adv. Mater.* 2001, vol. 13, no. 24, p. 1847-1857.

83. HOSSEINISIANAKI, A., VARLEY, C.J., TAYLOR, P.M., LACEY, D., MALINS, C. Comparison of electrorheological fluids based on silicone oil and liquid-crystalline materials. *J. Mater. Chem.* 1995, vol. 5, no. 11, p. 1853-1856.

84. UNAL, H.I., AGIRBAS, O., YILMAZ, H. Electrorheological properties of poly(Li-2-hydroxyethyl methacrylate) suspensions. *Colloid Surf. A-Physicochem. Eng. Asp.* 2006, vol. 274, no. 1-3, p. 77-84.

85. KOROBKO, E.V., DREVAL, V.E., SHULMAN, Z.P., KULICHIKHIN, V.G. Peculiar features in the rheological behavior of electrorheological suspensions. *Rheol. Acta*. 1994, vol. 33, no. 2, p. 117-124.

86. CHOI, H.J., KIM, T.W., CHO, M.S., KIM, S.G., JHON, M.S. Electrorheological characterization of polyaniline dispersions. *Eur. Polym. J.* 1997, vol. 33, no. 5, p. 699-703.

ORIGINAL PAPERS

PAPER I

Smart Mater. Struct. **19** (2010) 115008 (6pp) doi:10.1088/0964-1726/19/11/115008

Rheological properties of magnetorheological suspensions based on core–shell structured polyaniline-coated carbonyl iron particles

M Sedlačík[1], V Pavlínek[1], P Sáha[1], P Švrčinová[2], P Filip[2] and J Stejskal[3]

[1] Polymer Centre, Faculty of Technology, Tomas Bata University in Zlín, 762 72 Zlín, Czech Republic
[2] Institute of Hydrodynamics, Academy of Sciences of the Czech Republic, 166 12 Prague 6, Czech Republic
[3] Institute of Macromolecular Chemistry, Academy of Sciences of the Czech Republic, 162 06 Prague 6, Czech Republic

E-mail: pavlinek@ft.utb.cz

Received 23 February 2010, in final form 22 July 2010
Published 23 September 2010
Online at stacks.iop.org/SMS/19/115008

Abstract
The sedimentation caused by the high density of suspended particles used in magnetorheological fluids is a significant obstacle for their wider application. In the present paper, core–shell structured carbonyl iron–polyaniline particles in silicone oil were used as a magnetorheological suspension with enhanced dispersion stability. Bare carbonyl iron particles were suspended in silicone oil to create model magnetorheological suspensions of different loading. For a magnetorheological suspension of polyaniline-coated particles the results show a decrease in the base viscosity. Moreover, the polyaniline coating has a negligible influence on the MR properties under an external magnetic field B. The change in the viscoelastic properties of magnetorheological suspensions in the small-strain oscillatory shear flow as a function of the strain amplitude, the frequency and the magnetic flux density was also investigated.

1. Introduction

Magnetorheological fluid (MRF) is a suspension consisting of solid micrometer-sized magnetically polarizable particles dispersed in a non-magnetic carrier liquid such as mineral oil, which reversibly transforms from a liquid to a solid-like structure under an applied magnetic field in milliseconds. The transformation between these two states is due to the formation of chain clusters in the direction of the exerted external field, which has a consequence in changes of the rheological properties, such as the increase of the apparent yield stress and the shear viscosity [1, 2]. The importance of MRFs has considerably increased in the last 15 years. This is caused by the continuous growth of concrete applications utilizing these smart materials in many areas like damping systems [3], clutches [4], drug targeting [5, 6], prosthetic knees [7], etc. Many recent studies have also focused on the heating of ferrofluid (nanometer-sized ferromagnetic particles suspended in a carrier fluid) to achieve hyperthermia (the heating of certain tissues to temperatures between 41 and 46 °C) in cancer therapy [8].

However, since the density of the magnetic particles used for the MRF is considerably higher than that of the liquid phase, sedimentation represents a significant problem in the development of MRFs suitable for practical applications. The driving force of the sedimentation is the gravity that dominates in comparison with the Brownian motion for particles larger than approximately 0.1 μm. Nevertheless, if smaller particles are used, the Brownian motion also hinders the formation of internal structures in the fluid in a magnetic field. Thus the optimum particle size is in the range of 0.1–10 μm and further improvement of MRFs stability is necessary. Several

studies have been done to alter the sedimentation, e.g., the addition of thixotropic additives [9], non-spherical particles [2] to the suspension, or the choice of water-in-oil emulsion as a continuous phase [10]. Nevertheless, the additions of stabilization particles may deteriorate the chain structure of MR particles in external fields. A very interesting possibility of how to suppress sedimentation consists in an application of core–shell structures, where a magnetic particle creates either the core [11–15] or the shell [16, 17]. The former case represents different types of coatings improving the chemical and oxidation stability [18]. To prevent eventual fragmentation in shearing, the latter case requires a good bonding of the shell to the non-magnetic core. Both variants result in a decrease of the density of the dispersed phase, which improves the sedimentation stability and may also promote the MR effect of this smart system. This effect is defined as a difference between apparent viscosities in the absence and presence of the applied magnetic field.

Suspensions of carbonyl iron coated with a conducting polymer and carbon nanotubes have been proposed as a new type of MRF [14]. In the present study, core–shell composite particles with a carbonyl iron (CI) magnetic core and polyaniline (PANI) conducting shell were prepared by using a PANI colloidal dispersion in chloroform [18]. The effects of the PANI coating on the viscosity and MR properties, including the viscoelastic properties of the MR fluid containing core–shell particles stabilized further by fumed silica dispersed in silicone oil, have been evaluated.

2. Experimental details

2.1. Materials

For a model particle-suspended system, carbonyl iron (EA grade, BASF, Germany) and PANI were selected as a core and shell, respectively. The main material characteristics of bare CI according to the product information (G-CAS/BS0106 CIP2) are: the spherical shape of the particles with an average size of about 3.5 μm, the content of α-iron $>97\%$, and the silicated surface. The other chemicals for the PANI coating were of reagent grade (purchased from Sigma-Aldrich, USA).

2.2. Coating of CI powder by PANI

A schematic diagram of the CI particles coated with PANI is provided in figure 1. Briefly, the polymerization of aniline with ammonium peroxydisulfate was performed at room temperature in a chloroform/water emulsion in the presence of a sodium bis-(2-ethylhexyl) sulfosuccinate surfactant. These reaction conditions led to the separation of the colloidal dispersion of the PANI into the chloroform phase [18, 19]. CI was subsequently suspended in the PANI colloid in chloroform, separated on a filter, and dried.

2.3. Characterization of particles and magnetorheological fluids

The surface characteristics of the core–shell particles with a CI core and PANI shell were observed with SEM (scanning electron microscope VEGA II LMU, Tescan, Czech Republic) operated at 10 kV. The magnetic properties of the microspheres were examined using a VSM (vibration sample magnetometer, EG&G PARC 704, Lake Shore, USA) at room temperature.

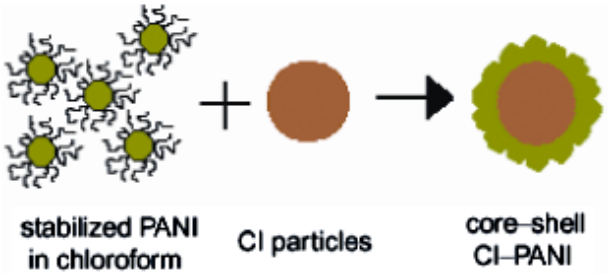

Figure 1. Schematic diagram of the synthesis of CI–PANI core–shell particles.

(This figure is in colour only in the electronic version)

MR fluid containing 60 and 80 wt% of bare CI and its PANI-coated analogue in silicone oil (Lukosiol M15, Chemical Works Kolin, Czech Republic; viscosity 14.5 mPa s, density 0.965 g cm^{-3}) were prepared. In both cases 0.5 wt% of nano-silica (average particle size $\sim$10 nm, Aerosil A 200, Degusa, Germany) was added. The suspensions were mechanically stirred before each measurement. The MR characteristics in steady shear and oscillatory regimes of the suspensions were examined using a Physica MCR501 rotational rheometer (Anton Paar GmbH, Austria) with a Physica MRD 180/1T magneto-cell at 25 and 40 °C. The true magnetic flux density was measured using a Hall probe and the temperature was checked with the help of an inserted thermocouple. Both the Hall probe and the thermocouple were rectangular, located in the bottom plate; for details see [20]. The temperature was set using an Anton Paar Viscotherm VT2 circulator with a temperature stability $\pm$0.02 °C. The maximum magnetic flux density used in all the measurements did not exceed 0.3 T, to ensure the sufficient homogeneity of the magnetic field perpendicular to the shear flow direction. A parallel-plate measuring system with a diameter of 20 mm and gap of 1 mm was used.

3. Results and discussion

3.1. Microstructure of particles

Figure 2 shows the size and surface morphology of both bare CI (a) and carbonyl iron–polyaniline (CI–PANI) core–shell particles (b) observed by SEM. The average size of the particles was slightly larger than that of the bare CI particles as a result of the coating layer not exceeding 0.5 μm. Moreover, the encapsulated particles with a smoother surface kept their spherical shape, which confirms the uniform and complete coating.

3.2. Magnetic properties of particles

The magnetization curve measurements of the bare CI powder and its PANI-coated analogue are depicted in figure 3. The

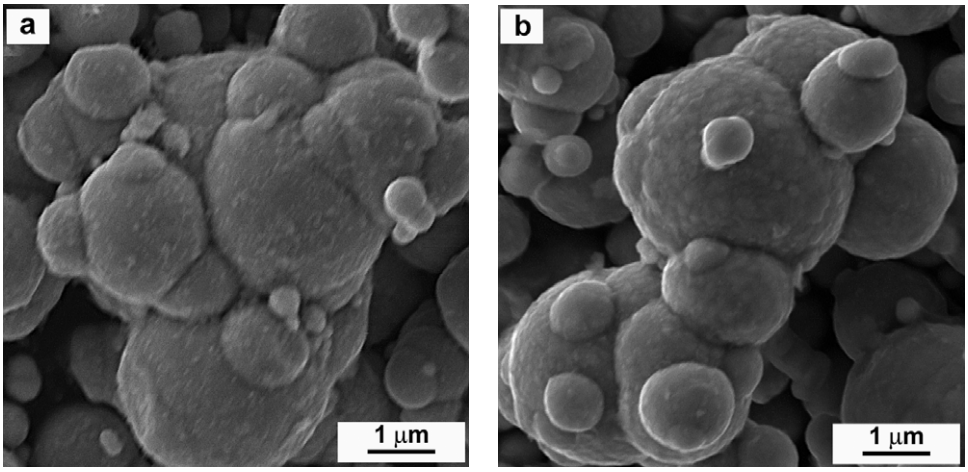

Figure 2. SEM images of (a) bare CI and (b) CI–PANI particles.

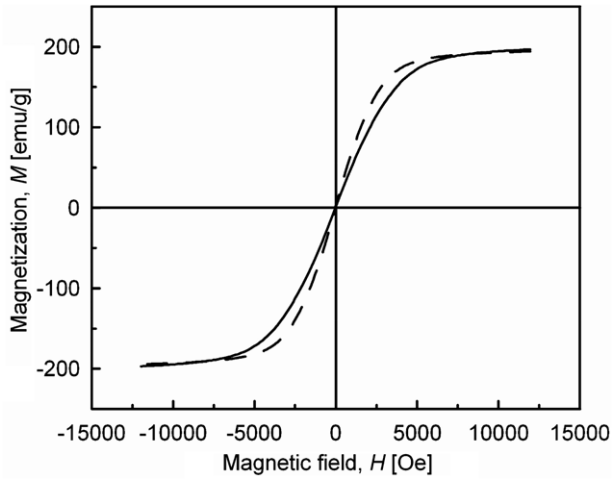

Figure 3. VSM image of bare CI (dashed line) and CI–PANI (solid line) particles.

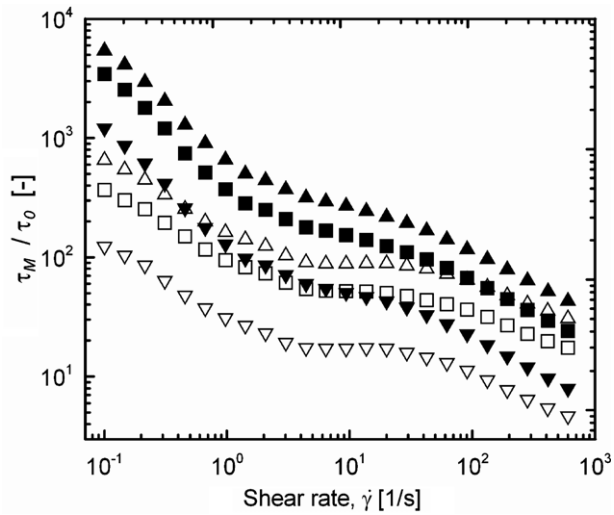

Figure 4. Ratio of shear stresses with/without a magnetic field (τ_M/τ_0) versus shear rate, $\dot{\gamma}$, for CI–PANI particles' (solid) and CI particles' (open) MR suspensions (80 wt%) in silicone oil in various magnetic fields applied at 25 °C. The symbols for the magnetic flux densities (mT): ▽ 99; □ 205; and △ 308.

saturation magnetization for the PANI-coated CI particles is comparable with uncoated CI. Hence, there is no significant influence of the polymeric coating on the magnetic properties, and an MR suspension based on CI–PANI core–shell particles exhibits similar MR performance as in the case of bare CI. Moreover, CI–PANI particles possess almost zero coercive force, which is the requested factor in cyclic applications for the maintenance of isothermal conditions in the system.

3.3. Steady shear and yield stress

The rheological behavior of MR fluids based on CI and CI–PANI particles was investigated in the controlled shear-rate mode. In all measurements the range of the shear rate tested was from 0.1 to 600 s^{-1} in a log scale with 6 pts/decade. The resulting flow responses were examined as a function of the magnetic flux density ranging from 0 to 0.3 T. During each run under a magnetic field, the MR fluid was first sheared ($\dot{\gamma} = 100\ s^{-1}$) at a zero field for 60 s to distribute the particles uniformly and after the measurement the system was completely demagnetized. Figure 4 shows the proportional changes of the MR effect expressed as a ratio of the shear stresses with/without a magnetic field for MR suspensions based on CI–PANI particles (solid symbols) and CI particles (open symbols). A noticeable increase in the shear stress with magnetic flux density is a typical feature of MR fluids and is caused by the formation of a robust chain structure [1]. Such a strong dependence on the external field is similar to the phenomenon observed for ER fluids [21]. The systems in figure 4 can be characterized by a Bingham plastic model with a yield stress, meaning that the suspension acts as a solid-like material when exposed to an external shear stress below this yield stress. In other words, the structure formed in the MR fluid by the magnetic field is sufficiently rigid to withstand certain deforming stresses without any external manifestation of flowing. In comparison with the literature [14], the smoother

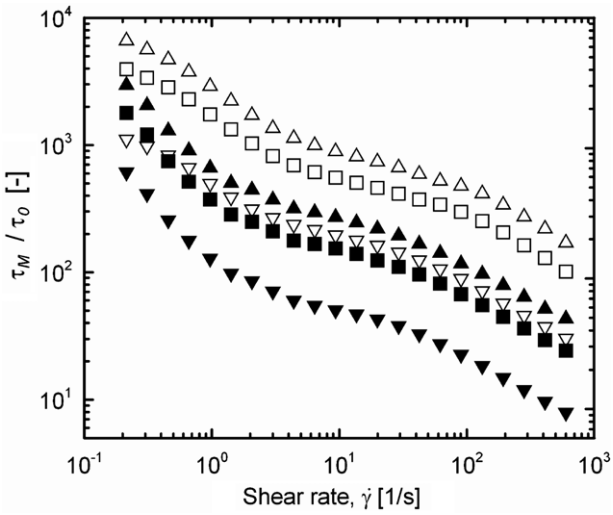

Figure 5. Ratio of the shear stresses with/without a magnetic field (τ_M/τ_0) versus shear rate, $\dot{\gamma}$, for core–shell particles based the MR suspensions in the various magnetic fields applied at 25 °C (solid) and 40 °C (open). The symbols for the magnetic flux densities (mT): ▼ 97; ■ 196; ▲ 297.

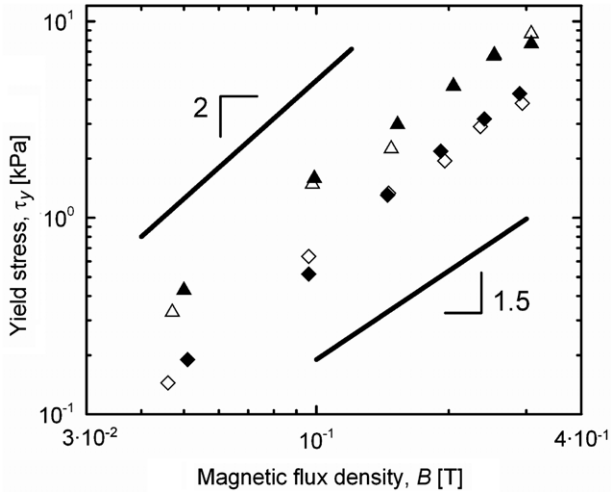

Figure 6. Dependence of the dynamic yield stress, τ_y, on the applied magnetic flux density, B, for 60 wt% (diamonds) and 80 wt% (triangles) concentrations of CI–PANI particles (solid symbols) or CI particles (open symbols) in silicone oil.

particles (CI–PANI) with nano-silica added used in this work seem to provide a reduction of the off-state viscosity and improve the sedimentation stability.

As can be seen in figure 4, the proportional change of the MR effect is higher in the case of the core–shell particles, which is due to lower zero field shear stress and viscosity of the MR suspension and confirms the fact that PANI coating reduces the density of suspended particles.

Furthermore, the MR effect defined as a difference between the flow curves in zero and applied magnetic fields can be increased by elevating the temperature. Figure 5 shows the proportional changes of the MR effect expressed as the ratio of shear stresses with/without a magnetic field for MR fluids with CI–PANI particles measured at 25 and 40 °C. It is worth noting that, in the absence of a magnetic field the system exhibits more Newtonian behavior at elevated temperatures due to stronger thermodynamic forces. However, the magnetic forces start to dominate over the thermodynamic ones in an applied magnetic field and the flow curves are very similar at both temperatures. Thus, the MR effect is higher at higher temperature.

In figure 6, the dynamic yield stresses of two different concentrations of MR suspensions based on CI and CI–PANI particles are shown as a function of the applied magnetic flux density B. The yield stresses in all cases increase with the external magnetic field following the dependence of the magnetic flux density in the range $B^{1.5-2}$. This value slightly deviates from the numerical and analytical models, according to which the dependence of the magnetic flux density is a consequence of the local saturation of the magnetization in the polar or contact zones of each particle [22, 23]. However, none of the curves in figure 6 show saturation of the system and all curves have the linear trend without any apparent yield stress plateau in the whole range of the applied magnetic flux densities. This is probably due to the presence of nano-silica in all MR suspensions. These sub-sized particles can fill the free space in the tetragonal column structure of magnetic particles, which might help the formation of more robust chain agglomerates resistant to the higher external stresses, which leads to higher yield stresses even above the saturation of magnetic particles [24].

3.4. Viscoelastic properties

As shown above, MR fluids exhibit Bingham plastic behavior with a yield stress and a system with such properties can be described as a viscoelastic material in the range of a small strain of oscillatory flow. In other words, oscillation experiments give information about the elastic (storage modulus, G') and viscous (loss modulus, G'') behavior of MR fluids. Figure 7(a) depicts the dependence of G' and G'' on the strain amplitude (γ) in oscillatory flow for 80 wt% CI–PANI suspension at 25 °C. The chain structure development with increasing magnetic flux density can be observed from the storage modulus increase and the loss modulus decrease. This trend indicates the solid-like character of MR fluids under these conditions. In a very small-strain amplitude, the viscoelastic modulus, especially its elastic part, is independent of the applied strain; this range is called the linear viscoelastic region (LVR). In the LVR, the structure of the MR fluid is basically undisturbed. However, with increasing strain amplitude, the chain structure starts to break and the system shows nonlinearity and deviations from the viscoelastic behavior. At higher values of strain (which were not measured in our experiment) the elastic and viscous moduli intersect each other ($G' = G''$), the chain structure of the MR fluid breaks rapidly and the system starts to flow.

For practical applications it is important to know the values of G' and G'' in LVR and their strain frequency dependence. Figure 7(b) shows G' and G'' as functions of the strain frequency for an 80 wt% CI–PANI suspension at 25 °C in LVR under a very small strain ($\gamma = 0.002\%$). The storage modulus of such an MR fluid slightly increases with increasing

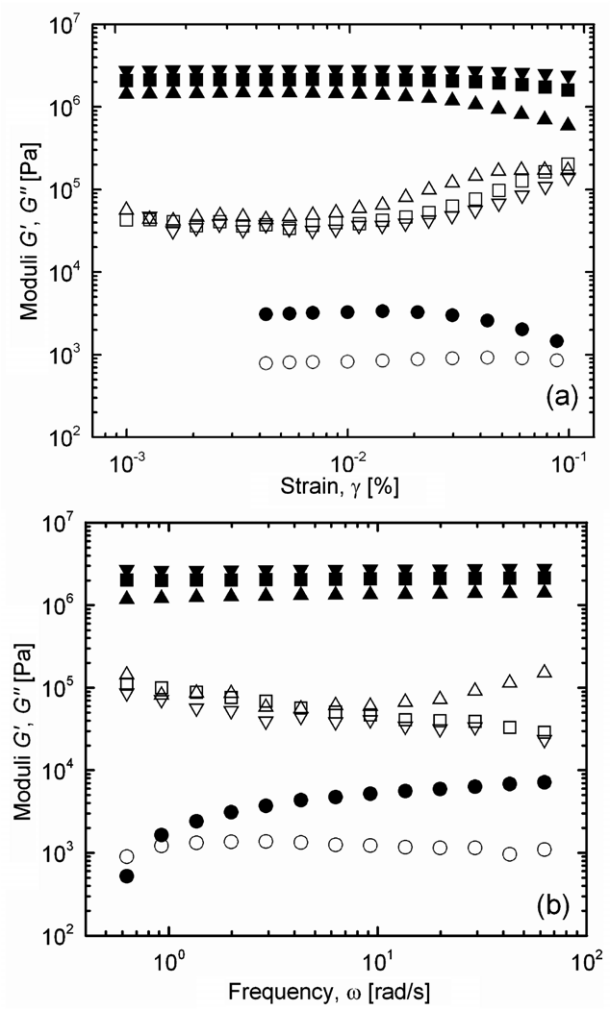

Figure 7. (a) Storage, G', (solid) and loss, G'', (open) moduli as a function of the strain amplitude and (b) storage, G', (solid) and loss, G'', (open) moduli as a function of the strain frequency in the various magnetic fields applied for an 80 wt% CI–PANI suspension in silicone oil at 25 °C. The symbols for magnetic flux densities (mT): ● 0; ▲ 96; ■ 200; and ▼ 307.

magnetic flux density. This is again evidence of the formation of higher magnetized structures. Moreover, the storage elastic modulus is constant over the wide range of driving frequencies. This trend confirms the fact that the thickness of the PANI coating layer used does not influence the magnetic properties of CI.

3.5. Sedimentation test

Finally, the effect of PANI coating on the sedimentation stability was investigated. MR fluids with the same weight fraction (60 wt%) but different dispersed particles were set in static conditions and the sedimentation ratios were measured until they approached asymptotic values. Figure 8 shows the sedimentation ratio as a function of time for bare CI and PANI-coated CI in suspensions with or without further stabilization by fumed silica. It is obvious that the CI–PANI suspension exhibits a higher sedimentation stability than that of bare the CI based one, in the same time period in a silica stabilized and also a non-stabilized MR suspension. Within the initial 10 hrs the uncoated particles settled much faster than the coated CI. Therefore, the coating of magnetic particles with polymers, such as PANI, can improve the sedimentation stability due to the reduction in the overall density. It is worth noting that the sedimentation stability can be further improved using higher concentrations of thixotropic additives such as nano-silica (0.5 wt% in our case). However, in both cases the positive role of PANI coating is apparent.

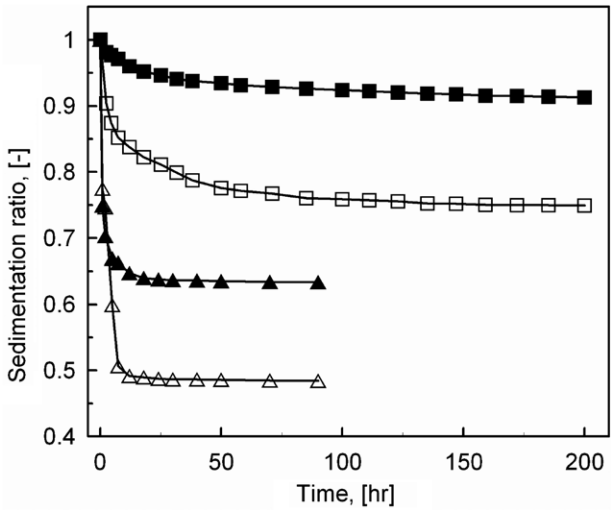

Figure 8. Sedimentation ratio of MR fluids (60 wt%) based on bare CI (□) or CI–PANI (■) particles with 0.5 wt% and bare CI (△) or CI–PANI (▲) particles without silica added.

4. Conclusions

Core–shell CI–PANI particles can be used as a dispersed phase in a novel MR fluid. Particles with the coating exhibit magnetic properties comparable to bare CI. Based on visual observation, the PANI coating contributes to reduced sedimentation, and thus to improved suspension stability. In addition, it lowers the interaction between the carrier fluid and the particles resulting in a decrease of the fluidity of the system in the absence of a magnetic field. Therefore the relative change in the magnetorheological effect is significantly higher. The temperature plays also a very important role in MRF activity, and the efficiency increases at elevated temperatures. The viscoelastic properties of the fluids suggest that the CI–PANI suspension exhibits strong elastic behavior within the linear viscoelastic region due to the robust chain structure under an applied magnetic field.

Acknowledgments

The authors thank the Ministry of Education, Youth, and Sports of the Czech Republic (MSM7088352101) and the Grant Agency of the Czech Republic (202/09/1626) for financial support.

References

[1] Bossis G, Volkova O, Lacis S and Meunier A 2002 Magnetorheology: fluids, structures and rheology *Lect. Notes Phys.* **594** 202–30

[2] Chin B D, Park J H, Kwon M H and Park O O 2001 Rheological properties and dispersion stability of magnetorheological (MR) suspensions *Rheol. Acta* **40** 211–9

[3] Yang G, Spencer B F Jr, Carlson J D and Sain M K 2002 Large-scale MR fluid dampers: modeling and dynamic performance considerations *Eng. Struct.* **24** 309–23

[4] Wang J and Meng G 2001 Magnetorheological fluid devices: principles, characteristics and applications in mechanical engineering *Proc. Inst. Mech. Eng.* L **215** 165–74

[5] Aviles M O, Ebner A D and Ritter J A 2007 Ferromagnetic seeding for the magnetic targeting of drugs and radiation in capillary beds *J. Magn. Magn. Mater.* **310** 131–44

[6] Arias J L, Linares-Molinero F, Gallardo V and Delgado A V 2007 Study of carbonyl iron/poly(butylcyanoacrylate) (core/shell) particles as anticancer drug delivery systems-loading and release properties *Eur. J. Pharm. Sci.* **33** 252–61

[7] Herr H and Wilkenfeld A 2003 User-adaptive control of a magnetorheological prosthetic knee *Indust. Robot.* **30** 42–55

[8] Jordan A, Scholz R, Wust P, Fahling H and Felix R 1999 Magnetic fluid hyperthermia (MFH): cancer treatment with AC magnetic field induced excitation of biocompatible superparamagnetic nanoparticles *J. Magn. Magn. Mater.* **201** 413–9

[9] de Vicente J, Lopez-Lopez M, Gonzales-Caballero F and Duran J D G 2003 Rheological study of the stabilization of magnetizable colloidal suspensions by addition of silica nanoparticles *J. Rheol.* **47** 1093–109

[10] Park J H, Chin B D and Park O O 2001 Rheological properties and stabilization of magnetorheological fluids in a water-in-oil emulsion *J. Colloid Interface Sci.* **240** 349–54

[11] You J L, Park B J, Choi H J, Choi S B and Jhon M S 2007 Preparation and magnetorheological characterization of CI/PVB core/shell particle suspended MR fluids *Int. J. Mod. Phys.* B **21** 4996–5002

[12] Ko S V, Lim J Y, Park B J, Yang M S and Choi H J 2009 Magnetorheological carbonyl iron particles doubly wrapped with polymer and carbon nanotube *J. Appl. Phys.* **105** 07E703

[13] Choi H J, Park B J, Cho M S and You J L 2007 Core–shell structured poly(methyl methacrylate) coated carbonyl iron particles and their magnetorheological characteristics *J. Magn. Magn. Mater.* **310** 2835–7

[14] Fang F F, Choi H J and Choi W S 2010 Two-layer coating with polymer and carbon nanotube on magnetic carbonyl iron particle and its magnetorheology *Colloid Polym. Sci.* **288** 359–63

[15] Fang F F, Choi H J and Seo Y 2010 Sequential coating of magnetic carbonyl iron particles with polystyrene and multiwalled carbon nanotubes and its effect on their magnetorheology *ACS Appl. Mater. Interfaces* **2** 54–60

[16] Pu H, Jiang F and Yang Z 2006 Preparation and properties of soft magnetic particles based on Fe_3O_4 and hollow polystyrene microsphere composite *Mater. Chem. Phys.* **100** 10–4

[17] Fang F F, Kim J H and Choi H J 2009 Synthesis of core–shell structured PS/Fe_3O_4 microbeads and their magnetorheology *Polymer* **50** 2290–3

[18] Abshinova M A, Kazantseva N E, Saha P, Sapurina I, Kovarova J and Stejskal J 2008 The enhancement of the oxidation resistance of carbonyl iron by polyaniline coating and consequent changes in electromagnetic properties *Polym. Degrad. Stab.* **93** 1826–31

[19] Sapurina I Y and Stejskal J 2006 The way of preparation of colloidally stable dispersion of a conducting polymer *Russian Patent Appl* 2,006,129,428

[20] Laun H M and Gabriel C 2007 Measurement modes of the response time of a magneto-rheological fluid (MRF) for changing magnetic flux density *Rheol. Acta* **46** 665–76

[21] Stenicka M, Pavlinek V, Saha P, Blinova N V, Stejskal J and Quadrat O 2009 The electrorheological efficiency of polyaniline particles with various conductivities suspended in silicone oil *Colloids Polym. Sci.* **287** 403–12

[22] Ginder J M, Davis L C and Elie L D 1996 Rheology of magnetorheological fluids: Models and measurements *Int. J. Mod. Phys.* B **10** 3293–303

[23] Fang F F, Choi H J and Jhon M S 2009 Magnetorheology of soft magnetic carbonyl iron suspension with single-walled carbon nanotube additive and its yield stress scaling function *Colloid Surf.* A **351** 46–51

[24] Lim S T, Cho M S, Jang I B and Choi H J 2004 Magnetorheological characterization of carbonyl iron based suspension stabilized by fumed silica *J. Magn. Magn. Mater.* **282** 170–3

PAPER II

Colloids and Surfaces A: Physicochem. Eng. Aspects 387 (2011) 99–103

Contents lists available at ScienceDirect

Colloids and Surfaces A: Physicochemical and Engineering Aspects

journal homepage: www.elsevier.com/locate/colsurfa

Plasma-treated carbonyl iron particles as a dispersed phase in magnetorheological fluids

Michal Sedlacik[a,b], Vladimir Pavlinek[a,b,*], Marian Lehocky[a], Ales Mracek[a,c], Ondrej Grulich[c], Petra Svrcinova[d], Petr Filip[d], Alenka Vesel[e]

[a] Centre of Polymer Systems, University Institute, Tomas Bata University in Zlin, Nad Ovcirnou 3685, 760 01 Zlin, Czech Republic
[b] Polymer Centre, Faculty of Technology, Tomas Bata University in Zlin, namesti T. G. Masaryka 275, 762 72 Zlin, Czech Republic
[c] Department of Physics and Materials Engineering, Faculty of Technology, Tomas Bata University in Zlin, namesti T. G. Masaryka 275, 762 72 Zlin, Czech Republic
[d] Institute of Hydrodynamics, Academy of Sciences of the Czech Republic, Pod Patankou 30/5, 160 00 Prague 6, Czech Republic
[e] Department for Surface Engineering and Optoelectronics, Jozef Stefan Institute, Jamova cesta 39, 1000 Ljubljana, Slovenia

ARTICLE INFO

Article history:
Received 8 June 2011
Received in revised form 21 July 2011
Accepted 23 July 2011
Available online 30 July 2011

Keywords:
Carbonyl iron
Magnetorheological fluid
Plasma
Viscoelasticity

ABSTRACT

The aim of this paper is to document suitability of plasma-treated carbonyl iron particles as a dispersed phase in magnetorheological fluids. Surface-modified carbonyl iron particles were prepared via their exposure to 50% argon and 50% octafluorocyclobutane plasma. The X-ray photoelectron spectroscopy was used for analysis of chemical bonding states in the surface layer. Plasma-treated particles were adopted for a dispersed phase in magnetorheological (MR) fluids, and the MR behaviour was investigated using rotational rheometer equipped with magnetic field generator. Viscoelasticity changes of MR fluids were measured in the small-strain oscillatory shear flow as a function of the strain amplitude, frequency and the magnetic flux density. The MR fluids based on plasma-treated particles exhibit promoted suspension stability, which is attributed to the interactions between fluorine bonded on particle surface and methyl groups of silicone oil.

1. Introduction

The possibility to control the flow and deformation of magnetorheological (MR) fluids by application of a magnetic field classified these systems into smart and intelligent materials. MR fluids are suspensions of non-colloidal (~1–10 μm), multi-domain ferromagnetic, ferrimagnetic particles dispersed in a non-magnetic carrier fluid [1–3]. The suspensions exhibit nearly Newtonian behaviour with values of apparent viscosity ranging from 0.1 to 1 Pa s at low shear rates in the absence of external magnetic field. However, when the field is applied, the particles become magnetized and the chain-like structures are formed within the fluid due to the dipolar magnetic interactions. The formation of internal structure leads to an abrupt transformation within milliseconds from liquid to solid-like state, which is caused by drastic changes of rheological properties of the suspension such as an enhancement of apparent viscosity, yield stress or viscoelastic moduli [4–6]. The particles can return to an unorganized state, and the apparent viscosity is reduced to the original value, when the magnetic field is removed. Analogous variant to MR fluids are electrorheological fluids, in which the chain-like structure is created under external electric field [7]. The ability of MR fluids to change the apparent viscosity depending on the intensity of external magnetic field can be used in torque transducers [8,9], active controllable dampers [10,11] as well as in cancer therapy [12,13], etc.

However, the poor stability of MR fluids due to sedimentation still hinders their larger utilization by reason that non-uniform particle distribution can interfere with MR response. The excessive gravitational settling is caused by the density mismatch between magnetic particles (e.g., bare carbonyl iron = 7.86 g cm^{-3}) and carrier liquid (e.g., silicone oil = 0.97 g cm^{-3}). To overcome this crucial problem, different methods such as the use of viscoplastic media [14], adding special type of additives (carbon nanotube) [15], core–shell structured particles [16,17], the use of aqueous suspensions stabilized by acrylic acid polymers [18], adding surfactants (oleic acid) [19], the use of bidisperse MR fluids [20] or choice of water-in-oil emulsion as a continuous phase [21] have been proposed. Nevertheless, further improvement of the stability of MR fluids is necessary.

Recently, there is growing interest in using low-temperature plasma to modify the surface of variety of materials [22,23]. It is a powerful technique, since the surface properties of materials can be changed without affecting of their bulk properties [24]. The Teflon-like surface thin film is prepared in plasma discharge using

* Corresponding author at: Polymer Centre, Faculty of Technology, Tomas Bata University in Zlin, namesti T. G. Masaryka 275, 762 72 Zlin, Czech Republic.
Tel.: +420 576 031 205; fax: +420 576 031 444.
E-mail address: pavlinek@ft.utb.cz (V. Pavlinek).

0927-7757/$ – see front matter © 2011 Elsevier B.V. All rights reserved.
doi:10.1016/j.colsurfa.2011.07.035

octafluorocyclobutane (C_4F_8) as a carrier gas with an admixture of argon [25,26].

In the present study, plasma-treated particles of carbonyl iron (CI) were obtained after exposition of bare magnetic particles in 50% argon +50% octafluorocyclobutane processing gas for different times of exposure. Effects of the surface modification on viscosity, viscoelastic properties of MR fluid containing plasma-treated particles and long-term stability were evaluated.

2. Materials and methods

2.1. Materials

Carbonyl iron particles (HQ and SL grades, BASF, Germany) were selected as magnetic agents. The main material characteristics of HQ and SL grades of bare CI are following: spherical shape of particles with the average size of about 1 μm and 9 μm, non-modified surface, and content of α-iron >97% and >99.5%, respectively. As components of processing gas, argon (Ar purity ≥99.998, Messer Industriegase GmbH, Germany) and octafluorocyclobutane (C_4F_8 purity ≥99.998, Linde AG, Germany) were used.

2.2. Plasma treatment of particles

The surface modification of CI particles was performed using a plasma reactor Diener Femto (Diener Electronic, USA) operating at frequency 40 kHz. The samples were inserted into the rotating rectangular parallelepiped glass reaction chamber, which was placed inside the plasma reactor. Such configuration enables the uniform modification of powdered samples. CI powders were exposed to 50% Ar and 50% C_4F_8 plasmas sustained at power of 50 W at processing gas pressures of approx. 30–40 Pa with the processing gas flow rate of 90 sccm. After certain time, the plasma was quenched and samples were kept under the atmosphere of processing gas for next 5 min. Three types of samples (B, C and D) were obtained in this way varying in the time of modification and CI grade (Table 1).

2.3. Characterization of particles surface composition

Surface characteristics of non-treated and plasma treated CI particles were observed with XPS (X-ray photoelectron spectroscopy, TFA XPS, Physical Electronics, USA). The base pressure in the chamber was about 6×10^{-8} Pa. The samples were excited with X-rays over a 400-μm spot area with a monochromatic Al $K\alpha_{1,2}$ radiation at 1486.6 eV. Photoelectrons were detected with a hemispherical analyzer positioned at the angle of 45° with respect to the sample surface. Survey-scan spectra were made at pass energy of 187.85 eV and an energy step was 0.4 eV. The concentrations of elements were determined by using MultiPak v7.3.1 software from Physical Electronics, which was supplied with the spectrometer [27].

2.4. Characterization of magnetorheological fluids

MR fluids containing 80 wt.% of bare CI (HQ or SL grade) or their plasma-treated analogues in silicone oil (Lukosiol M200, Chemical Works Kolín, Czech Republic; viscosity of 200 mPa s, density of 0.965 g cm^{-3}) were prepared. Suspensions were mechanically stirred before each measurement. MR characteristics of the suspensions in steady and oscillatory shear were examined using a rotational rheometer Physica MCR501 (Anton Paar GmbH, Austria) with the Physica MRD 180/1T magneto-cell at 25 °C. True magnetic flux density was measured using a Hall probe and temperature was checked with the help of an inserted thermocouple, for details see Ref. [28]. Temperature was set using an Anton Paar circulator Viscotherm VT2 with temperature stability ±0.02 °C. Maximum magnetic flux density used in all measurements did not exceed 0.3 T to ensure sufficient homogeneity of a magnetic field perpendicular to the shear flow direction. A parallel-plate measuring system with diameter of 20 mm and gap of 1 mm was used.

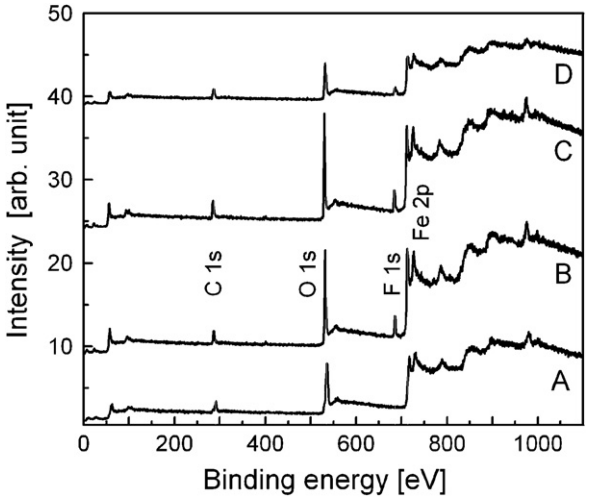

Fig. 1. XPS spectra for CI samples without and with exposure to Ar + C_4F_8 plasma.

2.5. Stability test

Stability of the various types of CI particles based MR suspensions was examined by a sedimentation ratio test, which is a simple naked-eye observation of sedimentation. In this method, a set of the samples were placed in test tubes and observed for 24 h. The settling of the macroscopic phase boundary between the concentration suspension and the relatively clear oil-rich phase was measured as a function of time. Then, the sedimentation ratio is defined as the height of particle-rich phase relative to the total suspension height.

3. Results and discussion

3.1. Surface composition

Chemical bonding states of the nano-surface layer of CI powders exposed to plasma were observed via X-ray photoelectron spectroscopy. Fig. 1 shows XPS spectra for bare and plasma-treated CI samples composed of four main components: C 1s peak at binding energy of 284.6 eV, O 1s peak at 531.6 eV, F 1s peak at 684.9 eV, and Fe 2s peak at 706.8 eV [27]. Here it should be noted that the other peaks are from signals of non-valent Auger electrons.

The results listed in Table 1 show that the amount of O 1s, which was presented on the CI surface may be due to oxidation of carbon and iron in the air, decreased due to Ar + C_4F_8 plasma. Furthermore, based on these data it was also suggested that the reduced O 1s was efficiently substituted by bonded F 1s. A certain amount of N 1s present in the particles surface layer after plasma treatment can be attributed to the post-plasmatic reaction ongoing in the air. Fig. 2 shows the atomic ratios of F/Fe on the surface of CI without and with exposure to Ar + C_4F_8 plasma. As can be seen, the ratio increases both with treatment time and with the particle size. The larger amount of bonded fluorine on larger particles can result from a fact that smaller particles had strong interface attractive forces and formed agglomerates, which implicated smaller surface area than larger ones. Above mentioned features indicate that the plasma treatment of CI particles can change their surface properties having a positive effect on their practical use.

Table 1
Parameters of samples and their surface composition from XPS.

Sample	Particle size [μm]	Treatment time [s]	C 1s [%]	O 1s [%]	N 1s [%]	F 1s [%]	Fe 2s [%]
A	1	0	22.2	50.1	0	0	27.7
B	1	120	15.5	45.0	2.2	6.5	30.8
C	1	300	27.9	40.7	1.6	6.4	23.4
D	9	120	25.9	41.3	0	7.4	25.4

3.2. Steady shear and yield stress

Rheological behaviour of MR suspensions based on non-treated and plasma-treated CI particles was investigated in a controlled shear-rate mode in static magnetic field ranging from 0 to 0.3 T. The measurements under given conditions were repeated twice and an average value was used for further evaluation. During each run under a magnetic field, the MR suspension was first sheared ($\dot{\gamma} = 100\,s^{-1}$) at zero magnetic field for 60 s to distribute the particles uniformly and after the measurement the system was completely demagnetized to disturb residual internal structures. Fig. 3 displays shear stress as a function of shear rate for samples A and B based MR fluids under different external magnetic flux densities.

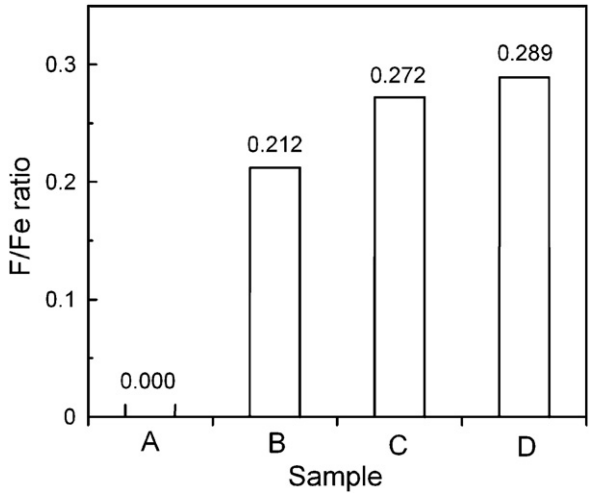

Fig. 2. Atomic ratio of F/Fe for CI samples without and with exposure to $Ar + C_4F_8$ plasma.

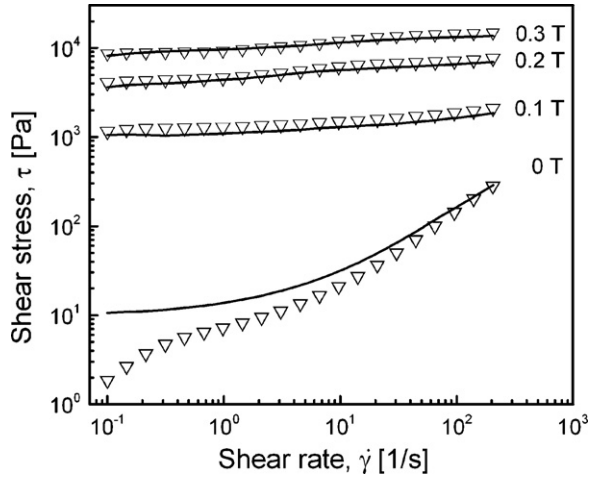

Fig. 3. Rheogram of 80 wt.% MR fluids based on samples A (open triangles) and B (lines) under various magnetic fields applied.

In the absence of magnetic field, the MR suspension containing non-treated particles exhibits nearly Newtonian behaviour, while suspensions with plasma-treated particles provide a certain value of yield stress, which can be generated due to interaction forces between fluorine bonded on CI particles and methyl groups of silicone oil. In the presence of magnetic field, both systems exhibit Bingham plastic behaviour showing that the magnetic particles were aligned into the chain-like structure sufficiently rigid to withstand certain deforming stresses without any external manifestation of flow. Typically for MR fluids, the shear stress of samples A and B based MR fluids increased for the entire shear rate region with the increase of magnetic flux density [29]. When magnetic field is applied, the magnetic forces between polarized particles strongly dominate over the interaction ones between plasma-treated particles and silicone oil, thus both MR suspensions have approximately the same values of shear stress irrespective of employed particles.

From the courses of shear stress–shear rate curves, dynamic yield stresses can be obtained by fitting the experimental data with the Cho–Choi–Jhon model [30]:

$$\tau = \frac{\tau_0}{1 + (t_2\dot{\gamma})^{\alpha}} + \eta_{\infty}\left(1 + \frac{1}{(t_3\dot{\gamma})^{\beta}}\right)\dot{\gamma} \quad (1)$$

Here, τ_0 is the dynamic yield stress, α is related to the decrease in the stress, t_2 and t_3 represent time constants, β is the exponent in the range $0 < \beta \leq 1$, and η_{∞} is the viscosity at high shear rates and is interpreted as the viscosity in the absence of a magnetic field [30].

Table 2 shows the yield stresses and optimal parameters for the Cho–Choi–Jhon model for MR suspensions based on CI particles (samples A–D) at the magnetic flux density of 0.3 T. Evidently from Table 2, suspension with CI particles of sample B exhibits almost the same value of τ_0 as non-treated particles (sample A) based MR suspension in the magnetic field of 0.3 T. Further, increase in time of plasma treatment (sample C) led to lower τ_0 and this can be explained by the lower iron content in the surface layer at the expense of higher carbon content. Thus, 120 s exposure appears as an optimal treatment time of CI particles from the magnetorheological point of view. It was also found from the results in Table 2, that larger CI particles (i.e. sample D) based MR suspension possesses almost twice-higher value of τ_0 due to larger magnetic domains.

3.3. Viscoelastic properties

Oscillatory shear tests represent an effective way to study the dynamic characteristics of microstructures formed in MR suspensions. Fig. 4 presents the storage modulus, G' (elastic behaviour) and loss modulus, G'' (viscous behaviour) versus strain for sample B suspension under various magnetic flux densities. Both G' and G'' increase rapidly from their original values upon the application of a magnetic field over the whole strain range ($\gamma = 10^{-5}$–10^{-2} in our case). Moreover, G' comes to be significantly higher than G'' in the linear viscoelastic region (LVR), i.e. in the range of independency of G' and G'' on strain amplitude, and the difference between these moduli grows also with magnetic flux density. This dramatic change in rheological properties originates from the mag-

Table 2
Parameters of the Cho–Choi–Jhon model obtained by linear regression for various treated CI particles-based MR fluids at the magnetic flux density of 0.3 T.

Parameters	A	B	C	D
τ_0 [Pa]	8 863	8 796	7 485	16 182
t_2 [s]	0.0011	0.0011	0.2150	0.7013
α [−]	0.0006	0.0006	0.1191	0.5641
η_∞ [Pa s]	1.1992	1.1992	1.1967	1.1992
t_3 [s]	7.8×10^{-5}	7.8×10^{-5}	7.4×10^{-5}	2.2×10^{-5}
β [−]	0.8820	0.8850	0.8433	0.7991

netic dipole–dipole interactions between CI particles resulting in the formation of chain-like structures.

Fig. 5 shows viscoelastic moduli G' and G'' as functions of angular frequency at a small strain of 2×10^{-4} in the LVR for 80 wt.% MR suspension based on CI particles of sample B under various magnetic fields. In the absence of magnetic field, G' is slightly larger than G'', which can be due to high CI particle loading in the suspension. Upon application of the external magnetic field G' and G'' increase in three and two orders of magnitude, respectively. As can be seen in Fig. 5, G' values are either constant or increase slightly as the angular frequency rises up to 100 rad s^{-1}. This is typical behaviour of stiff three-dimensional network formed by magnetized CI particles within MR fluid, which is sufficiently strong to transmit the elastic force in such system [31].

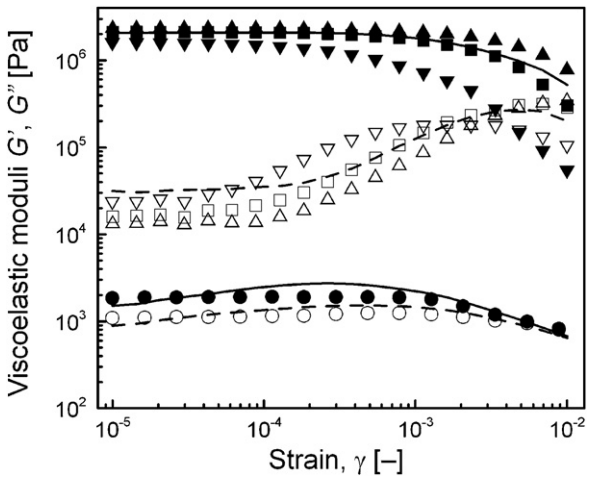

Fig. 4. Storage, G' (solid symbols or line) and loss, G'' (open symbols or dashed line) moduli versus strain, γ, at angular frequency of 62.83 rad s^{-1} for 80 wt.% MR fluid based on samples A (lines) particles under magnetic flux density (T) of 0 or 0.3, and B (symbols) particles under various magnetic fields applied. The symbols for magnetic flux densities (T): (●,○) 0; (▼,▽) 0.1; (■,□) 0.2; (▲,△) 0.3.

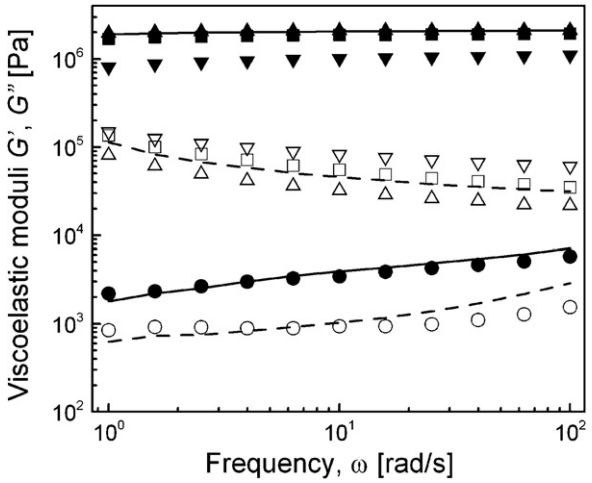

Fig. 5. Storage, G' (solid symbols or line) and loss, G'' (open symbols or dashed line) moduli versus angular frequency, ω, for samples A (lines) particles under magnetic flux density (T) of 0 or 0.3, and B particles based MR suspension (80 wt.%) under various magnetic fields applied. The symbols for magnetic flux densities (T): (●,○) 0; (▼,▽) 0.1; (■,□) 0.2; (▲,△) 0.3.

3.4. Sedimentation test

Finally, the effect of CI plasma treatment on the sedimentation stability was investigated. The MR fluids with overall fraction of 50 wt.% of HQ grade CI particles were set in static conditions and sedimentation ratios were measured for 24 h. Fig. 6 shows the effect of the exposure of CI particles to $Ar + C_4F_8$ plasma on the sedimentation stability of MR suspensions based on these particles. Three kinds of CI particles were used for the examination varying in treatment time (i.e. samples A, B and C). The inset photo shows final results of the sedimentation after 24 h for all suspensions. The interactions between fluorine bonded on the CI surface and methyl groups of silicone oil seem to be present, resulting in the retardation of sedimentation. Moreover, the MR suspension based on CI particles with 120 s exposure to plasma exerted the best suspension stability even better than in case of 300 s treated ones. This is probably caused by the growth of surface layer and so the overall particle size with increasing treatment time, which was confirmed using dynamic light scattering technique (Zetasizer, Malvern Instruments, UK). The particles size for 0, 120 and 300 s exposure to plasma time matched to 1, 1.026 and 1.038 μm, respectively. Therefore, there is an optimum plasma treatment time of 120 s for 1 μm CI particles ensuring the best combination of MR performance and suspension stability. However, 300 s plasma treated particles suspension possesses still higher stability due to the fluorine–methyl group interactions than for non-treated CI particles suspension. In other words it can be said that the retardation of sedimentation can be enhanced by surface modification of magnetic particles in plasma in order to improve the interac-

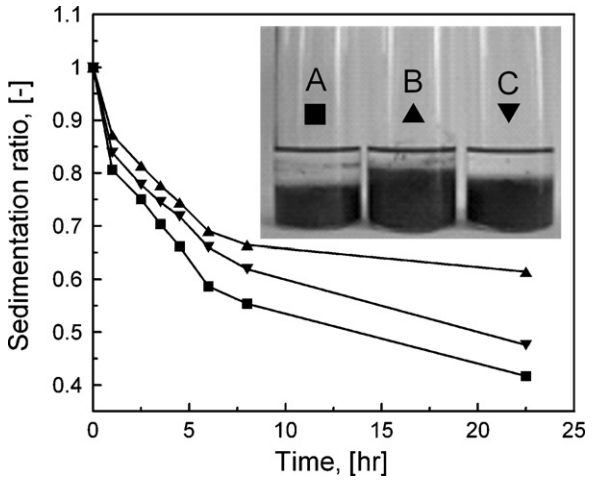

Fig. 6. Sedimentation ratio versus time for sample A (■), B (▲), C (▼) based MR suspensions (50 wt.%) in 200 mPa s silicone oil.

tions between particles and carrier liquid without the use of further viscosity modifying components [32].

4. Conclusions

Magnetic CI particles with different size were exposed to 50% argon and 50% octafluorocyclobutane plasma for different times for bonding of fluorine on their surface and its presence was confirmed via X-ray photoelectron spectroscopy. The plasma-treated particles based MR fluids show typical MR characteristics including high values of yield stresses and the sharp shear thinning behaviour under external magnetic field applied. The viscoelastic properties of the fluids suggest that plasma-treated CI particles MR suspensions exhibit strong elastic behaviour within the linear viscoelastic region due to the robust chain structure under a magnetic field applied. Compared with MR fluid based on bare CI, plasma-treated CI particles based MR fluids show enhanced sedimentation stability, and it seems to be due to the interaction forces between fluorine bonded on particle surface and methyl groups of silicone oil.

Acknowledgements

The authors wish to thank to the Ministry of Education, Youth and Sports of the Czech Republic (MSM7088352101) and the Czech Science Foundation (project 104/09/H080) for financial support.

This article was written with support of Operational Program Research and Development for Innovations co-funded by the European Regional Development Fund (ERDF) and national budget of Czech Republic, within the framework of project Centre of Polymer Systems (reg. number: CZ.1.05/2.1.00/03.0111).

References

[1] G. Bossis, O. Volkova, S. Lacis, A. Meunier, Magnetorheology: fluids, structures and rheology, Lect. Notes Phys. 594 (2002) 202–230.
[2] I. Bica, H.J. Choi, Preparation and electro-thermoconductive characteristics of magnetorheological suspensions, Int. J. Mod. Phys. B 22 (2008) 5041–5064.
[3] I. Bica, Advances in magnetorheological suspension: production and properties, J. Ind. Eng. Chem. 12 (2006) 501–515.
[4] J. de Vicente, D.J. Klingenberg, R. Hidalgo-Alvarez, Magnetorheological fluids: a review, Soft Matter 7 (2011) 3701–3710.
[5] B.J. Park, F.F. Fang, H.J. Choi, Magnetorheology: materials and application, Soft Matter 6 (2010) 5246–5253.
[6] L.K. Yang, F. Duan, A. Eriksson, Analysis of the optimal design strategy of a magnetorheological smart structure, Smart Mater. Struct. 17 (2008) 015047.
[7] M. Stenicka, V. Pavlinek, P. Saha, N.V. Blinova, J. Stejskal, O. Quadrat, Effect of hydrophilicity of polyaniline particles on their electrorheology: steady flow and dynamic behaviour, J. Colloid Interface Sci. 346 (2010) 236–240.
[8] V.A. Neelakantan, G.N. Washington, Modeling and reduction of centrifuging in magnetorheological (MR) transmission clutches for automotive applications, J. Intell. Mater. Syst. Struct. 16 (2005) 703–711.
[9] K.H. Gudmundsson, F. Jonsdottir, F. Thorsteinsson, A geometrical optimization of a magneto-rheological rotary brake in a prosthetic knee, Smart Mater. Struct. 19 (2010) 035023.
[10] S.N. Madhekar, R.S. Jangid, Variable dampers for earthquake protection of benchmark highway bridges, Smart Mater. Struct. 18 (2009) 115011.
[11] J.H. Koo, F.D. Goncalves, M. Ahmadian, A comprehensive analysis of the response time of MR dampers, Smart Mater. Struct. 15 (2006) 351–358.
[12] L.E. Udrea, N.J.C. Strachan, V. Badescu, O. Rotariu, An in vitro study of magnetic particle targeting in small blood vessels, Phys. Med. Biol. 51 (2006) 4869–4881.
[13] M.O. Aviles, A.D. Ebner, J.A. Ritter, Ferromagnetic seeding for the magnetic targeting of drugs and radiation in capillary beds, J. Magn. Magn. Mater. 310 (2007) 131–144.
[14] P.J. Rankin, A.T. Horvath, D.J. Klingenberg, Magnetorheology in viscoplastic media, Rheol. Acta 38 (1999) 471–477.
[15] F.F. Fang, H.J. Choi, M.S. Jhon, Magnetorheology of soft magnetic carbonyl iron suspension with single-walled carbon nanotube additive and its yield stress scaling function, Colloid Surf. A: Physicochem. Eng. Aspects 351 (2009) 46–51.
[16] M. Sedlacik, V. Pavlinek, P. Saha, P. Svrcinova, P. Filip, J. Stejskal, Rheological properties of magnetorheological suspensions based on core–shell structured polyaniline-coated carbonyl iron particles, Smart Mater. Struct. 19 (2010) 115008.
[17] F.F. Fang, H.J. Choi, Y. Seo, Sequential coating of magnetic carbonyliron particles with polystyrene and multiwalled carbon nanotubes and its effect on their magnetorheology, ACS Appl. Mater. Interfaces 2 (2010) 54–60.
[18] J.L. Viota, A.V. Delgado, J.L. Arias, J.D.G. Duran, Study of the magnetorheological response of aqueous magnetite suspensions stabilized by acrylic acid polymers, J. Colloid Interface Sci. 324 (2008) 199–204.
[19] M. Lopez-Lopez, J. de Vicente, F. Gonzales-Caballero, J.D.G. Duran, Stability of magnetizable colloidal suspensions by addition of oleic acid and silica nanoparticles, Colloid Surf. A 264 (2005) 75–81.
[20] N.M. Wereley, A. Chaudhuri, J.H. Yoo, S. John, S. Kotha, A. Suggs, R. Radhakrishnan, B.J. Love, T.S. Sudarshan, Bidisperse magnetorheological fluids using Fe particles at nanometer and micron scale, J. Intell. Mater. Syst. Struct. 17 (2006) 393–401.
[21] J.H. Park, B.D. Chin, O.O. Park, Rheological properties and stabilization of magnetorheological fluids in a water-in-oil emulsion, J. Colloid Interface Sci. 240 (2001) 349–354.
[22] M. Lehocky, H. Drnovska, B. Lapcikova, A.M. Barros-Timmons, T. Trindade, M. Zembala, L. Lapcik, Plasma surface modification of polyethylene, Colloid Surf. A: Physicochem. Eng. Aspects 222 (2003) 125–131.
[23] Z. Adamczyk, L. Szyk-Warszynska, M. Zembala, M. Lehocky, In situ studies of particle deposition on non-transparent substrates, Colloid Surf. A: Physicochem. Eng. Aspects 235 (2004) 65–72.
[24] M. Sowe, I. Novak, A. Vesel, I. Junkar, M. Lehocky, P. Saha, I. Chodak, Analysis and characterization of printed plasma-treated polyvinyl chloride, Int. J. Polym. Anal. Charact. 14 (2009) 641–651.
[25] M. Lehocky, P. Stahel, M. Koutny, J. Cech, J. Institoris, A. Mracek, Adhesion of Rhodococcus sp S3E2 and Rhodococcus sp S3E3 to plasma prepared Teflon-like and organosilicon surfaces, J. Mater. Process. Technol. 209 (2009) 2871–2875.
[26] M. Lehocky, P.F.F. Amaral, P. Stahel, M.A.Z. Coelho, A.M. Barros-Timmons, J.A.P. Coutinho, Deposition of *Yarrowia lipolytica* on plasma prepared teflonlike thin films, Surf. Eng. 24 (2008) 23–27.
[27] J.F. Moulder, W.F. Stickle, P.E. Sobol, K.D. Bomben, Handbook of X-Ray Photoelectron Spectroscopy, Eden Prairie, Minnesota, 1995.
[28] H.M. Laun, C. Gabriel, Measurement modes of the response time of a magnetorheological fluid (MRF) for changing magnetic flux density, Rheol. Acta 46 (2007) 665–676.
[29] B.J. Park, S.M. Kim, H.J. Choi, Fabrication and magnetorheological property of core/shell structured magnetic composite particle encapsulated with crosslinked poly(methyl methacrylate), Mater. Lett. 63 (2009) 2178–2180.
[30] M.S. Cho, H.J. Choi, M.S. Jhon, Shear stress analysis of a semiconducting polymer based electrorheological fluid system, Polymer 46 (2005) 11484–11488.
[31] K. Tsuda, Y. Takeda, H. Ogura, Y. Otsubo, Electrorheological behavior of whisker suspensions under oscillatory shear, Colloid Surf. A: Physicochem. Eng. Aspects 299 (2007) 262–267.
[32] J. de Vicente, M. Lopez-Lopez, F. Gonzales-Caballero, J.D.G. Duran, Rheological study of the stabilization of magnetizable colloidal suspensions by addition of silica nanoparticles, J. Rheol. 47 (2003) 1093–1109.

PAPER III

Modern Physics Letters B, Vol. 26, No. 3 (2012) 1150013

World Scientific
www.worldscientific.com

THE ROLE OF PARTICLES ANNEALING TEMPERATURE ON MAGNETORHEOLOGICAL EFFECT

M. SEDLACIK, V. PAVLINEK* and P. SAHA

Centre of Polymer Systems, University Institute,
Tomas Bata University in Zlin, Nad Ovcirnou 3685, 760 01, Zlin, Czech Republic
Polymer Centre, Faculty of Technology, Tomas Bata University in Zlin,
Nam. T. G. Masaryka 275, 762 72, Zlin, Czech Republic
**pavlinek@ft.utb.cz*

P. SVRCINOVA and P. FILIP

Institute of Hydrodynamics, Academy of Sciences of the Czech Republic,
Pod Patankou 5, 166 12 Prague 6, Czech Republic

Received 20 July 2011
Revised 5 October 2011

The spinel nanocrystalline cobalt ferrite ($CoFe_2O_4$) particles were prepared via a sol-gel method followed by the annealing process. Their structural, magnetic and magnetorheological (MR) properties depending upon the annealing temperature were investigated. The X-ray diffraction analysis revealed that the higher annealing temperature, the larger grain size of $CoFe_2O_4$ particles resulting in larger magnetic domains in particles. The saturation magnetization, determined via a vibrating sample magnetometry, increased with annealing temperature and, in contrast, the coercivity decreased. The rheological behavior of $CoFe_2O_4$ particles based MR suspensions determined under the small-strain oscillatory shear flow in magnetic field showed that higher annealing temperature reflects in larger changes of rheological properties.

Keywords: Magnetorheological suspensions; nanocrystalline cobalt ferrite; annealing; magnetic field.

1. Introduction

An important field of current research is represented by magnetorheological (MR) suspensions. These smart fluids enable an abrupt change of rheological properties such as yield stress, viscosity or viscoelastic moduli by transforming from liquid to solid-like structure under an applied magnetic field within milliseconds.[1,2]

Cobalt ferrite ($CoFe_2O_4$) as a typical example of ferromagnetic materials attracts a serious attention of researches in many areas due to its favorable properties like moderate saturation magnetization, high coercivity, as well as a good hardness and an excellent chemical stability. Especially, moderate saturation magnetization favors cobalt ferrite for successful application as a dispersed phase of intelligent

magnetorheological suspensions. On the other hand, the high coercivity is induced by the large anisotropy of Co^{2+} ion due to the spin-orbit coupling. Coercivity is an important feature in magnetic hyperthermia, the efficient and harmlessness method in medicine in cancer treatment causing the necroses of tumor cells due to heat generation by AC magnetic field on magnetic nanoparticles introduced into the diseased tissue.[3] Thus, from economic and time points of view it is very interesting to change the magnetic properties of one material dependent upon resulting application by small variation during the preparation.

To increase the variability of the use of $CoFe_2O_4$ particles, this work deals with the effect of temperature of the annealing process followed after the sol–gel synthesis of $CoFe_2O_4$ particles on their magnetic properties and rheological behavior of MR suspensions based on such particles.

2. Experimental

2.1. *Preparation of $CoFe_2O_4$ particles*

All the chemicals, except distilled water, used for preparation of ferrite particles were of reagent grade and purchased from Sigma–Aldrich (USA).

As can be seen in Fig. 1, cobalt ferrite particles were obtained via sol–gel method with subsequent annealing.[4] Briefly, the synthesis process starts with the preparation of solution consisting of cobalt acetate tetrahydrate (1/200 mol) and iron(III) nitrate nonahydrate (1/100 mol) dissolved in 2–methoxyethanol (100 ml) and water (15 ml). The solution was sonicated for 30 min and then refluxed at 70°C for 12 h. Afterwards the formed gel was dried at 100°C for 24 h and ground in a ball mill (Retsch MM 301, Retsch GmbH, Germany). Final step, and crucial for resulting magnetic properties of $CoFe_2O_4$ powders, was annealing in muffle furnace (LAC LMH 07/12, LAC, USA) with heating rate of 1°C/min up to 400°C or 850°C and holding for 3 h. Different annealing conditions were also studied but above mentioned appeared as the best variants from $CoFe_2O_4$ properties and economical point of view.

Structure of prepared particles was determined with an X-ray diffractometer (X'Pert PRO, Philips, The Netherlands) with Cu-K_α radiation ($\lambda = 0.154$ nm) in reflection mode and 2θ ranged from 25° to 70°. The morphology of prepared powder was determined with SEM (Scanning Electron Microscope VEGA II LMU, Tescan, Czech Republic) operated at 10 kV. Measurement of magnetic properties of $CoFe_2O_4$ was carried out at 25°C using a vibrating sample magnetometer (VSM, Lakeshore, USA) at high magnetic field of 12 kOe.

2.2. *Preparation of MR suspensions*

$CoFe_2O_4$ particles were dispersed by ultrasound in silicone oil (Lukosiol M15, Chemical Works Kolín, Czech Republic; viscosity $\eta = 14.5$ mPas, density $d = 0.965$ g/cm^3) to form stable suspensions with a particle weight fraction of 40% for materials annealed at 400°C or 850°C, respectively.

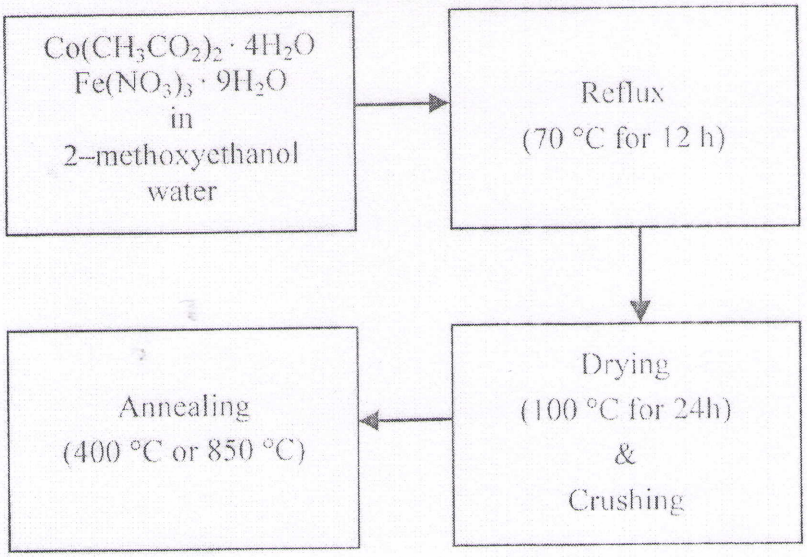

Fig. 1. Preparation procedure of $CoFe_2O_4$ particles.

Measurements of rheological properties of the prepared MR suspensions were carried out using a rotational rheometer Physica MCR501 (Anton Paar GmbH, Austria) with Physica MRD 180/1T magneto–cell at 25°C. True magnetic flux density (0–300 mT) was measured using a Hall probe. A parallel plate measuring system with a diameter of 20 mm and gap of 1 mm was used. The dynamic oscillation tests were performed by dynamic strain sweeps and frequency sweeps. The strain sweep was carried out with applied strains from 10^{-5} to 0.1 at angular frequency of 62.8 rad/s under a magnetic field to determine the linear viscoelastic region. Then, the rheological parameters were obtained from frequency sweep tests (0.628–62.8 rad/s) at fixed strain amplitude in the linear viscoelastic region.

3. Results and Discussion

3.1. *Characterization of $CoFe_2O_4$ particles*

The XRD patterns indicating the structure of $CoFe_2O_4$ particles annealed at 400°C or 850°C are shown in Fig. 2. All the diffraction peaks can be according to JCPDS card No. 22–1086 and JCPDS card No. 01–1121 indexed to the face centre structure of $CoFe_2O_4$. Moreover, no impurity peaks are detected. From Fig. 2 can be further seen the increase in intensity of the major peaks implying the growth of the grain size of $CoFe_2O_4$ particles with increasing annealing temperature. Based on the Scherrer formula,[5] the $CoFe_2O_4$ particle size was calculated as 16 nm and 35 nm for particles annealed at 400°C or 850°C, respectively.

SEM image in Fig. 3 demonstrates that single particles form larger agglomerates of mostly globular shape having the size in range from 100 nm to 1 μm.

The magnetic properties of prepared $CoFe_2O_4$ particles are depicted in Fig. 4. The magnetization saturations of annealed particles, 36 or 63 emu/g (annealed at

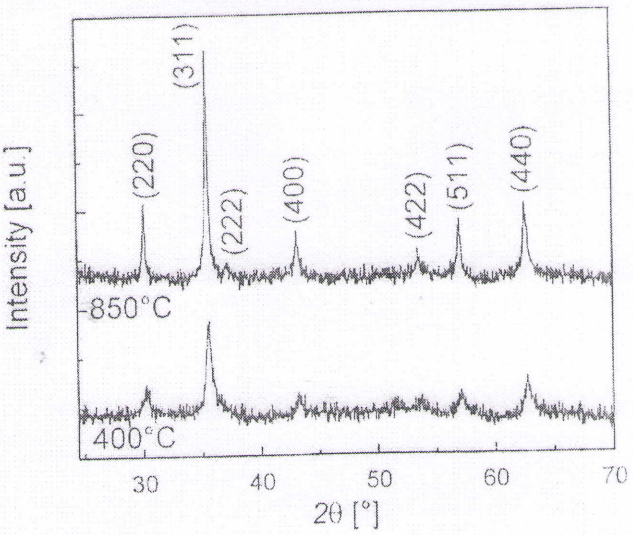

Fig. 2. X-ray diffraction patterns of the $CoFe_2O_4$ particles annealed at 400°C or 850°C.

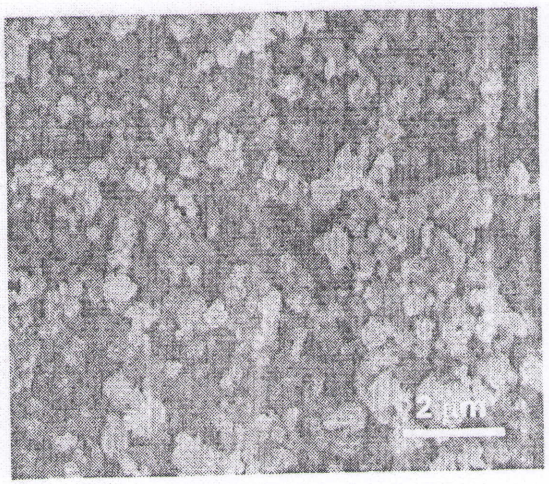

Fig. 3. SEM image of $CoFe_2O_4$ particles annealed at 850°C.

400°C or 850°C), are lower in comparison with bulk $CoFe_2O_4$ (72 emu/g)[6] confirming the nanocrystalline nature of prepared particles. In contrast to magnetization saturation values, the coercivity, which is unwanted property of dispersed particles in MR suspensions,[7] is higher for particles annealed at lower temperature. The existence of coercivity in the samples can be attributed to the large residual strain and defects in $CoFe_2O_4$ particles caused by milling during their preparation.[8] The differences in the magnetic properties of prepared $CoFe_2O_4$ can be due to different particle sizes (magnetic domains) depending upon annealing temperature.

3.2. *Rheological properties of MR suspensions*

An abrupt change of MR suspension internal structure under an external magnetic field causes a transition from nearly Newtonian liquid to solid-like state in several

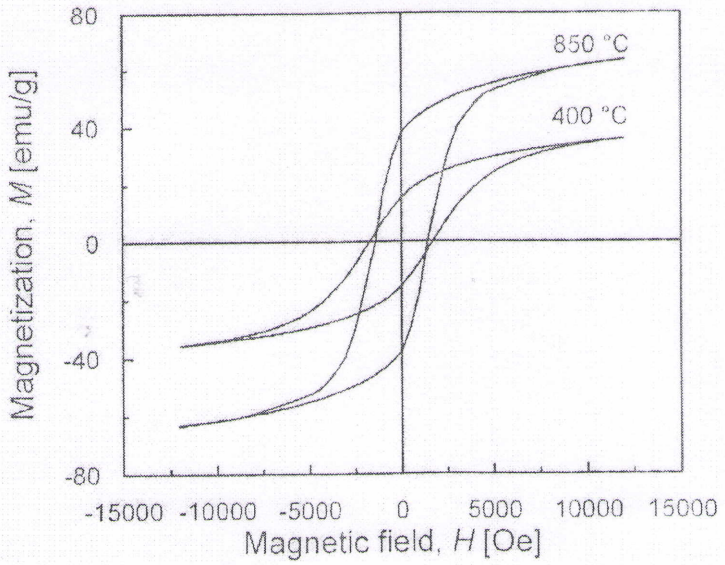

Fig. 4. Magnetization curves of $CoFe_2O_4$ particles annealed at 400°C or 850°C.

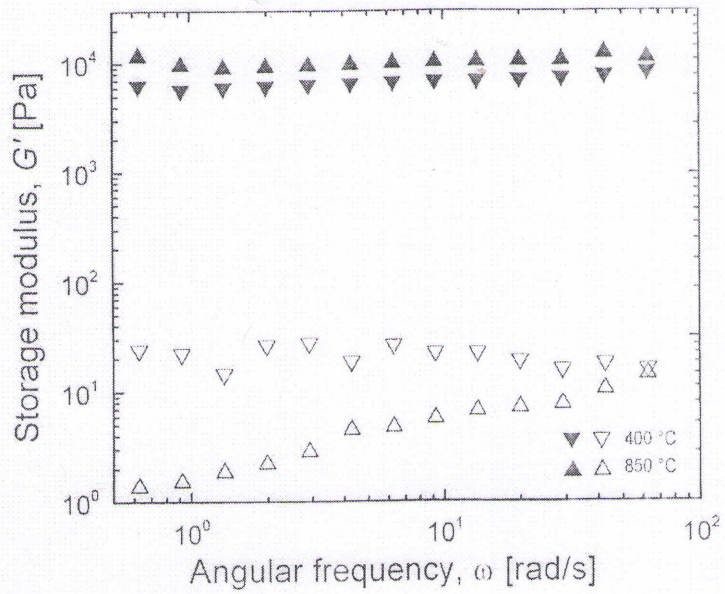

Fig. 5. Frequency dependence of storage modulus, G', for 40 wt.% suspension of $CoFe_2O_4$ annealed at 400°C or 850°C at different magnetic flux densities: 0 mT (open symbols); 260 mT (solid symbols).

milliseconds. A possible method for the investigation of such transition is a dynamic oscillation test, in which storage, G', and loss, G'', moduli describe the change of the suspension internal structure.[9] First of all, the range of the independency of G' and G'' on strain amplitude, so called linear viscoelastic region, must be determined and that was until strain amplitude $\gamma = 2\times10^{-4}$ in our experiment.

Figure 5 shows storage modulus, G', for MR suspensions of two kinds of $CoFe_2O_4$ particles differing in the annealing temperature as a function of angular frequency

in the linear viscoelastic region. In the absence of a field, G' is dependent on the frequency, especially in case of particles annealed at 850°C. However, it increases significantly and becomes independent of the frequency upon a magnetic field. Suspension of $CoFe_2O_4$ particles annealed at 850°C exhibits higher G'. Moreover, the higher annealing temperature of particles results in lower G' of MR suspensions in the absence of magnetic field and thus in higher MR efficiency. Thus, MR suspensions based on nanoparticles can demonstrate typical MR characteristics due to the formation of rigid internal structure of magnetized particles imposed to magnetic field.[10]

4. Conclusions

The synthesis of cobalt ferrite via sol–gel method with subsequent annealing enable to tailor properties of such particles in dependence on required application, which can also be effective from economical point of view. It means that $CoFe_2O_4$ particles annealed at higher temperature are good candidates for classical magnetorheology while those annealed at lower temperature can be used in magnetic hyperthermia.

Acknowledgments

This work was financially supported by the Ministry of Education, Youth and Sports of the Czech Republic (MSM 7088352101) and the Grant Agency of the Czech Republic (202/09/1626).

This article was written with support of Operational Programme Research and Development for Innovations co-funded by the European Regional Development Fund (ERDF) and national budget of the Czech Republic, within the framework of project Centre of Polymer Systems (reg. number: CZ.1.05/2.1.00/03.0111).

References

1. B. J. Park, F. F. Fang and H. J. Choi, *Soft Matter* **6** (2010) 5246.
2. A. J. F. Bombard and J. V. R. Teodoro, *Int. J. Mod. Phys. B* **25** (2011) 943.
3. D. H. Kim, D. E. Nikles, D. T. Johnson and C. S. Brazel, *J. Magn. Magn. Mater.* **320** (2008) 2390.
4. J. G. Lee, J. Y. Park and C. S. Kim, *J. Mater. Sci.* **33** (1998) 1965.
5. A. Patterson, *Phys. Rev.* **56** (1939) 978.
6. E. Kneller, *Magnetism and Metallurgy*, eds. A. E. Berkowitz and E. Kneller (Academic Press, New York, 1969), p. 621.
7. J. De Vicente, J. D. G. Duran, A. V. Delgado, F. Gonzales-Caballero and G. Bossis, *Int. J. Mod. Phys. B* **16** (2002) 2576.
8. M. V. Limaye, S. B. Singh, S. K. Date, D. Kothari, V. R. Reddy, A. Gupta, V. Sathe, R. J. Choudhary and S. K. Kulkami, *J. Phys. Chem: B* **113** (2009) 9070.
9. F. F. Fang, J. H. Kim and H. J. Choi,*Int. J. Mod. Phys. B* **23** (2009) 3613.
10. I. G. Kim, K. H. Song, B. O. Park, B. I. Choi and H. J. Choi, *Colloid Polym. Sci.* **289** (2011) 79.

PAPER IV

Colloid Polym Sci (2012) 290:41–48
DOI 10.1007/s00396-011-2521-x

ORIGINAL CONTRIBUTION

Electrorheological properties of suspensions of hollow globular titanium oxide/polypyrrole particles

M. Sedlačík · M. Mrlík · V. Pavlínek · P. Sáha · O. Quadrat

Received: 29 April 2011 / Revised: 21 September 2011 / Accepted: 22 September 2011 / Published online: 6 October 2011

Abstract Hollow globular clusters of titanium oxide (TiO_2) nanoparticles were synthesized by a simple hydrothermal method. The prepared particles were consequently coated by in situ polymerization of conductive polymer polypyrrole (PPy) to obtain novel core–shell structured particles as a dispersed phase in electrorheological (ER) suspensions. The X-ray diffraction analysis and scanning electron microscopy provided information on particle composition and morphology. It appeared that PPy coating improved the compatibility of dispersed particles with silicone oil which results in higher sedimentation stability compared to that of mere TiO_2 particles-based ER suspension. The ER properties were investigated under both steady and oscillatory shears. It was found that TiO_2/PPy particles-based suspension showed higher ER activity than that of mere TiO_2 hollow globular clusters. These observations were elucidated well in view of their dielectric spectra analysis; a larger dielectric loss enhancement and faster interfacial polarization were responsible for a higher ER activity of core–shell structured TiO_2/PPy-based suspensions. Investigation of changes in ER properties of prepared suspensions as a function of particles concentration, viscosity of silicone oil used as a suspension medium, and electric field strength applied was also performed.

Keywords Electrorheology · Titanium oxide · Hollow globular clusters · Polypyrrole coating · Core–shell particles · Dielectric properties

M. Sedlačík · M. Mrlík · V. Pavlínek · P. Sáha
Centre of Polymer Systems, University Institute,
Tomas Bata University in Zlin,
Nad Ovcirnou 3685,
760 01 Zlin, Czech Republic

M. Sedlačík (✉) · M. Mrlík · V. Pavlínek · P. Sáha
Polymer Centre, Faculty of Technology,
Tomas Bata University in Zlin,
namesti T. G. Masaryka 275,
762 72 Zlin, Czech Republic
e-mail: msedlacik@ft.utb.cz

O. Quadrat
Institute of Macromolecular Chemistry,
Academy of Sciences of the Czech Republic,
Heyrovsky Sq. 2,
162 06 Prague 6, Czech Republic

Introduction

Electrorheological (ER) behavior of suspensions of electrically polarizable particles dispersed in an insulating fluid has been the object of investigations of many researchers in the past. The ability to suddenly change rheological properties due to formation of a stiff chain-like structure of polarized particles in the electric field ranges these fluids among smart materials with a great potential in engineering applications [1–3]. The nature of this effect enabling the remote-controlled transition from liquid to quasi-solid state has been discussed in review articles [4–7]. The broader using of ER effect in practice is still hindered by several problems such as low polarization forces and temperature dependence, leaking current through the suspension and particle sedimentation. To overcome these drawbacks, various ER materials differing in shape [8] and organic [9, 10] or inorganic [11] nature have been developed. In addition, a dispersed phase of particles with modified structure as metal-doped titania [12], polymer/inorganic hybrid [13, 14], and core–shell composites [15] have also been used in ER fluids.

It is well known that the interfacial polarization takes dominant role in determination of the ER performance, and

dielectric and electric properties of particles are main factors affecting the ER activity. At present great attention has been paid to titanium oxide (TiO_2) because of its high dielectric constant. Its weak ER activity mainly originating from its low active natural structure could be improved by changing its molecular or crystalline structure or microstructure [16]. In this study, with a view to prepare a novel material with good ER performance, the hollow globular clusters of titanium oxide nanoparticles coated with a polypyrrole (TiO_2/PPy) were synthesized and steady-state and oscillatory flow behavior of their silicone oil suspensions related to dielectric properties were analyzed.

Experimental

Materials

Potassium titanium oxide oxalate dihydrate (TiO) $(OCO\text{-}COOK)_2$; PTO, technical grade), hydrogen peroxide solution (H_2O_2, 30 wt.%), hydrochloric acid (HCl, ≥37%), pyrrole (Py, ≥98%) and ammonium persulfate (APS, 98%) were purchased from Sigma–Aldrich Incorporation (St. Louis, USA). Cetyltrimethylammonium bromide (CTAB, 98%) was obtained from Lach–Ner, s.r.o. (Neratovice, Czech Republic). All chemicals were used without further purification.

Synthesis of TiO_2/PPy particles

The mere TiO_2 hollow clusters were prepared according to the report [17], with a minor modification. PTO 1.416 g (4 mmol) was dissolved in 30 ml of distilled water and to a dark red solution 30 ml of 30% H_2O_2 and 3 ml of 37% HCl were added. The mixture was transferred to a 100-ml Teflon-lined autoclave and filled up with distilled water up to 90% of the total volume. The autoclave was sealed, heated at 150 °C for 8 h, and cooled down to room temperature. The suspension of TiO_2 clusters was filtered, the precipitate rinsed with distilled water several times, and dried at 60 °C in the vacuum for 6 h. The yield was around 83% (approximately 0.281 g).

To obtain TiO_2/PPy particles, 1.845 g of CTAB was dissolved in 100 ml of distilled water and 2 g of TiO_2 clusters was added. The suspension was sonicated for 30 min and cooled to 0–5 °C during vigorous stirring. Then, 4 ml of precooled Py monomer and 13.28 g of precooled initiator APS were added to the mixture dropwise. The polymerization reaction was carried out at 0–5 °C for 8 h and kept under room temperature another 12 h. The powder of TiO_2/PPy particles was collected on the filter and rinsed with distilled water several times. In order to decrease the conductivity of PPy coating, the sample was dispersed in fivefold molar excess of 1 M ammonium hydroxide for 5 h. Then, after filtration, TiO_2/PPy was rinsed with distilled water and dried as above. The weight fraction of PPy in the composite determined by thermogravimetric analysis (Setaram SetSys Evolution 1200, USA) was 34 wt.%.

Particle characterization

The structural analysis of prepared materials was carried out on an X'Pert PRO (Philips, the Netherlands) X-ray diffractometer, fitted with copper target, K_α ray, scanning rate of 4° min^{-1} for the recording data in the range of 2θ= 20–80° (360 kV, 20 mA). Elicited phase and purity from powder XRD patterns are shown in Fig. 1. All the diffraction peaks can be indexed to a pure tetragonal rutile phase according to JCPDS card No. 21–1276 with lattice constants a=4.602 Å and c=2.956 Å. In obtained XRD patterns, no other impurity peaks are detected. The peaks are not so sharp, and a small amorphous halo due to PPy appears in TiO_2/PPy particles XRD pattern.

The morphologies of the TiO_2/PPy powder as well as its PPy-coated variants were determined with SEM (Scanning Electron Microscope VEGA II LMU; Tescan, Czech Republic) operated at 10 kV and is shown by scanning electron micrograph in Fig. 2. As can be seen, the particles are hollow globular clusters of TiO_2 primary nanoparticles with the size of around 1 μm. PPy coating can be recognized on the surface.

Preparation of ER fluids

Five, 15, and 25 wt.% of uncoated and PPy-coated hollow globular clusters were dispersed by ultrasonic mixing in silicone oils Lukosiol M15 (Chemical Works Kolín, Czech Republic; viscosity 14.5 mPa s, density 0.965 g cm^{-3}) and Lukosiol M200 (Chemical Works Kolín, Czech Republic;

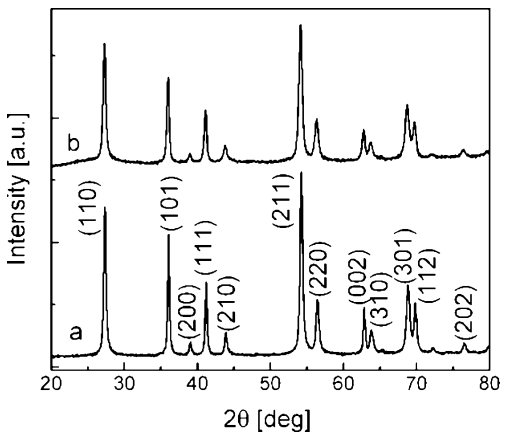

Fig. 1 Powder XRD patterns of the mere TiO_2 clusters (**a**) and TiO_2/PPy particles (**b**)

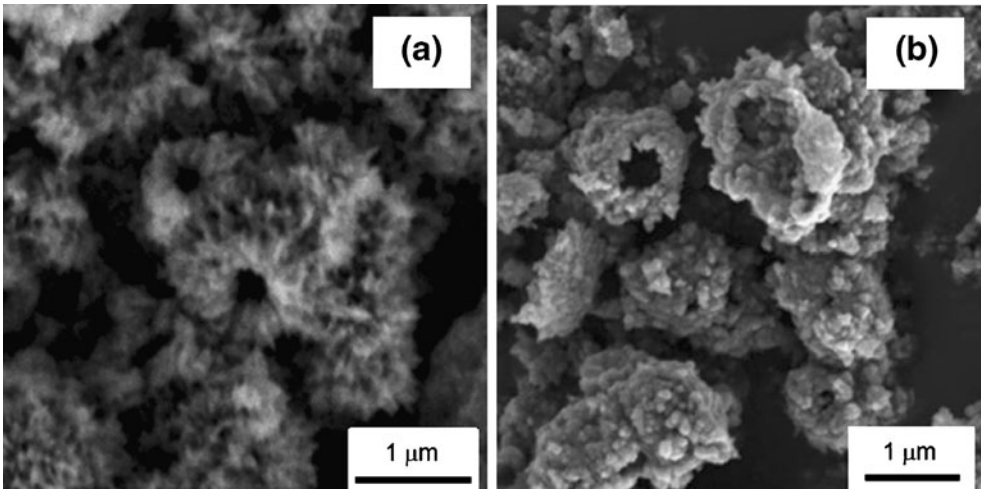

Fig. 2 SEM images of TiO_2 (**a**) and TiO_2/PPy (**b**) hollow globular clusters

viscosity 194 mPa s, density 0.965 g cm^{-3}). To avoid the influence of moisture, both silicone oils were dried at 80 °C for 24 h.

Electrorheological measurements

The ER properties of the fluids under investigation were measured using a rotational rheometer (Bohlin Gemini, Malvern Instruments, UK), with coaxial cylinder geometry (length 27.4 mm, inner cylinder of 14 mm in diameter and the outer cylinder separated by a 0.7-mm gap), modified for ER experiments. A DC voltage (0.35 until 2.1 kV) corresponded to the electric field strength range 0.5–3 kV mm^{-1} was generated by a DC high-voltage source TREK (TREK 668B, USA). All steady-flow measurements in the controlled shear rate (CSR) mode were performed in the shear rate range 0.1–300 s^{-1}. The oscillatory tests were carried out through dynamic strain sweeps and frequency sweeps. The strain sweeps were performed in the applied strain range of 10^{-4} to 10^{-2} at a fixed angular frequency of 6.28 rad s^{-1} under an electric field in order to get the position of the linear viscoelastic region (LVR). Afterwards, the viscoelastic moduli were obtained from the frequency sweep tests (0.5 to 100 rad s^{-1}) at fixed strain amplitude in the LVR. All the oscillatory measurements were performed in the CSR mode.

In both modes before each measurement at new electric field strength used, the formed internal structure within the suspension was destroyed by shearing of the sample at a shear rate 20 s^{-1} for 150 s. The temperature in all experiments was kept at 25 °C.

Dielectric properties

Dielectric properties in the frequency range of 40–5×10^6 Hz were measured with an impedance analyzer (Agilent 4524, Japan). Although the Cole–Cole equation has been frequently used for investigation of dielectric properties of many ER fluids [18], the dielectric spectra (Fig. 3) expressed by complex permittivity ε^* were analyzed in this study using Havriliak–Negami equation by which the asymmetry of relaxation peak can be more properly fitted [19]:

$$\varepsilon^* = \varepsilon'_\infty + \frac{(\varepsilon'_0 - \varepsilon'_\infty)}{(1 + (i\omega \cdot t_{\mathrm{rel}})^a)^b} \quad (1)$$

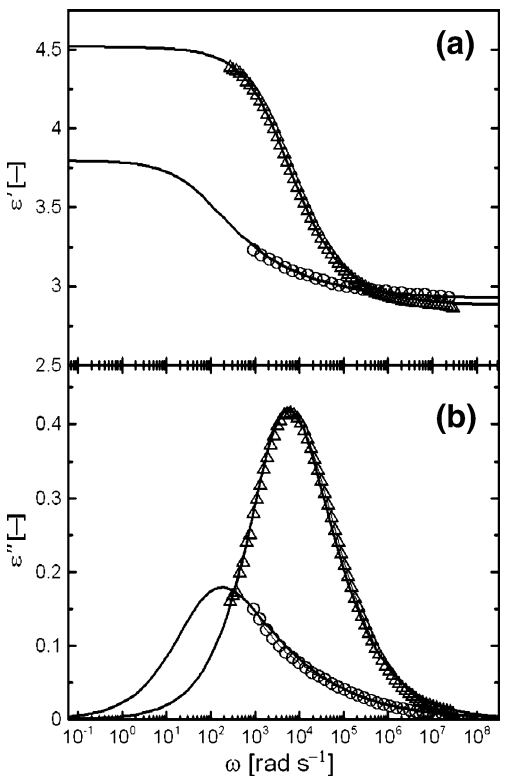

Fig. 3 Relative permittivity, ε', (**a**) and dielectric loss factor, ε'', (**b**) as a function of the angular frequency, ω, for 5 wt.% suspension of TiO_2 hollow globular clusters (*empty circle*) and TiO_2/PPy (*empty triangle*) particles

where polarizability, $\Delta\varepsilon'$, is defined as the difference between static ε'_0 and high-frequency ε'_∞ relative permittivity, ω is angular frequency, t_{rel} is the relaxation time, and a and b are shape parameters which describe the symmetric and asymmetric broadening of the dielectric function, $0<a$, $a\cdot b<1$. The parameters a and b are related to the limiting behavior of the dielectric function at low and high frequencies. The relaxation frequency, at which the dielectric loss factor ε'' has a maximum, is proportional to the rate of polarization of suspension particles.

Sedimentation behavior

Stability of ER fluid consisted of 25 wt.% TiO_2 hollow clusters and their PPy-coated variant in silicone oil M15 was examined by sedimentation ratio test based on a simple naked eye observation of sedimentation velocity (Fig. 4). Within this method, the samples were placed into test tubes and observed for 220 h. The settling of macroscopic phase boundary between the concentrated suspension and the relatively clear oil-rich phase was measured as a function of time. Then, the sedimentation ratio is defined as the height of particle-rich phase relative to the total suspension height. As can be seen, the ER fluids keep stable for a long time because of hollow structure. Furthermore, TiO_2/PPy suspension exhibits higher sedimentation stability than that of TiO_2 particles based one in the same time period which is caused by improved particles compatibility with the oil medium due to PPy coating.

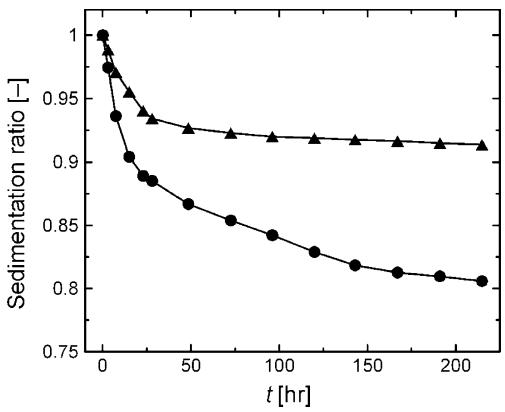

Fig. 4 Sedimentation ratio/time dependence of 25 wt.% ER suspensions of TiO_2 (*filled circle*) and TiO_2/PPy (*filled triangle*) particles in silicone oil M15

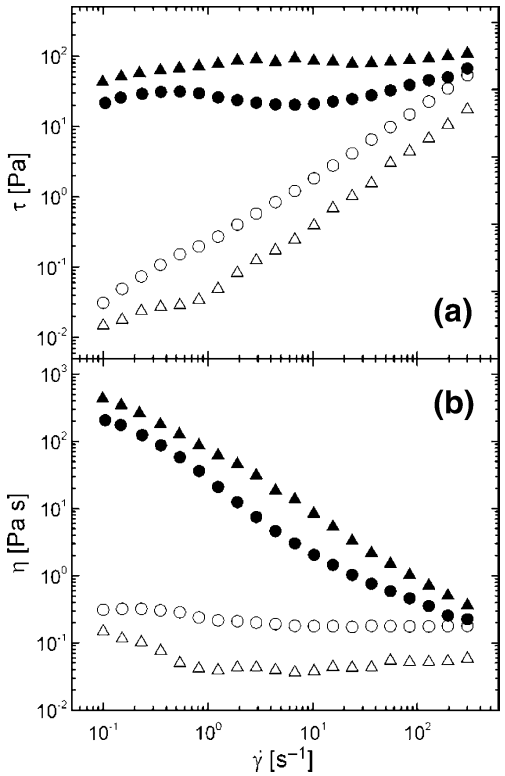

Fig. 5 Double-logarithmic plots of the shear stress, τ, (**a**) and the viscosity, η, (**b**) vs. shear rate, $\dot{\gamma}$, for 5 wt.% suspension of TiO_2 (*filled circle*, *empty circle*) and TiO_2/PPy (*filled triangle*, *empty triangle*) particles in silicone oil M15. The electric field strengths (in kilovolts per millimeter): 0 (*empty circle*, *empty triangle*), 3 (*filled circle*, *filled triangle*)

Results and discussion

ER effect and dielectric properties

Figure 5 illustrates an increase in ER activity of the mere TiO_2 clusters after PPy coating. Almost linear log–log plot of the shear stress on the rate of shear for suspension of both coated and uncoated particles in the absence of the electric field suggests almost Newtonian behavior characteristic for suspension of non-polarized particles (Fig. 5a). Viscosity of the sample of mere TiO_2 particles predominates (Fig. 5b) probably due to their more hydrophilic surface than PPy layer and, consequently, worse particle compatibility with the hydrophobic oil medium [9, 20]. Under electric field application, the low-shear apparent viscosity of both suspensions increased. The flow became pseudoplastic, and the ER response of PPy-coated particles was higher. As seen in Fig. 5a, the peak in the shear stress develops during shearing of the suspension in the electric field. This phenomenon is attributed to the rearrangement in

Table 1 Parameters in Eq. 1 and polarizability of ER fluids

Parameter	TiO_2	TiO_2/PPy
ε'_0	3.8	4.52
ε'_∞	2.92	2.88
$\Delta\varepsilon'$	0.88	1.64
t_{rel}	1.63E−02	2.64E−04

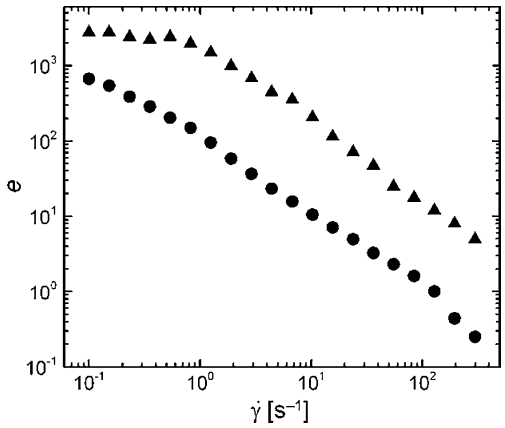

Fig. 6 The dependence of the performance, e, on the shear rate, $\dot{\gamma}$, for 5 wt.% suspension of mere TiO_2 particles (*filled circle*) and TiO_2/PPy-coated particles (*filled triangle*) in silicone oil M15

ER structures from chain-like structures spanning the gap between electrodes to lamellar structures as has been demonstrated in several ER fluids [21]. Because the rearrangement requires both electrostatic and hydrodynamic forces, it has been suggested that due to the thermodynamic reasons, the lamellar structures spontaneously form, driven by a lowering of the free energy in the system [22].

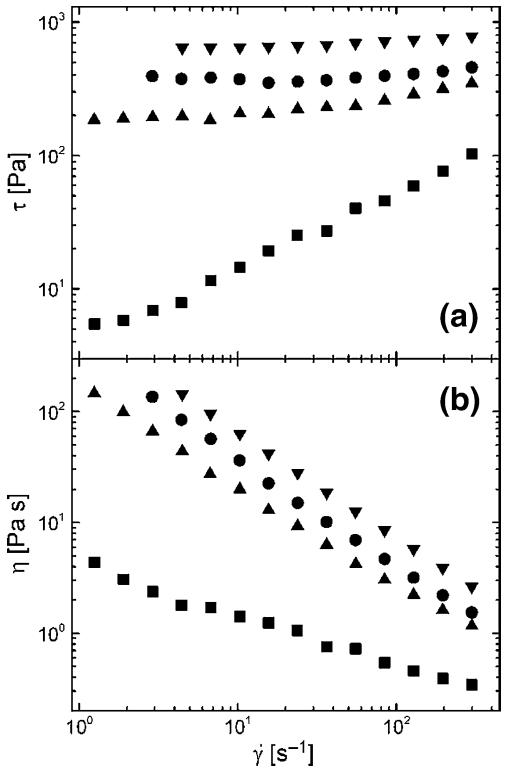

Fig. 7 Double-logarithmic plot of the shear stress, τ, (**a**) and viscosity, η, (**b**) vs. shear rate, $\dot{\gamma}$, for 25 wt.% ER fluid of TiO_2/PPy particles in silicone oil M15 at various electric field strengths E (in kilovolts per millimeter): 0 (*filled square*), 1 (*filled triangle*), 2 (*filled circle*), 3 (*filled inverted triangle*)

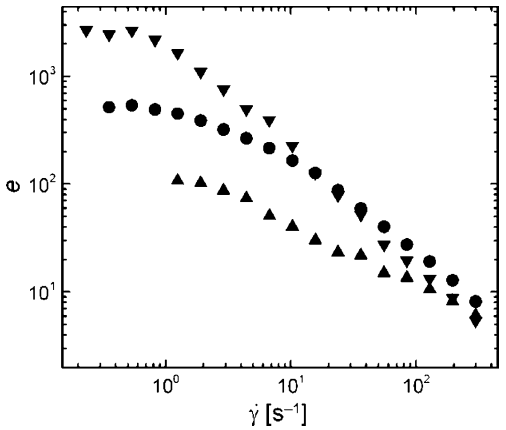

Fig. 8 The dependence of performance, e, on the shear rate, $\dot{\gamma}$, for suspension of TiO_2/PPy particles in silicone oil M15. Particle concentrations (in weight percent): 5 (*filled inverted triangle*), 15 (*filled circle*), 25 (*filled triangle*)

Especially mere TiO_2 hollow globular clusters suspension exhibits during the initial stages of shearing under electric field rearrangement from static aligned particles chain-like structure into another dynamic one.

It is generally accepted that interfacial polarization of particles and formation of chain-like structures in ER materials are closely related to dielectric phenomena. The dielectric spectra (Fig. 3) and their characteristics in the Table 1 indicate that PPy coating of particles enhanced the magnitude of particle polarizability, $\Delta\varepsilon'$, and decreased the relaxation time, t_{rel}. As a result, highly polarized particles with higher mobility were organized in a stiffer ER structure of suspension with higher viscosity.

For practical use, in addition to viscosity of suspension reached at the electric field strength used, also electric field-off value must be considered for evaluation of the efficiency of ER phenomenon. Thus, the performance of the ER liquid corresponding to a relative increase in electroviscosity,

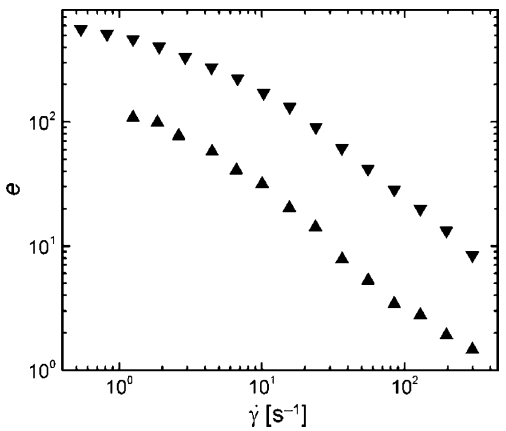

Fig. 9 The dependence of ER performance, e, on the shear rate, $\dot{\gamma}$, of 15 wt.% suspension of TiO_2/PPy particles in M15 (*filled inverted triangle*) and M200 (*filled triangle*) silicone oil

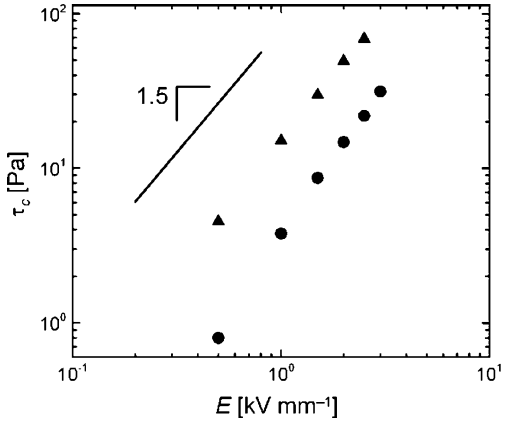

Fig. 10 Double-logarithmic plot of the shear stress, τ_c, vs. electric field strength, E, for 5 wt.% suspension of TiO_2 (*filled circle*) and TiO_2/PPy (*filled triangle*) particles in silicone oil M15

$\Delta\eta_E=\eta_E-\eta_0$, due to electric field application can be expressed as $e=(\eta_E-\eta_0)/\eta_0$, where η_E is a viscosity of ER structure [23]. It is worth to noting here the case of nanoparticles-based ER fluids providing a giant ER effect [24]. Unfortunately, no information about ER performance has been found in the literature dealing with such systems. However, one can expect that the ER performance could be comparable with conventionally used ER systems due to very high off-state viscosity of giant ER fluids, which could also be a problem in some practical applications.

In our study it is obvious that the ER efficiency is significantly higher for system based on coated particles due to higher viscosity in the low-shear rate region under electric field applied and lower field-off viscosity (Fig. 6).

Steady-state flow properties

The rigidity of the particles chain structure in suspension of TiO_2/PPy particles under electric field influence steeply increased with particle concentration. The shear stress of

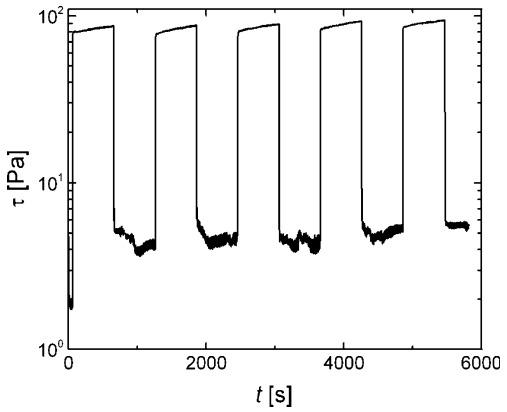

Fig. 11 Time dependence of the shear stress, τ, in the alternate switching on (E=1.5 kV mm^{-1})/off regime of 15 wt.% suspension of TiO_2/PPy particles in silicone oil M15 at the constant shear rate $\dot{\gamma} = 5\ s^{-1}$

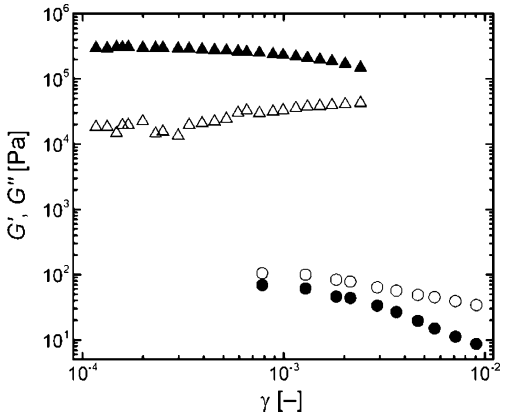

Fig. 12 Storage, G', (*solid symbols*) and loss, G'', (*open symbols*) moduli vs. strain, γ, at angular frequency 6.28 rad s^{-1} for 25 wt.% suspension of TiO_2/PPy particles in silicone oil M15. Electric field strengths E (in kilovolts per millimeter): 0 (*filled circle*, *empty circle*), 3 (*filled triangle*, *empty triangle*)

25 wt.% suspension at low shear rates at the field strength 3 kV mm^{-1} reached about 0.7 kPa (Fig. 7). However, due to steeper increase in the field-off value, the performance with particle concentration decreased (Fig. 8).

The higher viscosity of suspension medium caused lower relative increase in electroviscosity and, consequently, lower ER performance (Fig. 9).

The response to the electric field

The determination of the dynamic yield stress by extrapolation of the shear stress to zero shear rate is problematic because of unsteady flow at low shear rates caused by deformation, destruction, and reformation of formed chain-like and columnar ER structures [25]. Thus the shear stresses, τ_c, at the low shear rates $\dot{\gamma}_c = 0.5\ s^{-1}$ have been

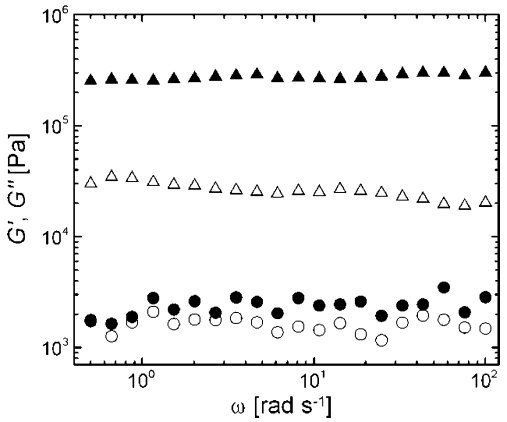

Fig. 13 Storage, G', (*solid symbols*) and loss, G'', (*open symbols*) moduli vs. angular frequency, ω, for 25 wt.% suspension of TiO_2/PPy particles in silicone oil M15. Electric field strengths E (in kilovolts per millimeter): 0 (*filled circle*, *empty circle*), 3 (*filled triangle*, *empty triangle*)

used as a criterion of rigidity of static particle chain-like structure. The dependence of this quantity on the electric field strength, E, (Fig. 10) illustrates the improvement in the ER activity of TiO_2 hollow clusters by PPy coating. The linear log–log plot of τ_c vs. E obeys the power law $\tau_c = q\,E^{\alpha}$, where the response of particles on the electric field strength $\alpha = 1.46–1.58$ corresponds to the theoretical predictions for well-developed ER structure ($\alpha = 1.5$) [26]. The higher q value for suspension of TiO_2/PPy particles confirms strong increase in ER efficiency due to particle coating.

Reproducibility of ER structure

The reproducibility of ER phenomenon is another basic factor for the use of ER liquids in practice. Thus, the alternate switching on and off the electric field should provide the same increase or decrease in suspension viscosity and reach during milliseconds virtually the same ER structure. Figure 11 demonstrates that the shear stress reached after switching on/off cycles with 15 wt.% ER suspension based on TiO_2/PPy particles in silicone oil M15 sheared at 5 s^{-1} and 1.5 kV mm^{-1} fulfills the requirements.

Dynamic oscillatory experiments

The formation of the internal chain-like structure of polarized particles under electric field application is also accompanied by a change of viscoelastic characteristics. Figure 12 depicts the dependence of G' and G'' on the strain amplitude (γ) in oscillatory flow for 25 wt.% TiO_2/PPy particles suspension. Without the electric field, the viscous modulus, G'', in the suspension is dominant over elastic one, G'. When the electric field is applied, however, G' becomes significantly higher than G'' in the linear viscoelastic region and both moduli increase rapidly in several orders of magnitude from their electric field-off values. When the strain acting on the internal structure increases beyond a certain degree, the elastic and viscous moduli intersect each other ($G' = G''$), the chain structure of the ER fluid breaks rapidly and the system starts to flow [27].

For practical applications it is important to know the moduli in linear viscoelastic region and their angular frequency dependence. Figure 13 presents the change in G' and G'' of 25 wt.% suspension of TiO_2/PPy particles at the small strain of 3×10^{-4} under electric field strength 3 kV mm^{-1}. In the absence of electric field, G' and G'' exhibited the similar values. Relatively high G' is probably due to the presence of irregular shaped TiO_2/PPy particles, which can form aggregates in the flow even in the absence of electric field, and so increase the elastic portion within the ER suspension. Under electric field application, unlike G'' an increase in G' about two orders of magnitude was much higher. The elastic modulus was substantially larger than the viscous modulus and the ER suspension exhibited solid-like behavior, i.e., G' became nearly independent of frequency. This plateau of the frequency-dependent viscoelastic modulus is a characteristic of aligned 3D microstructures under electric field application [28].

Conclusions

Hollow globular clusters of titanium oxide nanoparticles coated with polypyrrole were prepared as a dispersed phase of a novel ER fluid. The steady-state flow and dynamic measurement showed that unlike mere uncoated particles, their ER efficiency after polypyrrole coating was significantly higher. This result is in good agreement with the dielectric properties indicating higher particles polarizability and lower relaxation frequency. The reproducibility and speed of the formation and breaking of the ER structure met the requirements. The performance characterized by a relative increase in electroviscosity appeared to be significantly affected by particle content and viscosity of suspension medium.

Acknowledgments The authors wish to thank the Ministry of Education, Youth and Sports of the Czech Republic (MSM 7088352101) and the Grant Agency of the Czech Republic (202/09/1626) for financial support. This article was written with support of Operational Programme Research and Development for Innovations cofunded by the European Regional Development Fund (ERDF) and national budget of the Czech Republic, within the framework of Centre of Polymer Systems project (reg. number: CZ.1.05/2.1.00/03.0111).

References

1. Papadopoulos CA (1998) Brakes and clutches using ER fluids. Mechatronics 8:719–726
2. Choi SB, Lee DY (2005) Rotational motion control of a washing machine using electrorheological clutches and brakes. Proc Inst Mech Eng Part C J Eng Mech Eng Sci 219:627–637
3. Dragasius E, Navickaite S, Rugaityte V (2008) Development and Investigation of Electrorheological Clutch. Proc 7th Inter Conf Vibroeng 32–34
4. Parthasarathy M, Klingenberg DJ (1996) Electrorheology: mechanisms and models. Mater Sci Eng R Rep 17:57–103
5. Hao T (2002) Electrorheological fluids. Adv Colloid Interface Sci 97:1–35
6. Yin JB, Zhao XP (2006) Advances in electrorheological fluids based on inorganic dielectric materials. J Ind Eng Chem 12:184–198
7. Quadrat O, Stejskal J (2006) Polyaniline in electrorheology. J Ind Eng Chem 12:352–361
8. Cheng QL, Pavlinek V, He Y, Lengalova A, Li CZ, Saha P (2008) Structural and electrorheological properties of mesoporous silica modified with triethanolamine. Colloid Surface Physicochem Eng Aspect 318:169–174
9. Stenicka M, Pavlinek V, Saha P, Blinova NV, Stejskal J, Quadrat O (2010) Effect of hydrophilicity of polyaniline particles on their

electrorheology: steady flow and dynamic behaviour. J Colloid Interface Sci 346:236–240
10. Hong CH, Sung JH, Choi HJ (2009) Effects of medium oil on electroresponsive characteristics of chitosan suspensions. Colloid Polym Sci 287:583–589
11. Cheng QL, Pavlinek V, He Y, Yan YF, Li CZ, Saha P (2011) Synthesis and electrorheological characteristics of sea urchin-like TiO_2 hollow spheres. Colloid Polym Sci 289:799–805
12. Yin JB, Zhao XP, Xiang LQ, Xia X, Zhang ZS (2009) Enhanced electrorheology of suspensions containing sea-urchin-like hierarchical Cr-doped titania particles. Soft Matter 5:4687–4697
13. Fang FF, Choi HJ, Ahn WS (2010) Electrorheology of a mesoporous silica having conducting polypyrrole inside expanded pores. Microporous Mesoporous Mat 130:338–343
14. Choi HJ, Jhon MS (2009) Electrorheology of polymers and nanocomposites. Soft Matter 5:1562–1567
15. Liu YD, Fang FF, Choi HJ (2011) Silica nanoparticle decorated polyaniline nanofiber and its electrorheological response. Soft Matter 7:2782–2789
16. Liu FH, Xu GJ, Wu JH, Cheng YC, Guo JJ, Cui P (2010) Synthesis and electrorheological properties of oxalate group-modified amorphous titanium oxide nanoparticles. Colloid Polym Sci 288:1739–1744
17. Li XX, Xiong YJ, Li ZQ, Xie Y (2006) Large-scale fabrication of TiO_2 hierarchical hollow spheres. Inorg Chem 45:3493–3495
18. Liu YD, Fang FF, Choi HJ (2010) Core–shell structured semiconducting PMMA/polyaniline snowman-like anisotropic microparticles and their electrorheology. Langmuir 26:12849–12854
19. Havriliak S, Negami S (1966) A complex plane analysis of alpha-dispersions in some polymer systems. J Polym Sci C 16:99–117
20. Stenicka M, Pavlinek V, Saha P, Blinova NV, Stejskal J, Quadrat O (2011) Structure changes of electrorheological fluids based on polyaniline particles with various hydrophilicities and time dependence of shear stress and conductivity during flow. Colloid Polym Sci 289:409–414
21. Vieira SL, Neto LBP, Arruda ACF (2000) Transient behavior of an electrorheological fluid in shear flow mode. J Rheol 44:1139–1149
22. Henley S, Filisko FE (1999) Flow profiles of electrorheological suspensions: an alternative model for ER activity. J Rheol 43:1323–1336
23. Lengalova A, Pavlinek V, Saha P, Quadrat O, Kitano T, Stejskal J (2003) Influence of particle concentration on the electrorheological efficiency of polyaniline suspensions. Eur Polym J 39:641–645
24. Huang XX, Wen WJ, Yang SH, Sheng P (2006) Mechanisms of the giant electrorheological effect. Solid State Commun 139:581–588
25. Cho MS, Choi HJ, Jhon MS (2005) Shear stress analysis of a semiconducting polymer based electrorheological fluid system. Polymer 46:11484–11488
26. Davis LC (1997) Time-dependent and nonlinear effects in electrorheological fluids. J Appl Phys 81:1985–1991
27. Cheng QL, Pavlinek V, He Y, Li CZ, Saha P (2009) Electrorheological characteristics of polyaniline/titanate composite nanotube suspensions. Colloid Polym Sci 287:435–441
28. Tsuda K, Takede Y, Ogura H, Otsubo Y (2007) Electrorheological behavior of whisker suspensions under oscillatory shear. Colloid Surface Physicochem Eng Aspect 299:262–267

PAPER V

"manuscript"

Synthesis and electrorheology of rod-like TiO_2 particles prepared via microwave-assisted molten-salt method

M. Sedlacik[a,b], M. Mrlik[a,b], Z. Kozakova[a,b], V. Pavlinek[a,b*], I. Kuritka[a,b]

[a] Centre of Polymer Systems, University Institute, Tomas Bata University in Zlin, Nad Ovcirnou 3685, 760 01 Zlin, Czech Republic

[b] Polymer Centre, Faculty of Technology, Tomas Bata University in Zlin, namesti T. G. Masaryka 275, 762 72 Zlin, Czech Republic

[*]Corresponding author. Tel.: +420 57 603 1205; fax: +420 57 603 1444.

E-mail: pavlinek@ft.utb.cz

Abstract

Rod-like titanium dioxide (TiO_2) particles were synthesized by a simple and rapid microwave-assisted molten-salt method. The X-ray diffraction analysis revealed that phase composition transform from anatase phase of TiO_2 starting nanomaterial to the rutile phase of high crystallinity. The scanning electron microscopy proved the conversion of originally spherical particles of starting anatase TiO_2 having the size from 200 to 500 nm into rods with the length from 5 to 10 μm and the diameter from 0.5 to 2 μm. The ER measurements performed under steady-state flow showed that suspension of rutile rod-like TiO_2 particles-based fluid exhibits much higher ER activity than that of anatase starting TiO_2 material particles. These observations were further clarified well in a view of their dielectric spectra analysis. The changes in ER properties of studied fluid as a function of the applied electric field strength and particles concentration were also performed.

Keywords: Electrorheology, Titanium oxide, Rod-like particles, Rutile, Anatase, Microwave-assisted molten-salt method, Dielectric properties

1 Introduction

Electrorheological (ER) fluids are basically two phase systems consisted of polarizable semiconducting particles homogenously dispersed within the insulating carrier liquid. These systems evoke expressive research and applicative interest by means of their phase-controllable behaviour under external electric field. In principle, the imposed electric field polarizes originally randomly dispersed particles and, consequently, the chain-like or columnar internal structure of particles spanning the gap between electrodes is formed [1-4]. In other words, ER fluids are able to change their rheological properties such as shear stress, apparent viscosity or viscoelastic moduli in several orders of magnitude in the presence of external electric field. All the changes generated within the system are moreover very rapid and reversible. Such electric field-dependent behaviour can be used in various damping systems, hydraulic valves or clutches [5].

Recently, the development in fabrication of one dimensional inorganic particle has passed considerable progress. These materials seem to be very promising as a dispersed phase of novel ER fluids since they exhibit enhanced polarizability and so improved ER performance under external electric field compared to classical globular particular systems [6-9]. The previous studies concentrated on the synthesis of one dimensional particle suitable for ER fluids were based on hydrothermal methods under alkali condition [10,11]. However, these methods are time-consuming and the use of hydroxides under high temperature and pressure can be dangerous for the human as well as for environment.

This paper is focused on the study of the ER properties of suspensions of rod-like titanium dioxide (TiO_2) particles prepared by molten-salt microwave-assisted method [12]. Molten-salt synthesis is one of the simple one-step methods to obtain desired product with high crystallinity and is based on the use of low-melting solvent to accelerate diffusion and thus formation of required structure. While further introducing microwaves into the synthesis process, uniform heating can provide faster reaction in comparison to conventional heating. Correlation of the steady shear ER behaviour of particle suspensions of both TiO_2 varieties with dielectric properties has been performed.

2 Experimental

2.1 Materials

Titanium(IV) dioxide powder consisted of anatase crystalline phase (99.8 % trace metal basis, Sigma-Aldrich, USA) was used as a precursor for the synthesis. Sodium chloride

(NaCl, Penta, Czech Republic) and sodium phosphate dibasic dodecahydrate ($Na_2HPO_4 \cdot 12\ H_2O$, Penta, Czech Republic) which has an eutectic at 735 °C while molar ratio of disodium phosphate is 20 % [13] were used as a molten environment. All chemicals were used without further purification.

2.2 Synthesis of rutile TiO_2 rod-like particles

TiO_2 rod-like particles were obtained applying a simple and rapid microwave-assisted molten-salt method in the presence of molten sodium salts flux (Fig. 1). The first step of synthesis was grinding of TiO_2 powder with eutectic mixture of $NaCl/Na_2HPO_4 \cdot 12\ H_2O$ in a mortar for 10 min in order to obtain homogenous reaction mixture. The ratio of raw material to the flux mixture was set 4:5. This mixture was subsequently poured into the corundum crucible and covered by corundum lid. Crucible was placed into the special ceramic kiln suitable for heating in microwaves. Inside of the cover of this kiln is coated by microwave absorbing layer which speeds up heating while exposed to microwaves and, thus, enables rapid rise of the temperature inside the kiln. The kiln was placed into the cavity of common domestic microwave oven and exposed to microwaves for 30 min at 750 W. After the heating, kiln was removed from the oven and allowed to cool to room temperature. Obtained powder was washed several times with demineralized water, filtered off and as-prepared product was dried at 60 °C in the vacuum for 24 h.

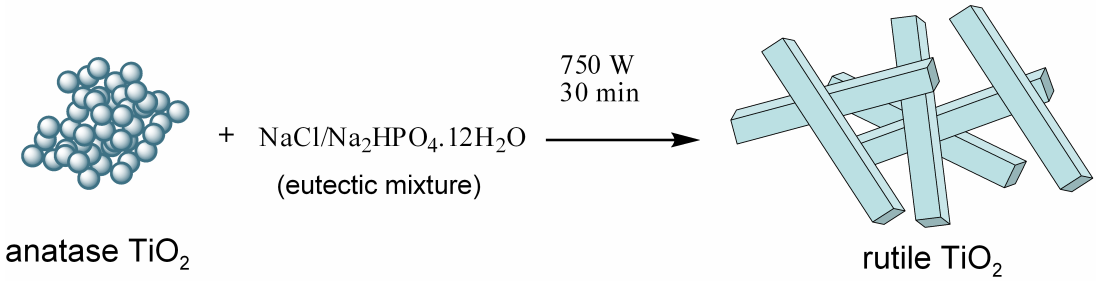

Fig. 1 Schematic illustration of the formation of rutile TiO_2 rod-like particles

2.3 Particle characterization

The crystallinity and phase composition of starting TiO_2 with anatase phase and prepared particles were examined via the X-ray diffraction (XRD) patterns collected on an X'Pert PRO (Philips, the Netherlands) diffractometer with Cu $K_{\alpha 1}$ radiation (λ = 1.54 Å) and scanning rate of 4° min^{-1} for the recording data in the wide range of 2θ = 10° – 95°. Moreover, the obtained

patterns were evaluated by a semi quantitative analysis performed by PANalytical X'Pert High Score works on the basis of reference intensity ratio values.

Elicited TiO_2 phases of anatase starting material and prepared rod-like particles from powder XRD patterns are shown in Fig. 2. It is worth noting that there are presented also diffraction peaks of anatase phase in the XRD pattern of prepared rod-like particles. However, the crystalline ratio is 92 % of rutile and 8 % of anatase in the sample according to the semi quantitative analysis of XRD pattern. Moreover, the narrow and most intensive peaks signify very good crystallinity and can be indexed to the tetragonal rutile phase according to JCPDS card No. 21-1276 with lattice constants a = 4.593 Å and c = 2.959 Å. Hence, the use of molten-salt microwave-assisted synthesis with reaction time of 30 min is sufficient for the TiO_2 phase transformation from anatase phase to rutile phase with high crystallinity.

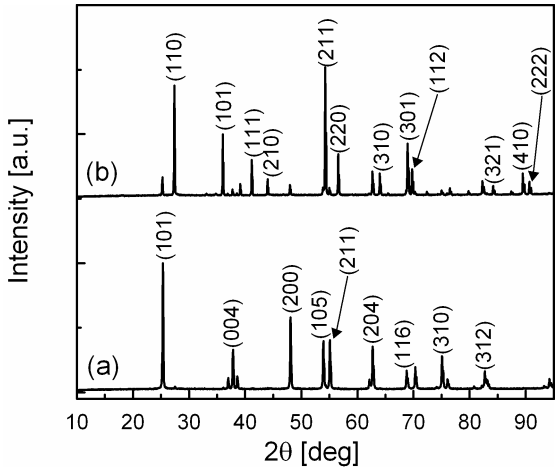

Fig. 2 Powder XRD patterns of the starting anatase TiO_2 particles **(a)** and prepared rod-like TiO_2 particles **(b)**

The size and morphology of studied particles were further observed with SEM (Scanning Electron Microscope VEGA II LMU, Tescan, Czech Republic) operated at 30 kV for the starting anatase TiO_2 and 10 kV for the prepared rutile TiO_2 (Fig. 3). As can be seen, the starting TiO_2 particles of anatase phase have rather spherical shape with the size ranging from 200 to 500 nm. On the other hand, TiO_2 particles of rutile phase prepared via molten-salt microwave-assisted synthesis have rod-like shape with the length from 5 to 10 μm and the diameter from 0.5 to 2 μm. Correspondingly, the geometric aspect ratio, *L/D*, of prepared TiO_2 particles is ranging from 2.5 to 20.

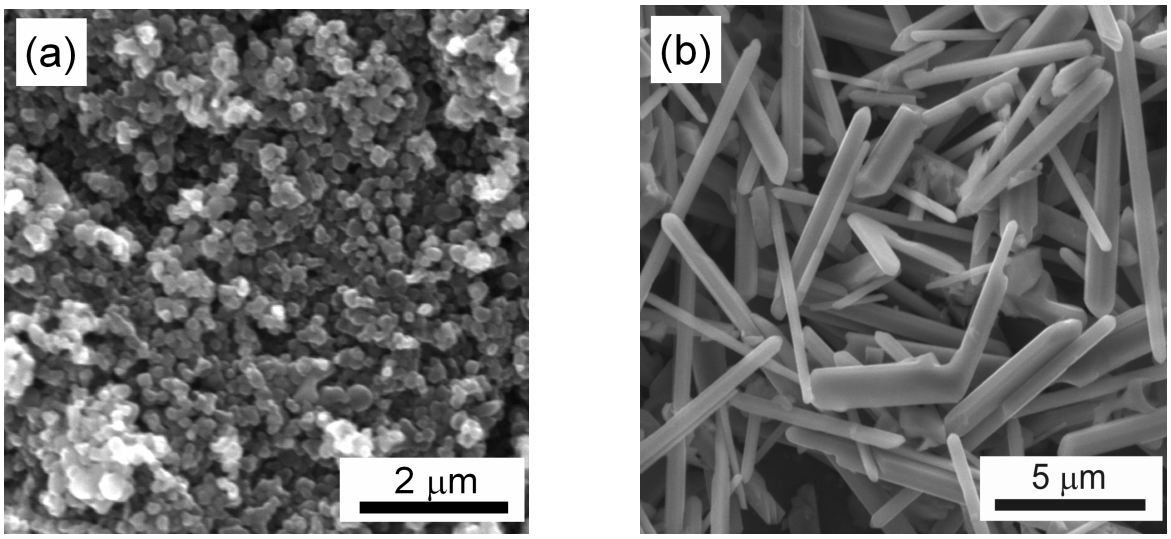

Fig. 3 SEM images of starting anatase TiO_2 **(a)** and prepared rutile TiO_2 **(b)** particles prepared via molten-salt microwave-assisted synthesis

2.4 Preparation of ER fluids

The ER fluids (5, 10, 15 wt.%) were prepared by mixing anatase powder or rutile TiO_2 rod-like particles with a corresponding volume of silicone oil (Lukosiol M200, Chemical Works Kolín, Czech Republic, viscosity $\eta_c = 200$ mPa·s, density $\rho_c = 0.965$ g·cm^{-3}, conductivity $\sigma_c \approx 10^{-11}$ S·cm^{-1}, relative permittivity $\varepsilon'_c = 2.6$, loss factor tan $\delta = 0.002$). To avoid the influence of moisture the silicone oil was dried at 80 °C for 24 h. The ER fluids were stirred mechanically and then placed in an ultrasonic bath for 60 s before each measurement.

2.5 Electrorheological measurements

Measurements of rheological properties of prepared ER fluids were carried out at 25 °C using a rotational rheometer (Bohlin Gemini, Malvern Instruments, UK), with coaxial cylinder geometry (length 27.4 mm, inner cylinder of 14 mm in diameter and the outer cylinder separated by a 0.7–mm gap), modified for ER experiments. A DC voltage (0.35 kV until 2.1 kV) corresponded to the electric field strength range 0.5 – 3 kV·mm^{-1} was generated by a DC high-voltage source TREK (TREK 668B, USA). A DC voltage was applied for 60 s to generate the equilibrium chain-like structure of particles before shearing. All steady-flow tests were performed in the shear rate range 0.1 – 300 s^{-1} (controlled shear rate mode). After the measurement at given electric field strength, the formed internal structure within the fluid was destroyed by shearing of the sample at a shear rate 20 s^{-1} for 120 s prior to characterization at a different electric field values.

2.6 Dielectric properties

Dielectric properties involving the frequency spectra of relative permittivity, ε', and dielectric loss factor, ε'', in the frequency range $4\times10^1 - 5\times10^6$ Hz have been measured with an impedance analyzer (Agilent 4524, Japan). The dielectric spectra (Fig. 4) characteristics of ER fluids were obtained from the Havriliak–Negami empirical model (Eq. 1) fitted by least square method [14]:

$$\varepsilon^* = \varepsilon'_\infty + \frac{(\varepsilon'_0 - \varepsilon'_\infty)}{\left(1 + (i\omega \cdot t_{\mathrm{rel}})^a\right)^b} \tag{1}$$

where ε^* is a complex fluid permittivity, the particle polarizability, $\Delta\varepsilon'$, is defined as the difference between ε'_0 and ε'_∞, which are the limit values of the relative permittivity at the frequencies below and above the relaxation frequencies, ω is angular frequency (= $2\pi f$), t_{rel} is the relaxation time, a is the scattering degree of relaxation times, and b is related to the asymmetry of the relaxation time spectrum. The relaxation frequency, at which the dielectric loss factor ε'' has a maximum, is proportional to the rate of polarization of suspension particles.

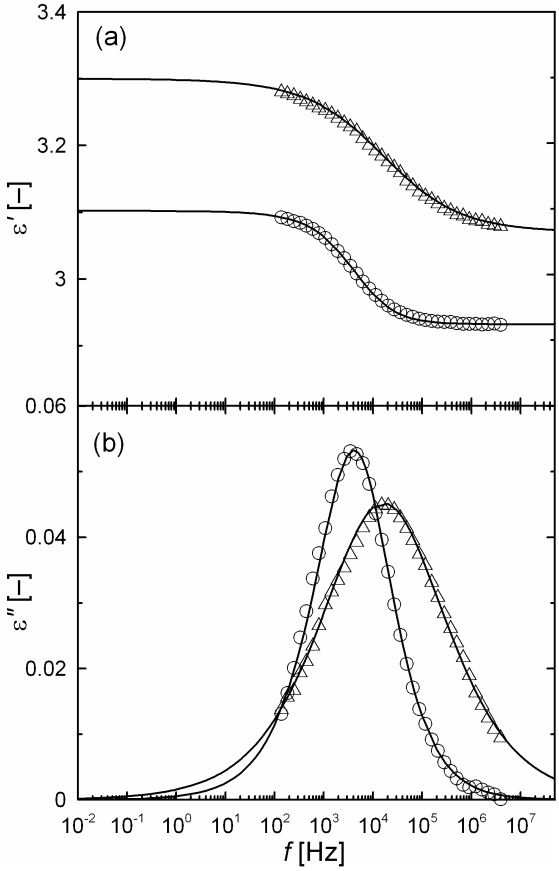

Fig. 4 Relative permittivity, ε', **(a)** and dielectric loss factor, ε'', **(b)** as a function of the frequency, f, for 5 wt.% suspension of starting anatase TiO_2 particles (○) and prepared TiO_2 rod-like particles (△)

Table 1. Dielectric parameters in Eq. 1 for starting anatase TiO_2 particles and prepared rod-like TiO_2 particles based ER fluids of 5 wt.% concentration

Parameter	Anatase TiO_2	TiO_2 rod-like
ε'_0	3.1	3.3
ε'_∞	2.93	3.07
$\Delta\varepsilon'$	0.17	0.23
t_{rel}	3.00×10^{-5}	9.06×10^{-6}

3 Results and discussion

3.1 ER activity and dielectric properties

The curves of the shear stress and viscosity versus shear rate for the starting anatase TiO_2 particle and prepared rutile TiO_2 rod-like particle based ER fluids are plotted in Fig. 5. The field-off shear stress depends almost linearly on the shear rate indicating a Newtonian flow of non-polarized particles (Fig. 5a). Viscosity of the starting anatase TiO_2 particle based ER fluid predominates (Fig. 5b) probably due to the nano-sized nature of particles having much larger surface area. Under electric field application, both ER fluids exhibit a typical Bingham plastic behaviour in the low-shear rate region, showing the prevalent feature of the ER activity. The flow became pseudoplastic, and the ER response of rutile TiO_2 rod-like particles was higher as the stronger chain-like structure developed due to better particles polarization [15]. Both systems show also typical shear thinning behaviour as the deformation rate of chain-like structure given by hydrodynamic forces becomes faster than its reformation rate given by polarization of particles with an increase in the shear rate. Generally, the chain-like structure is formed by induced electrostatic interactions between dispersed dielectric particles which are caused by their interfacial polarization. The dielectric spectra (Fig. 4) and their characteristics in the Table 1 indicate that rod-like TiO_2 particles exhibit enhanced magnitude of particle polarizability, $\Delta\varepsilon'$, and decreased the relaxation time, t_{rel}, compared to starting TiO_2 particles due to higher induced charges on the interface between the particle [16].

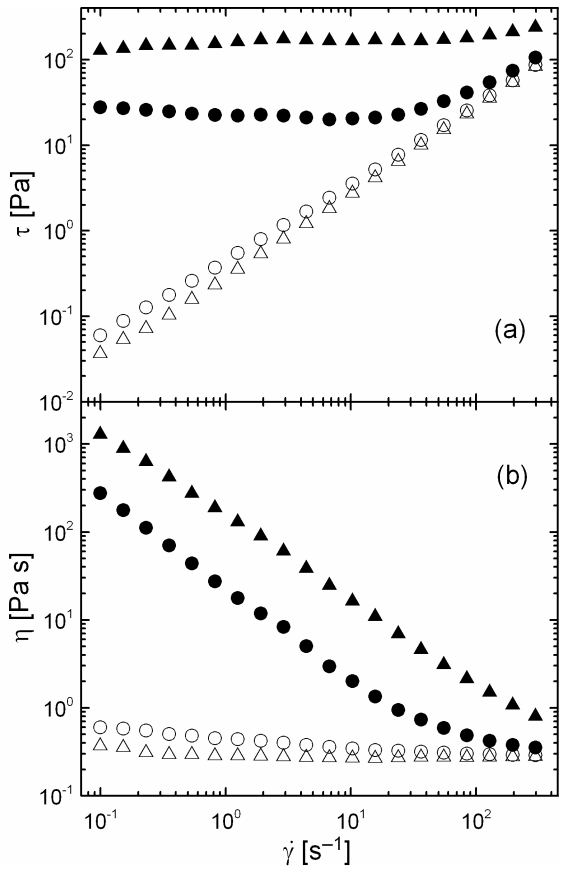

Fig. 5 Double-logarithmic plot of the shear stress, τ, **(a)** and the apparent viscosity, η, **(b)** vs. shear rate, $\dot{\gamma}$, for 15 wt.% suspension of starting anatase TiO_2 (●,○) and prepared rutile TiO_2 rod-like (▲,△) particles in silicone oil M200. The electric field strengths ($kV \cdot mm^{-1}$): 0 (○,△), 3 (●,▲)

3.2 Steady-state flow properties

As a representative of rutile TiO_2 rod-like particles, Fig. 6 shows typical flow and viscosity curves for 15 wt.% ER suspension under different electric field strengths. It is noteworthy that the peak in the shear stress develops during shearing of the suspension at moderate shear rates in higher electric field strengths. This phenomenon is attributed to the rearrangement in the ER structures from chain-like structures to lamellar ones due to the lowering of the free energy in the system [17,18].

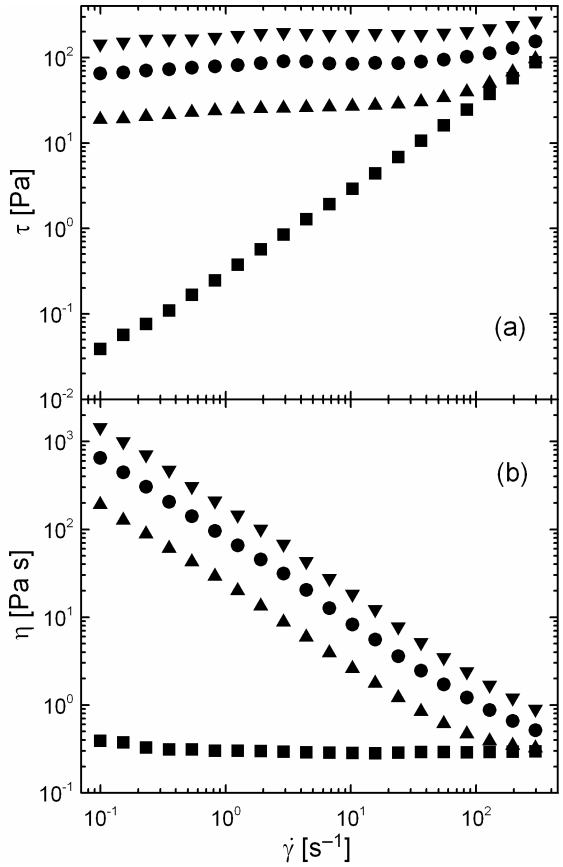

Fig. 6 Double-logarithmic plot of the shear stress, τ, **(a)** and viscosity, η, **(b)** vs. shear rate, $\dot{\gamma}$, for 15 wt.% ER fluid of rutile TiO_2 rod-like particles in silicone oil M200 at various electric field strengths, E (kV·mm^{-1}): 0 ■, 1 ▲, 2 ●, 3 ▼

Furthermore, the value of electric field-off viscosity is another important factor for the evaluation of the efficiency of ER phenomenon for practical use. The efficiency of the ER effect corresponding to a relative increase in electroviscosity, $\Delta\eta_E = \eta_E - \eta_0$, can be characterized by a quantity $e = (\eta_E - \eta_0)/\eta_0$, where η_E is a viscosity of ER structure [19]. The ER efficiencies for ER fluids based on rutile TiO_2 rod-like particles of different weight concentrations are shown in Fig. 7. Obviously, the efficiency of ER fluid increases with the particle concentration indicating that the maximal concentration for which the ER efficiency will attain a maximum, $e_{max.}$, was still not reached in this study. Comparing these results with those obtained for ER fluids consisted of spherical rutile TiO_2 particles [20], it is evident, that rod-like particles posses higher ER efficiency probably due to lower field-off viscosity and higher particle polarization both given by one dimensional morphology of particle.

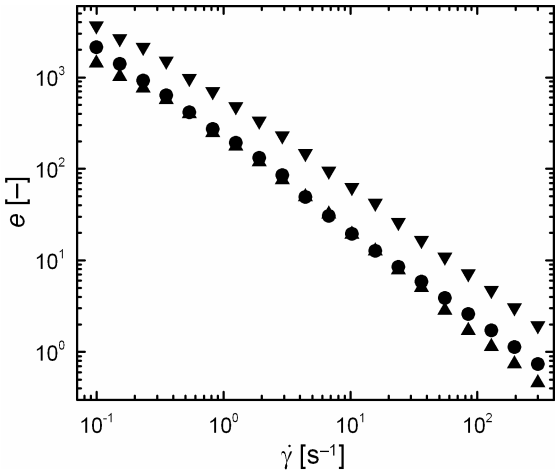

Fig. 7 The dependence of ER performance, e, on the shear rate, $\dot{\gamma}$, for suspension of rutile TiO_2 rod-like particles in silicone oil M200. Particle concentrations (wt.%): 5 ▲, 10 ●, 15 ▼

3.3 The response to electric field

The increase in the rigidity of formed internal structures within the ER fluids with electric field applied is shown in Fig. 8. The shear stresses, τ_c, at low shear rates $\dot{\gamma} = 0.23\ s^{-1}$ have been used as a criterion of rigidity of static particle chain-like structure due to the problematic determination of dynamic yield stress by extrapolation of the shear stress to zero shear rate. Evidently, the log τ_c vs. log E obeys the power law $\tau_c = q \cdot E^{\alpha}$. The response of particles on the electric field strength $\alpha = 2$ as expected from polarization model [21]. The almost one order of magnitude higher q value for suspension of rod-like TiO_2 particle confirms strong increase in ER activity.

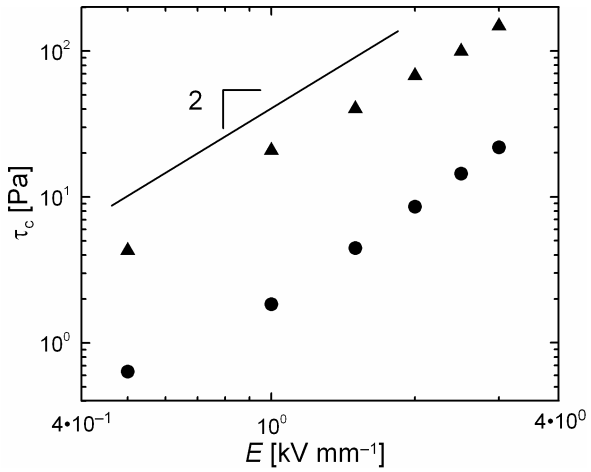

Fig. 8 Double-logarithmic plot of the shear stress, τ_c, vs. electric field strength, E, for 15 wt.% suspension of starting anatase TiO_2 (●) and rutile TiO_2 rod-like (▲) particles in silicone oil M200

3.4 Reproducibility of ER structure

The reproducibility of ER phenomenon is also very important factor for practical application of ER fluids. The alternate switching on/off the electric field should provide the same ER efficiency, i.e. the same ER structure should be formed rapidly. Fig. 9 depicts that the reproducibility after switching on/off cycles for rutile TiO_2 rod-like particles based ER fluid sheared at 1 s^{-1} and 1.5 $kV \cdot mm^{-1}$ is fulfilled.

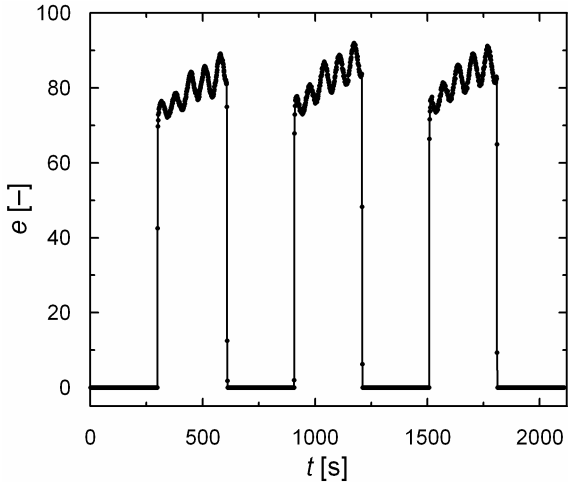

Fig. 9 Time dependence of ER performance, e, in the alternate switching on (E = 1.5 $kV \cdot mm^{-1}$)/off regime for 15 wt.% suspension of rutile TiO_2 rod-like particles in silicone oil M200 at the constant shear rate $\dot{\gamma}$ = 1 s^{-1}

4 Conclusions

Rutile TiO_2 rod-like particles were prepared via microwave-assisted molten-salt synthesis as a dispersed phase of a novel ER fluid. To gain an insight into the ER activity of these particles based ER fluids, rheological properties were evaluated under various experimental conditions, such as shear rate, electric field strength, and particle weight concentration. The steady-state flow measurements showed that the ER efficiency of rod-like TiO_2 particles was significantly higher compared to starting anatase TiO_2 particles. Moreover, the higher ER activity was in a good correlation with dielectric spectroscopy measurements as the particles polarizability was improved and relaxation time lowered for rod-like particles. The maximal ER efficiency was moved to higher weight concentrations for rod-like particles used as a dispersed phase probably due to lower field-off viscosity and better particle polarization. Finally, the reproducibility and speed of the formation and destruction of ER structure met the requirements for practical applications.

Acknowledgements

The authors wish to thank the internal grant of TBU in Zlín No. IGA/FT/2012/039 funded from the resources of specific university research for financial support.

This article was written with support of Operational Programme Research and Development for Innovations co-funded by the European Regional Development Fund (ERDF) and national budget of the Czech Republic, within the framework of Centre of Polymer Systems project (reg. number: CZ.1.05/2.1.00/03.0111).

References

[1] Wen WJ, Huang XX, Sheng P (2008) Electrorheological fluids: structures and mechanisms. Soft Matter 4:200–210

[2] Parthasarathy M, Klingenberg DJ (1996) Electrorheology: Mechanisms and models. Mater Sci Eng R-Rep 17:57–103

[3] Hao T (2002) Electrorheological fluids. Adv Colloid Interface Sci 97:1–35

[4] Yin JB, Zhao XP (2006) Advances in electrorheological fluids based on inorganic dielectric materials. J Ind Eng Chem 12:184–198

[5] Stanway R, Sproston JL, ElWahed AK (1996) Applications of electro-rheological fluids in vibration control: A survey. Smart Mater Struct 5:464–482

[6] Liu YD, Fang FF, Choi HJ (2011) Silica nanoparticle decorated polyaniline nanofiber and its electrorheological response. Soft Matter 7:2782–2789

[7] Cheng QL, Pavlinek V, He Y, Li CZ, Saha P (2009) Electrorheological characteristics of polyaniline/titanate composite nanotube suspensions. Colloid Polym Sci 287:435–441

[8] Mrlik M, Pavlinek V, Saha P, Quadrat O (2011) Electrorheological properties of suspension of polypyrrole-coated titanate nanorods. Appl Rheol 21:52365

[9] Lu XF, Zhang WJ, Wang C, Wen TC, Wei Y (2011) One-dimensional conducting polymer nanocomposites: Synthesis, properties and applications. Prog Polym Sci 36:671–712

[10] Yin JB, Zhao XP (2008) Electrorheological properties of titanate nanotube suspensions. Colloid Surf A-Physicochem Eng Asp 329:153–160

[11] Cheng QL, Pavlinek V, He Y, Li CZ, Lengalova A, Saha P (2007) Facile fabrication and characterization of novel polyaniline/titanate composite nanotubes directed by block copolymer. Europ Polym J 43:3780–3786

[12] Li HL, Du ZN, Wang GL, Zhang YC (2010) Low temperature molten salt synthesis of SrTiO(3) submicron crystallites and nanocrystals in the eutectic NaCl-KCl. Mater Lett 64:431–434

[13] Wang TX., Liu SZ, Chen J (2011) Molten salt synthesis of SrTiO(3) nanocrystals using nanocrystalline TiO(2) as a precursor. Powder Technol 205:289-291

[14] Havriliak S, Negami S (1966) A complex plane analysis of alpha-dispersions in some polymer systems. J Polym Sci C 16:99–117

[15] Hong JY, Choi M, Kim C, Jang J (2010) Geometrical study of electrorheological activity with shape-controlled titania-coated silica nanomaterials. J. Colloid Interface Sci 347:177–182

[16] Sanchis A, Sancho M, Martinez G, Sebastian JL, Munoz S (2004) Interparticle forces in electrorheological fluids: effects of polydispersity and shape. Colloid Surf A-Physicochem Eng Asp 249:119-122

[17] Vieira SL, Neto LBP, Arruda ACF (2000) Transient behavior of an electrorheological fluid in shear flow mode. J Rheol 44:1139–1149

[18] Henley S, Filisko FE (1999) Flow profiles of electrorheological suspensions: An alternative model for ER activity. J Rheol 43:1323–1336

[19] Lengalova A, Pavlinek V, Saha P, Quadrat O, Kitano T, Stejskal J (2003) Influence of particle concentration on the electrorheological efficiency of polyaniline suspensions. Europ Polym J 39:641–645

[20] Sedlacik M, Mrlik M, Pavlinek V, Saha P, Quadrat O (2012) Electrorheological properties of suspensions of hollow globular titanium oxide/polypyrrole particles. Colloid Polym Sci 290:41–48

[21] Kim SG, Lim JY, Sung JH, Choi HJ, Seo Y (2007) Emulsion polymerized polyaniline synthesized with dodecylbenzenesulfonic acid and its electrorheological characteristics: Temperature effect. Polymer 48:6622-6631